

CRUISE REPORT

Geochemical Evaluation of Deep Sediment Hydrate Deposits on Alaminos Canyon, Block 818, Texas-Louisiana Shelf

Coauthors:

Richard Coffin, NRL

Leila Hamdan, NRL

Joseph P. Smith, NRC-NRL

Kelly Rose, NETL

Ross Downer, Milbar Hydrotest Inc.

Douglas Edsall, USNA (retired)

Joan Gardner, NRL

Rick Hagen, NRL

Warren Wood, NRL

POC:

Richard B. Coffin, Code 6114

Marine Biogeochemistry Section

Naval Research Laboratory

Washington, DC.

PHONE: 202-767-0065

EMAIL: richard.coffin@nrl.navy.mil

TABLE OF CONTENTS

| | |
|--|----|
| TABLE of CONTENTS | 2 |
| TABLE of FIGURES | 3 |
| TABLE of TABLES | 4 |
| I. OVERVIEW | 5 |
| II. INTRODUCTION | 5 |
| III. CRUISE PARTICIPANTS | 6 |
| IV. SITE DESCRIPTION | 7 |
| V. METHODS | 9 |
| A. Acoustic Profiling | 9 |
| B. Acoustic Positioning | 9 |
| C. Piston Coring | 9 |
| D. Shipboard Laboratory Analysis | 9 |
| E. Land Based Laboratory Analysis | 10 |
| F. Seismic Data Interpretation | 10 |
| G. Heat Flow | 11 |
| VI. RESULTS | 12 |
| A. Seismic Data Overview | 12 |
| B. Geochemical Data Overview | 16 |
| C. Heat Flow Data Overview | 28 |
| VII. PRELIMINARY SUMMARY | 29 |
| VIII. LITERATURE CITED | 30 |
| APPENDIX 1: Daily Activity Log | 31 |
| APPENDIX 2: Preliminary Porewater Data | 36 |
| APPENDIX 3: On Board Chemistry Lab lay out | 47 |
| APPENDIX 4: Geologic Core Descriptions | 49 |

TABLE OF FIGURES

| | |
|---|----|
| Figure 1. Alaminos Canyon Block 818 location in the Gulf of Mexico | 7 |
| Figure 2: Piston core and heat flow locations along the seismic inlines 986, 1006, 1016, 1026 and 1046. Inline and crossline sample points are interpreted to latitude and longitude in Table 2 | 8 |
| Figure 3: “Lister-type” heat flow probe | 11 |
| Figure 4: Interpretation of seismic data for shallow piston core geochemical interpretation of seismic profiles. Data presents potential hydrate deposits located above free gas zones and free gas venting. Piston core points on inline 986 are listed | 13 |
| Figure 5: Interpretation of seismic data for shallow piston core geochemical interpretation of seismic profiles. Data presents potential hydrate deposits located above free gas zones and free gas venting. Piston core points on inline 1006 are listed | 14 |
| Figure 6: Interpretation of seismic data for shallow piston core geochemical interpretation of seismic profiles. Data presents potential hydrate deposits located above free gas zones and free gas venting. Piston core points on inline 1016 are listed | 14 |
| Figure 7: Interpretation of seismic data for shallow piston core geochemical interpretation of seismic profiles. Data presents potential hydrate deposits located above free gas zones and free gas venting. Piston core points on inline 1026 are listed | 15 |
| Figure 8: Interpretation of seismic data for shallow piston core geochemical interpretation of seismic profiles. Data presents potential hydrate deposits located above free gas zones and free gas venting. Piston core points on inline 1046 are listed | 15 |
| Figure 9: Sediment methane concentration through vertical core profiles. A spatial description for the variations in concentrations is presented in the text | 18 |
| Figure 10: Porewater chloride concentration profiles through piston cores taken at all locations on Block 818. The dashed vertical line represents the background seawater chloride concentration of 559 mM | 19 |
| Figure 11: Piston core porewater sulfate profiles compared to shallow 3.5 kHz and deep seismic data. Data in the three plots are separated along inline 986 for western, mid and eastern seismic line data groups | 20 |
| Figure 12: Piston core porewater DIC profiles compared to shallow 3.5 kHz and deep seismic data. Data in the three plots are separated along inline 986 for western, mid and eastern seismic line data groups | 21 |
| Figure 13: Piston core porewater sulfate and DIC profiles compared to shallow 3.5 kHz | |

| | |
|---|----|
| and deep inline 1006 seismic data. Porewater data are plotted separately for the sulfate and DIC concentrations | 22 |
| Figure 14: Piston core porewater sulfate and DIC profiles compared to shallow 3.5 kHz and deep inline 1016 seismic data. Porewater data are plotted separately for the sulfate and DIC concentrations | 23 |
| Figure 15: Piston core porewater sulfate and DIC profiles compared to shallow 3.5 kHz and deep inline 1026 seismic data. Porewater data are plotted separately for the sulfate and DIC concentrations | 24 |
| Figure 16: Piston core porewater sulfate and DIC profiles compared to shallow 3.5 kHz and deep inline 1046 seismic data. Porewater data are plotted separately for the sulfate and DIC concentrations | 25 |
| Figure 17: Selected porewater sulfate and sediment methane profiles to provide an overview of the spatial variation in profiles | 26 |
| Figure 18: Sediment SMI depths calculated from sediment porewater profiles and core sites located on the inline and cross line points | 27 |
| Figure 19: Geothermal gradients measured through crosslines from inline 986 up to Inline | 28 |

TABLE OF TABLES

| | |
|---|----|
| Table 1: Contact information for cruise participants onboard and related key personnel. ... | 6 |
| Table 2. Core locations and background information. | 16 |

I. OVERVIEW

The project was designed to initiate characterization of deep sediment methane hydrates in the Alaminos Canyon, Block 818, on the Texas-Louisiana Shelf in the Gulf of Mexico. Work included the gathering of geochemical and fluid migration data as well as bacteria samples in a cold seep environment as part of the Seep and Methane Hydrate Advanced Research Initiative (ARI) model development. Fieldwork planning integrated a preliminary geochemical survey for the Chevron-Texaco Joint Industry Program (JIP) drilling on Alaminos Canyon, Block 818 with the NRL ARI on shallow sediment methane seeps. Data acquired during this survey supported both program goals. Locations for field sampling and data collection were based on seismic profiles provide by WesternGeco after review by WesternGeco, NRL, NETL and MMS geophysists and geochemists (Appendixes 1). The NRL data will be compared with evaluation of this region for deep drilling conducted by the JIP to further develop the use of seismic and geochemical data to conduct preliminary site characterization of deep sediment hydrate deposits. The NRL program addresses biogeochemical cycling of methane in shallow sediments.

Data from this survey provide a preliminary shallow porewater geochemical prediction of possible deep sediment methane for hydrate exploration. Geochemical profiles in shallow sediment porewaters were used for spatial comparison of vertical methane flux (advection and diffusion). Heat flow, profiles indicative of vertical fluid migration, was coupled with geochemical profiles to contribute to interpretation of the vertical methane flux. This report provides a preliminary data overview. With analysis of all of the samples taken during this cruise, project objectives relative to the JIP include:

1. Determine porewater gas source(s) in sub-samples from piston cores.
2. Estimate the vertical methane flux in terms of the sulfate-methane interface (SMI) and sulfate gradients.
3. Provide supporting data on vertical methane flux with comparison of chloride, sulfide, dissolved inorganic carbon (DIC), and $\delta^{13}\text{C}$ DIC analysis of porewater.
4. Integrate data interpretation with seismic, heat flow and geochemical data.

Research objectives related to the NRL ARI include:

1. Assess the influence of deep ocean waters on vertical methane fluxes.
2. Study the shallow biogeochemical cycling of deep sediment methane.
3. Relate the vertical methane flux to horizontal and vertical variation in the microbial community diversity.
4. Characterize this region for methane seeps into the water column.

II. INTRODUCTION

Currently, preliminary evaluation of deep sediment hydrate beds is accomplished using seismic surveys to define zones with strong bottom simulating reflectors (BSRs) of acoustic velocity transitioning through sediment and into free gas. The first observed correlation between BSR and gas hydrate was in seismic data collected at Blake Ridge. This finding was further studied using single and multichannel seismic measurements to summarize BSR profiles for prediction of

hydrate reservoirs. Recent research in methane hydrate exploration off the mid-Chilean Margin and Atwater Valley in the Gulf of Mexico coupled seismic data with heat flow data and pore water geochemical profiles to provide a thorough evaluation of methane cycling. Conflicting geochemical and seismic data over strong seismic blanking regions indicate a need to combine these parameters for deep sediment gas hydrate surveys.

The biogeochemical cycles in shallow sediment over methane hydrate beds are active in response to upward vertical methane diffusion and advection from deep sediments, and the downward diffusion of sulfate from seawater. The interface between upward methane diffusion and downward sulfate diffusion is known as the sulfate methane interface (SMI)¹. At the SMI anaerobic oxidation of methane (AOM) can occur resulting in the oxidation of methane and reduction of sulfate. These coupled metabolic processes are commonly conducted via a syntrophic consortium of archaea and bacteria. Anaerobic oxidation of methane is the dominant process responsible for methane oxidation in oceanic sediments around the world.

This expedition on Alaminos Canyon was planned to combine porewater geochemical profiles with thermal gradients and seismic surveys to assess potential deep sediment gas and gas hydrate distribution at and around a seafloor seep. Basic research on microbial community diversity and sulfate and methane cycling was coupled with this field survey. Also pursuant to JIP needs, coring and thermometry in this area was planned to help quantify the lateral variability of flux. A highly variable seafloor flux regime may require closely spaced drill holes to achieve ultimate JIP goals of characterizing the gas hydrate accumulation at this site. The coring and thermometry from this expedition will provide valuable guidance in generating a JIP drilling plan.

III. CRUISE PARTICIPANTS

Table 1: Contact information for cruise participants onboard and related key personnel.

| Onboard | Phone number | email |
|--------------------------------------|---------------------|--|
| Warren T. Wood (NRL SSC) | (228) 688 5311 | warren.wood@nrlssc.navy.mil |
| Rick Coffin (NRL DC) | (202) 727-0065 | richard.coffin@nrl.navy.mil |
| Leila Hamdan (NRL DC) | (202) 727-3364 | leila.hamdan@nrl.navy.mil |
| Joseph P. Smith (NRL DC) | (202) 404-6416 | joseph.smith@nrl.navy.mil |
| Jody Bruton (NRL SSC) | (228) 688-5310 | jody.bruton@nrlssc.navy.mil |
| Ross Downer (Milbar Hydrotest-Inc) | (318) 227-8210 | rdowner@milbar.net |
| Layton Bryant (Milbar Hydrotest-Inc) | (318) 227-8210 | lbryant@milbar.net |
| Joan Gardner (NRL DC) | (202) 404-1094 | gardner@nrl.navy.mil |
| Rick Hagen (NRL DC) | (202) 404-1125 | rick.hagen@nrl.navy.mil |
| Mara Daugherty (U. Maryland) | | mdoughe6@umd.edu |
| Kelly Rose (NETL DoE) | (304) 285-4157 | Kelly.Rose@NETL.DOE.GOV |
| Eilis Rosenbaum (NETL DoE) | (412) 386-6019 | Eilis.Rosenbaum@NETL.DOE.GOV |
| Brandon Yoza (U Hawaii) | | byoza@hawaii.edu |
| Other Contacts | | |
| Joe Gettrust (NRL SSC) | (228) 688 5475 | joe.gettrust@nrlssc.navy.mil |
| Joe Ustach (R/V Cape Hatteras) | (252) 504-7579 | joeu@duke.edu |
| John D. Wilder | (252)-504-7580 | jwilder@duke.edu |
| Rebecca Plummer (NRL DC) | (202) 404 1735 | rebecca.plummer@nrl.navy.mil |

¹ SMI (sediment-methane interface) and SMT (sediment-methane transition) are referenced in different publications. Data interpretation for analysis of SMI and SMT are the same.

IV. SITE DESCRIPTION

The Alaminos Canyon (AC), Block 818 (Figure 1) is located in the northwestern Gulf of Mexico off the Texas Deltas with dominant coastal input beyond the base of the slope fan. This site is in the Perdido Fold Belt and contains oil accumulations in a variety of turbidite deposits from sand sheets to amalgamated and leveed channel systems (Meyer et al. 2005). Recent surveys of this area conducted in ROV and manned submersible sub dives found locations for chemosynthetic communities at the sediment water column interface². Seismic reflection maps indicate a series seeps that manifest themselves along the region which is characterized by subtle differences in reflection amplitude that are likely a result of high concentrations of sand below a 10 m thick pelagic drape. The seeps are located along a small ridge associated with the up-thrown side of a fault. No gas chimneys are visible in 3-D seismic data. Sediment piston coring and heat flow probing was conducted around the AC 818 well where sonic and resistivity logs used to estimate depth at the base of gas hydrate stability indicate a thick 5 to 50 meters of hydrate laden, sand-rich sediment. Because the well exists in an area of seafloor seeps, characterizing these seeps (quantifying the nature of fluid and methane flux) is the best way to estimate the flux associated with the suspected occurrence of gas hydrates. Chemical and thermal gradients can be used as inputs (boundary conditions) to finite element models of seafloor fluid flux. This study site, in contrast to another recent site in the Gulf of Mexico, Atwater Valley site, is closer to shore in the proximity of the Mississippi Fan fold belt. The belt runs 300 km eastward across a 50 km wide path and contains basinward-verging anticlines and underlain southern verging thrust faults. Fold strata were formed during the Late Jurassic to the Miocene geologic periods and in some regions are influenced by salt tongues and sheets that may reduce hydrate stability and increase the rate of vertical methane flux to the shallow sediment (Coffin et al., 2008).

Field work was conducted on board the *RV Cape Hatteras* with site selection based on seismic profiles provided by WesternGeco and reviewed by MMS, USGS, NRL, and WesternGeco. Sediment piston coring and heat flow probing was conducted across seismic inlines 986, 1006, 1016, 1026 and 1046 (Figure 2). Selection of the crosslines was based on seismic patterns indicating strong bottom simulating reflection (BSR) and potential vertical fluid migration as well as other information provided by recent surveys in this region. The daily log for field work during this cruise is outlined in Appendix 2.

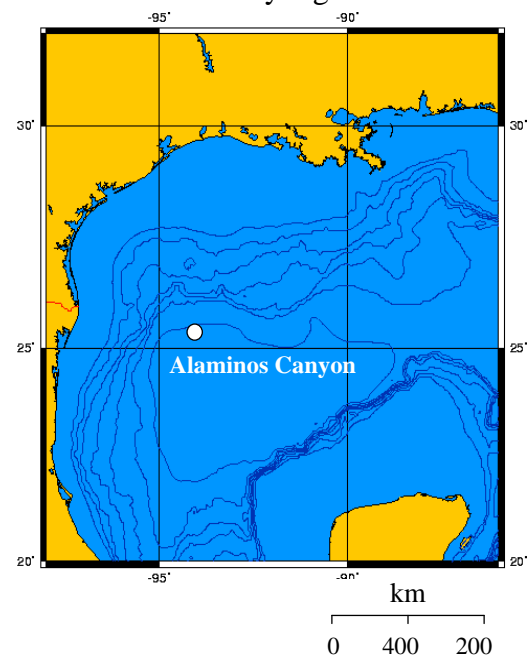


Figure 1. Alaminos Canyon Block 818 location relative to coastal slope fans.

² <http://www.oceanexplorer.noaa.gov/explorations/07mexico/welcome.html>

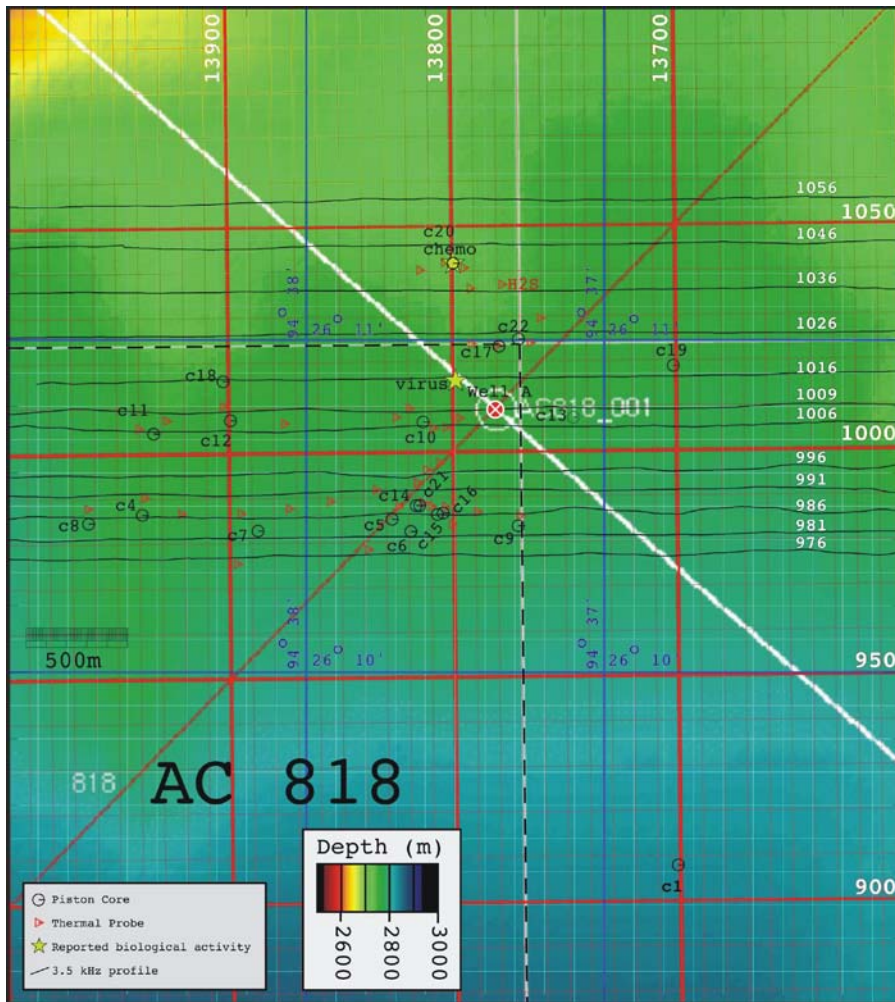


Figure 2: Piston core and heat flow locations along the seismic inlines 986, 1006, 1016, 1026 and 1046. Inline and crossline sample points are converted to latitude and longitude in Table 2.

V. METHODS

A. Acoustic Profiling

Acoustic profiles at 3.5 and/or 12 kHz were collected on a grid through the study region on inlines 986, 1006, 1016, 1026 and 1046. Selection of the piston core and thermal probe locations were determined on board with comparison of this acoustic profiling and the seismic images provided by WesternGeco.

B. Acoustic Positioning

An NRL Sonardyne USBL was used to provide acoustic positioning on all thermal probe deployments and on all but one piston core deployments. Several pre-mature piston core drops in the water column damaged the brackets holding the acoustic transponder to the cable so brackets belonging to the ship were refit to the NRL transponder. On subsequent deployments, the transponder was attached 200-300m above the core head instead of 100m. On the thermal probe deployments the transponder was attached 300-400 m above the weight stand. This instrument

provided improved accuracy in positioning as deep currents were responsible for drifts of up to 130 m from the ship's position on the surface. The Hatteras was able to maneuver within a range of 10 to 40 m in the range of the acoustic positioning.

C. Piston Coring

The piston coring system provided by Milbar (R. Downer) had been designed to collect samples within the hydrate stability zone. The core weight was approximately 3,000 lbs. The system includes trigger assemblies, trigger weights, wire terminations, piston immobilizers and specially designed N-80 alloy core barrels complete with modified Atlas Bradford connections. Two or three, 3 m core barrels lined with 3" diameter polycarbonate liners were used for each deployment. The safety trigger design for the system was developed by Milbar. Trigger weights were set initially at 12 - 15 meters. Typical core penetration depths were between 6-7m.

D. Shipboard Laboratory Analysis

A thorough presentation of instruments installed for geochemical analysis on the research vessel is available for cruise reports of research conducted of the mid Chilean Margin, Atwater Valley in the Gulf of Mexico and the Hikurangi Margin off New Zealand (Coffin et al., 2006; 2008; 2007). The following text is a brief summary of the on board geochemical laboratory analyses.

1. Porewater Press Loading and Squeezing – After recovery, cores were placed horizontally on deck. Core liners were removed and cut in 10 cm sections at 25 to 45 cm intervals. Sampling intervals were selected based upon observations of dark (black) sediment and hydrogen sulfide odor (observational indicators of sulfide production associated with the SMT) and the appearance of core gas pockets. Fewer samples were taken toward the sediment-water interface and resolution was increased toward the suspected depth of the SMT. On average, 20 sediment sections were sampled from each core. Sediment plugs were immediately collected from each section in a 3 ml polyethylene syringe with the end cut off, and transferred to pre-weighed 20 ml serum vials to measure the headspace CH₄ concentrations (Hoehler et al., 2000). Whole round core sections were then taken to the ship wet laboratory for processing. Approximately 5 g of wet sediment from each section were collected in pre-weighed 31-mm snap-tight Petri-dishes and frozen for measurements of sediment porosity and percent organic carbon. Immediately after the subsample collection, porewater was pressed from the remaining sediment from each section using 70 ml Reeburgh-style PVC press containers pressurized to ~400 KPa (~60 psi) by low-pressure air applied to a latex sheet placed between the core sections and press gas inflow. Porewater was pre-filtered through Grade 1 Qualitative Filter Paper into gas-tight 60-ml polypropylene syringes. It was subsequently filtered through 0.2-µm Acrodisc PES syringe filters (Pall) into ashed (4 h at 450°C) 20 ml vials and dispensed into 1-10 ml ashed vials for analysis. Pressed sediment was wrapped in ashed aluminum foil and stored frozen at -20°C during transport to the land-based laboratory.

2. Sulfate and Chloride Concentrations – Porewater sulfate and chloride concentration were measured with a Dionex DX-120 ion chromatograph equipped with an AS-9HC column, Anion Self-Regenerating Suppressor (ASRS Ultra II), and an AS-40 autosampler. Samples were diluted

1:50 (vol/vol) prior to analysis and measured using standard solutions referenced against a 1:50 diluted IAPSO standard seawater (28.9 mM SO_4^{2-} , 559 mM Cl^-). Analytical precision was $\pm 1\%$ of the reference standard. Chloride concentrations lower than values measured in seawater were used to indicate porewater freshening due to hydrate dissociation in the core. The measured porewater sulfate gradient and depth of depleted sulfate concentrations (limits of detection ~ 0.1 mM) were used to predict the depth of the SMI.

3. Pore Water Methane Concentrations – Methane concentrations were determined from 3-ml sediment plugs using headspace techniques and were quantified against certified gas standards (Scott Gas, Plumbsteadville PA). Headspace analysis was performed on board using a GC-FID Shimadzu GC-14A gas chromatograph equipped with a Hayesep 0.80/100 column. Methane concentrations are presented in millimolar units (mM).

4. Pore Water DIC Concentrations – Porewater DIC concentrations were measured using a UIC CO_2 coulometer and standardized to a certified seawater reference material (University of California, San Diego, CA). Conversion of DIC to CO_2 and separation from interfering sulfides was conducted according to Boehme et al. (1996).

E. Land Based Laboratory Analysis

1. Sediment Porosity – Frozen samples (~ 5 -6 g) were thawed and allowed to equilibrate to room temperature. Samples were then weighed wet and placed in a drying oven (~ 50 -60°C) for 24-48 hours. Samples were weighed again after drying. Sediment water content was determined by the difference between wet and dry weight, assuming constant pore water (ρ_{pw}) and bottom water (ρ_{sw}) density, and porosity profiles were then determined using the following equation:

$$\text{Porosity } (\phi) = \rho_{sm} WC \times [1/(\rho_{sm} WC + \rho_{pw} (1-WC))]$$

Where:

$$\text{Assumed solid matter density } (\rho_{sm}) = 2.50 \text{ g/cm}^3$$

2. Sediment Geological Summary – Sediment geological surveys from piston cores were conducted by Kelly Rose at NETL. Lithostratigraphic and subsea geologic evaluation was conducted onboard and in the laboratory. These data will be used to construct a detailed geologic and lithostratigraphic framework for the region and each coring site. Shipboard sedimentology techniques and procedures will include detailed visual core descriptions to help constrain the detailed lithostratigraphy. In the laboratory targeted xrd/xrf analyses, and smear slide and coarse fraction descriptions are used to identify the mineral and biogenic composition of sediments from major and minor lithologies. Sediment subsamples are also collected for particle size analyses correlative with the major and minor lithology sedimentology sample sites. These data contribute to the detailed geologic interpretation at each site and, when integrated with geophysical and other core sample analyses, help identify the geologic controls and constraints on carbon sources and cycling in the region. Geological data are in Appendix 5.

3. Porewater Cation Analysis – Major cation concentrations (Na^+ , Ca^{+2} , Mg^{+2} , K^+) were measured in sediment porewater in the laboratory using a Dionex DX-120 ion chromatograph

equipped with an AS-40 autosampler. A 20mM methanesulfonic acid ($\text{CH}_3\text{SO}_2\text{OH}$) eluent was used with a CS-12 column and a Cation Self-Regenerating Suppressor (CSRS Ultra II) at a flow rate of ~ 0.7 ml/min. Samples were diluted 1:50 (vol/vol). Calibration standards were prepared in the laboratory and diluted (1:50) IAPSO standard seawater was used as a reference standard. Analytical precision was ± 2 -3%. (Cation data will be presented in subsequent manuscripts. The data are not included in this report. Contact Joseph Smith (joseph.smith@nrl.navy.mil).)

F. Seismic Data Interpretation

Seismic blanking on seismic reflection records can indicate the presence and relative concentration of methane hydrates above the BSR. The BSR is not always present and an absence does not exclude the presence of methane hydrates. Regions of strong “wipe out or amplitude blanking” of acoustic signature often occur above the BSR. Blanking or reduction of amplitude of the acoustic reflectors above the BSR may indicate the presence of gas hydrates in the pore space which can act as a cement that reduces the velocity and density contrasts between the various strata and thus lessens the intensity of the return. Gas hydrate in sediments acts as a higher velocity material for seismic transmission relative to sediment filled with porewater. When water is preferentially replaced with hydrate, velocity becomes near or equal that of the adjacent, faster strata and thus eliminates the acoustic impedance contrast and any reflection at the strata boundary. More ill-defined BSRs reflect the subsequent dissociation of the methane hydrate and the upward migration of methane gas, especially along existing faults or stratigraphic pinchouts. Areas of seismic blanking above the BSR may reflect methane hydrate accumulations. With this interpretation of seismic profiles, methane hydrate formation is assumed within the HSZ where T and P conditions are at stable conditions. Vertical migration of gas will preferentially occur along faults, and will reach the sea floor where these faults extend upwards and intersect it. For preliminary seismic data interpretation four different features were surveyed; 1) a high amplitude reflector located above the BSR; 2) the BSR; 3) zones of amplitude blanking above the BSR; and 4) zones of amplitude blanking below the BSR containing varying amounts of free gas in the pore spaces.

G. Heat Flow

Thermal data collected in the upper few meters of the seafloor using a heat flow instrument has proven to be reliable for a proxy for fluid flow and helps define the limits of active flows around methane seeps and mud volcanoes associated with methane seeps and hydrates. The heat flow instrument used was a 3.5-meter-long “violin bow” or “Lister-type” instrument (Figure 3) consisting of eleven thermistors arranged 30 centimeters apart in a 1-cm-diameter tube held in tension parallel to a solid steel strength member. There was also a temperature sensor mounted on the top of the weight stand which recorded the water temperature near the sediment-water interface. The system measures both the temperature gradient and thermal conductivity in-



Figure 3: Lister-type heatflow probe.

situ. Sediment temperatures were calculated from the decay of the frictional heat caused by penetration of the instrument into the sediment. Thermal conductivity was determined from the decay of a calibrated thermal pulse applied after a preset period of time. Heat flow values were determined at each station by computing thermal resistance values at each thermistor,

$$R = \int (1/\lambda) dz,$$

where λ is the thermal conductivity. In a situation of steady-state conductivity the heat flow is equal to the slope of the line on a Bullard Plot, a plot of temperature vs. thermal resistance. For each station, any non-linear data that might be attributed to bottom water warming were removed so as not to bias the statistics. A heat flow value was determined from the slope of the linear regression fit to the remaining data. All heat flow values were corrected for instrument tilt. High resolution transects were done over the seeps and mounds to get an accurate summary of elevated thermal signatures. Stations were typically set no more than 100 meters apart to allow for the distinction of local fluid flow variations as opposed to those associated with the lateral distribution of seafloor seeps. Data showed clear anomalies in sediment temperature and heat flow associated with the mounds and seeps.

VI. RESULTS

A. Seismic Data Overview

As previously stated, Alaminos Canyon seismic data were provided by WesternGeo, Inc. to assist in the selection of porewater geochemistry and heat flow sample. In the seismic profiles, the base of the gas hydrate (solid phase) stability field is assumed to manifest as a bottom simulating reflector (BSR). Regions of high-amplitude acoustic reflectors often occur beneath the BSR. Enhanced reflection signal strength below the BSR appears to be caused by strong acoustic impedance contrasts due to the presence of free gas. Our approach for identifying methane hydrates and free gas in this area is similar to the approach used in other margins. The BSR seen in the seismic data is used as a first indicator of the regional base of hydrate stability. We assume that the methane transport responsible for the emplacement of methane at and around the BSR is diffusion dominated with linear geothermal profiles. Where the geothermal profiles are non-linear we expect a locally advective system, with a decreased depth to free gas, higher overall concentrations CH_4 and elevated sulfate SO_4^{2-} gradients in sediment porewater recovered from shallow piston cores.

Various features in the sub-bottom strata were identified and delineated with visual reviews (Figures 4-8). Immediately recognizable and present from one seismic profile to another were the sea floor, BSR's, major subbottom-anticlinal folds, faults, areas of seismic blanking (greatly reduced amplitude), and high amplitude reflectors. An anticlinal fold is recognizable below the BSR in the inline 986 seismic profile as well as in the four other west-east transects. The existence of a seismic wipeout on western limb of each crossing of the anticline suggests the source of methane above the basal BSR is towards the west in the adjacent syncline (Figure 4). The presence of methane gas in the eastern end of each profile is also interpreted, although the absence of severe faulting may have helped trapped this gas at the very strong BSR and limited its vertical ascent. The presence of faults above the western limb of the anticline and possible existence of an additional, shallow BSR suggests upward migration of gas and/or fluids from depth

and subsequent accumulation of hydrate in the region above basal BSR. This shallower BSR may be an example of a “perched” BSR. This suggests that the base of hydrate stability zone may have a significant temporal component.

The seismic lines parallel to line 986 cuts cross the same anticlinal feature, although the anticline plunges to the south on successive profiles from 1046 towards 986 (Figures 4 to 8). The seismic wipeout on the western limb of each crossing is again observed, as are numerous faults with vertical offsets, possible perched and relict BSRs, areas of apparent seismic blanking, and other high amplitude reflectors. The depth to the BSR is deeper on the eastern side of the anticline on each profile suggesting far less extensive faulting in the east, so the interpretation of methane hydrate and free gas is relatively easier on the eastern ends of the five profiles. We expect free gas exists beneath the very clearly defined BSR. Within the sedimentary sequence above this BSR there are areas of apparent seismic blanking interspersed with weak seismic reflectors. We expect methane hydrate to be present (in at least small amounts) above the BSR at various depths, with variable lateral extent, and therefore variable total volumes. This semi-quantitative overview of the seismic profiles was made with the interpretation of subsequent heat flow and porewater geochemical profiles. On the western limb of this anticlinal feature, crossed on lines 986, 1006, 1016, 1026 and 1046, free gas is present closer to the present ocean floor and might occur beneath both the perched BSR and the deeper BSR. We expect ethane hydrate accumulations should occur within the shallow sequence above the perched BSR and between the perched and deeper BSRs. Accumulations of free gas are predicted to be larger and more localized in the west but the presence of buried faults must be taken into consideration as they provide the avenues for the vertical migration of the free gas.

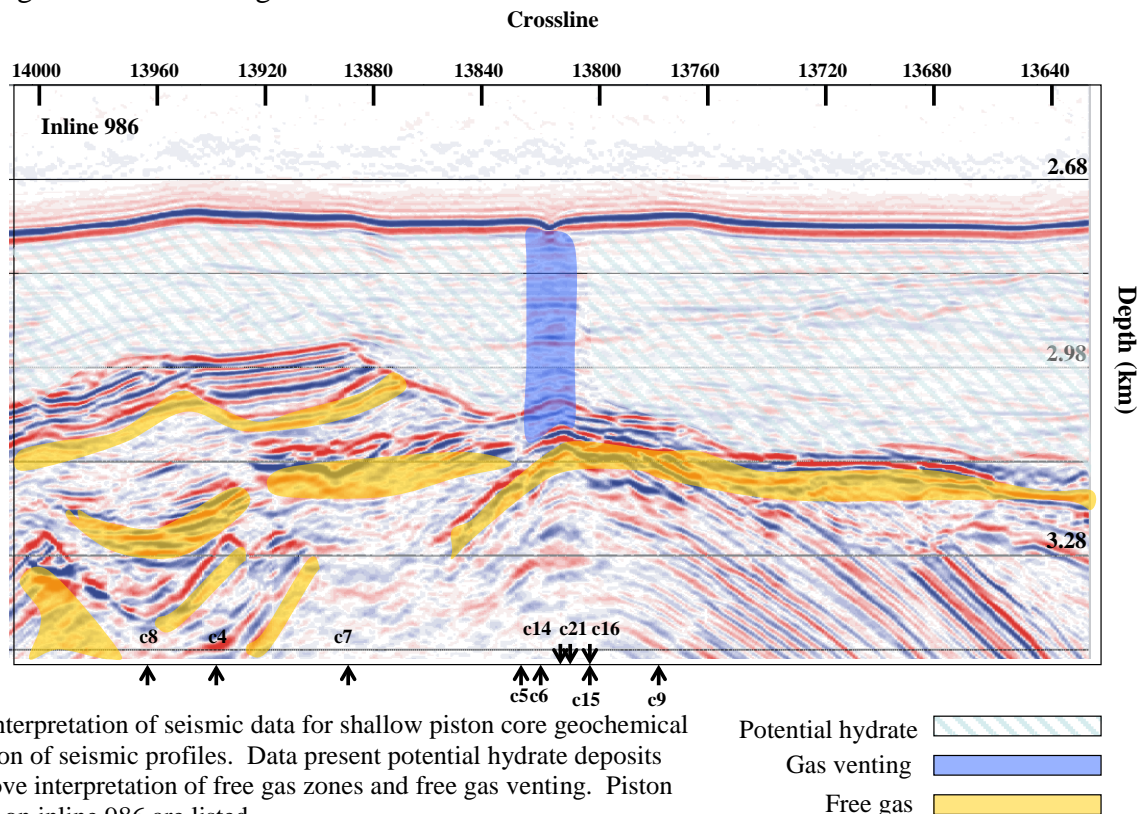


Figure 4: Interpretation of seismic data for shallow piston core geochemical interpretation of seismic profiles. Data present potential hydrate deposits located above interpretation of free gas zones and free gas venting. Piston core points on inline 986 are listed.

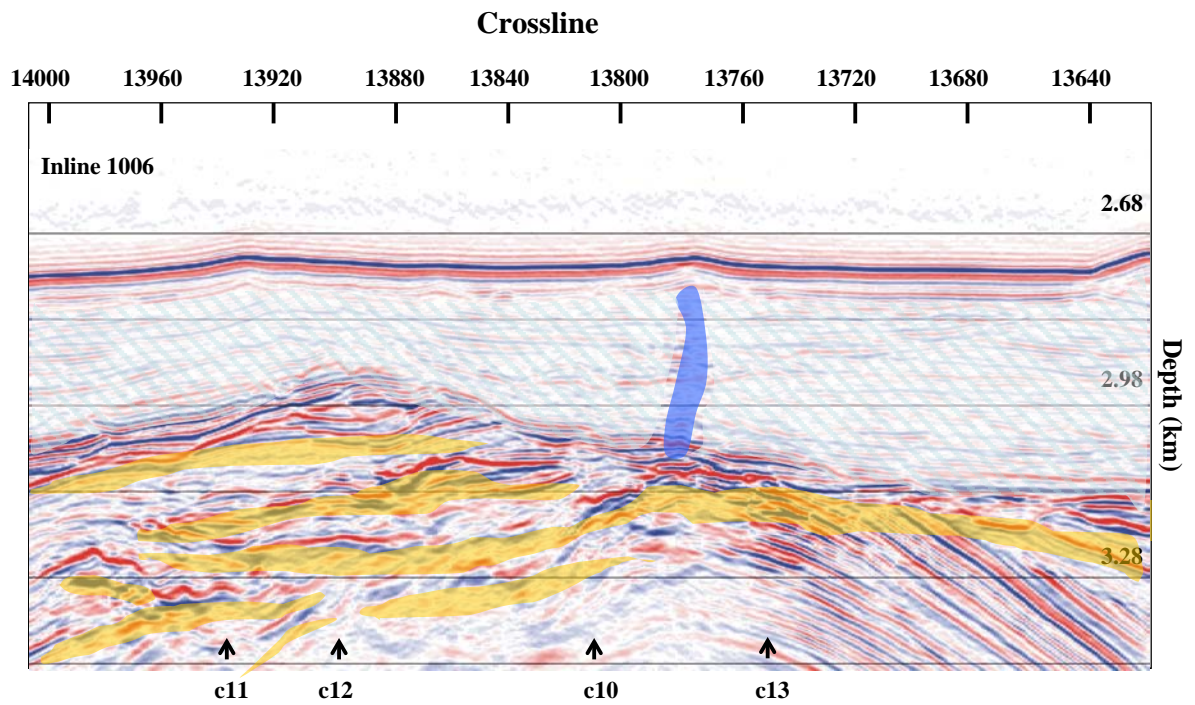


Figure 5: Interpretation of seismic data for shallow piston core geochemical interpretation of seismic profiles. Data present potential hydrate deposits located above interpretation of free gas zones and free gas venting. Piston core points on inline 1006 are listed.

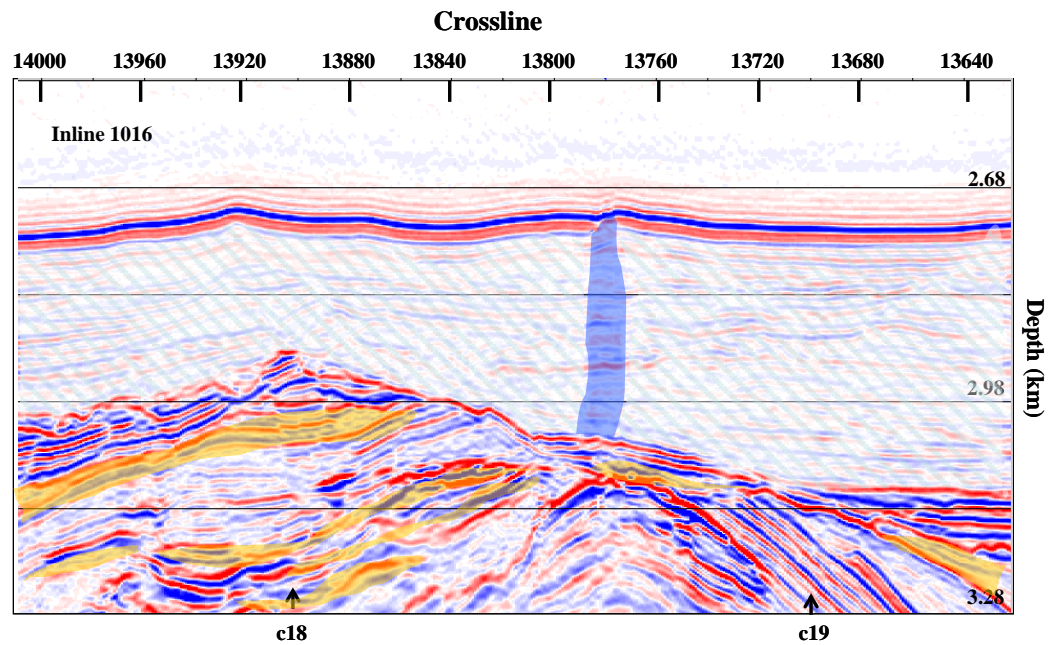


Figure 6: Interpretation of seismic data for shallow piston core geochemical interpretation of seismic profiles. Data present potential hydrate deposits located above interpretation of free gas zones and free gas venting. Piston core points on inline 1016 are listed.

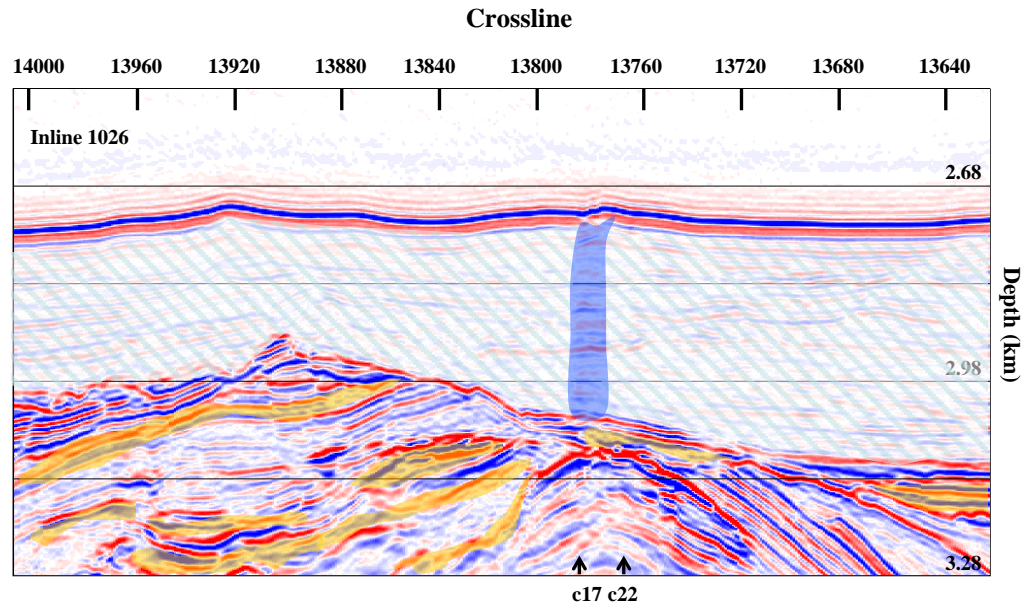





Figure 7: Interpretation of seismic data for shallow piston core geochemical interpretation of seismic profiles. Data present potential hydrate deposits located above interpretation of free gas zones and free gas venting. Piston core points on inline 1026 are listed.

Potential hydrate 
 Gas venting 
 Free gas 

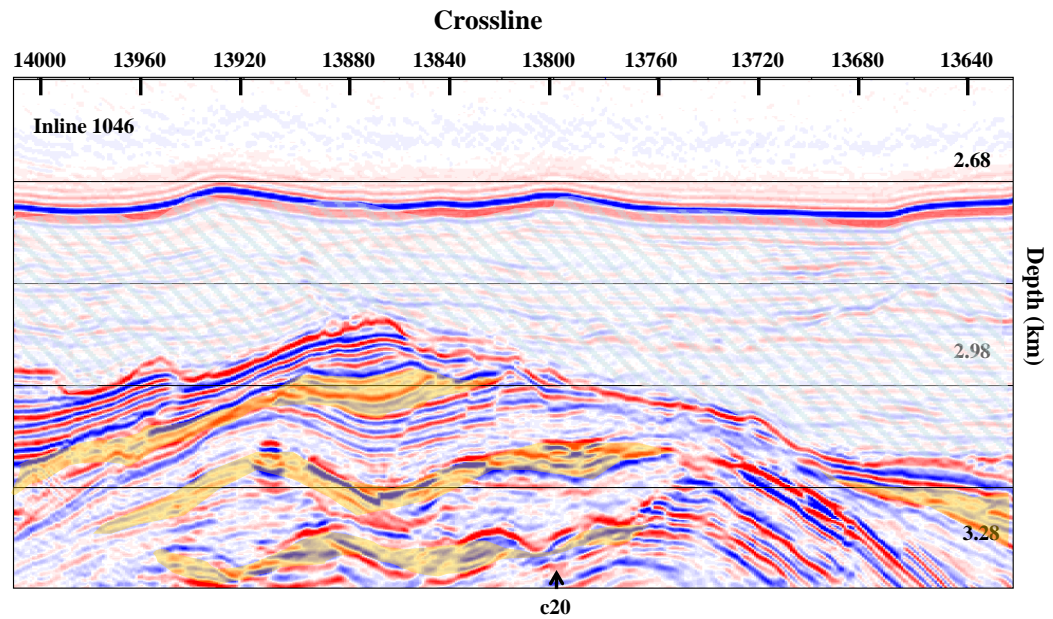





Figure 8: Interpretation of seismic data for shallow piston core geochemical interpretation of seismic profiles. Data present potential hydrate deposits located above interpretation of free gas zones and free gas venting. Piston core points on inline 1046 are listed.

Potential hydrate 
 Gas venting 
 Free gas 

B. Geochemical Data Overview

Twenty piston cores were retrieved during 22 deployments (Figure 2, Table 2). Core lengths ranged from 2.76 to 7.51 m. Onboard geochemical analysis included sediment (headspace) methane, and porewater sulfate, chloride, sulfide, and dissolved inorganic carbon concentrations (Appendix 3). Detailed descriptions were logged for each core that noted visually recognizable variations in core composition, specifically the noting the presence of clay, silt and sand layers (Appendix 5). Stable carbon isotope ratios, sediment porosity, and other sediment chemical parameters were measure at the onshore laboratory. Initial data interpretation used porewater CH₄ and SO₄⁻² profiles to estimate CH₄ fluxes and suggest relative rates of uncoupled organoclastic SO₄⁻² reduction (SR) and SR coupled to the anaerobic oxidation of methane (AOM) (Borowski et al., 1999). Anaerobic oxidation of methane is conducted through a metabolic partnership between methanogen-like archaea that oxidize CH₄ and SO₄⁻² reducing bacteria. The net equation describing AOM can be written as:



In many marine locations organoclastic SR is the dominant biogeochemical pathway for sediment sulfate consumption. However, in sediments over CH₄ gas seeps and hydrates with vertical CH₄ flux, AOM is the dominant pathway for SO₄⁻² reduction (Borowski et al., 1996; Boetius et al., 2000; Pancost et al., 2000). In such locations, rates of AOM are controlled by the rate of vertical CH₄ flux (diffusive and advective) and downward SO₄⁻² diffusion (Borowski et al., 1996; 1999). where they are consumed through AOM at a 1:1 stoichiometric ratio is known as the sulfate methane interface (SMI) (Borowski et al., 1999; Valentine, 2002). Where AOM is the dominant process for reduction of porewater SO₄⁻², an estimate of the SO₄⁻² diffusion rate can be used to estimate the CH₄ vertical flux. Quantifying lateral variations in SMI depths and SO₄⁻² diffusion rates across features on the seafloor or in the subsurface (imaged by seismic data) can assist in locating areas with significant CH₄ fluxes and potentially significant methane hydrate deposits (Borowski et al., 1999; Paull et al., 2005). Porewater DIC concentrations are influenced by microbial CO₂ respiration and assimilation, DIC advection, and porewater DIC solubility so these data assist in providing some qualitative interpretation of the SO₄⁻² and CH₄ flux and transport in the core profiles. Stable carbon isotope analysis of porewater DIC also provides additional interpretation of methane oxidation and contribution to the DIC pool.

Table 2. Core locations and background information.

| PC | GMT at hit | Lngth | Ship | Lat. | Ship | Lon | Rng | | | | Core | Core | Comments |
|----|--------------|-------|------|--------|------|--------|------|-----|-----------|----------|----------|---------|----------------------------|
| # | Bottom | (m) | Deg. | Min. | Deg. | Min. | dist | deg | X | y | Lt. Min. | Ln. Min | |
| 1 | 206:17:36:36 | 6.48 | 26 | 9.428 | 94 | 36.724 | 50 | 251 | -47.2759 | -16.2784 | 9.419 | 36.752 | Control, No visible seeps |
| 2 | 0 | 0 | 26 | 0.000 | 94 | 0.000 | 0 | 0 | 0.0000 | 0.0000 | 0.000 | 0.000 | Misfire in water column |
| 3 | 0 | 0 | 26 | 0.000 | 94 | 0.000 | 0 | 0 | 0.0000 | 0.0000 | 0.000 | 0.000 | Misfire in water column |
| 4 | 208:00:00:36 | 7.18 | 26 | 10.470 | 94 | 38.550 | 0 | 0 | 0.0000 | 0.0000 | 10.470 | 38.550 | Inline 986, bathy high |
| 5 | 209:03:50:43 | 7.56 | 26 | 10.459 | 94 | 37.562 | 250 | 270 | -250.0000 | 0.0000 | 10.459 | 37.712 | Inline 986 off pckmk |
| 6 | 209:15:36:10 | 3.04 | 26 | 10.435 | 94 | 37.616 | 60 | 247 | -55.2303 | -23.4439 | 10.422 | 37.649 | Inline 986 pckmk center |
| 7 | 209:21:01:13 | 7.51 | 26 | 10.450 | 94 | 38.126 | 78 | 230 | -59.7515 | -50.1374 | 10.423 | 38.162 | Inline 986, East shldr |
| 8 | 210:01:01:10 | 7.51 | 26 | 10.455 | 94 | 38.709 | 40 | 240 | -34.6410 | -20.0000 | 10.444 | 38.730 | Inline 986, West shldr |
| 9 | 210:14:23:53 | 7.69 | 26 | 10.460 | 94 | 37.269 | 50 | 220 | -32.1394 | -38.3022 | 10.439 | 37.288 | Inline 986, E. of pckmrk |
| 10 | 210:17:18:40 | 6.99 | 26 | 10.760 | 94 | 37.572 | 62 | 254 | -59.5982 | -17.0895 | 10.751 | 37.608 | Inline 1006, near well A |
| 11 | 210:20:55:44 | 6.87 | 26 | 10.738 | 94 | 38.485 | 63 | 224 | -43.7635 | -45.3184 | 10.714 | 38.511 | Inline 1006, west mound |
| 12 | 211:00:25:36 | 7.26 | 26 | 10.746 | 94 | 38.199 | 93 | 280 | -91.5871 | 16.1493 | 10.755 | 38.254 | Inline 1006, East shldr |
| 13 | 211:14:13:20 | 6.93 | 26 | 10.751 | 94 | 37.087 | 40 | 315 | -28.2843 | 28.2843 | 10.766 | 37.104 | Inline 1006, E of Well A |
| 14 | 211:16:59:44 | 7.01 | 26 | 10.481 | 94 | 37.610 | 50 | 315 | -35.3553 | 35.3553 | 10.500 | 37.631 | Inline 986, Pckmk Cntr |
| 15 | 211:20:10:18 | 2.76 | 26 | 10.484 | 94 | 37.543 | 34 | 234 | -27.5066 | -19.9847 | 10.473 | 37.560 | Inline 986, Pckmk E. Flank |
| 16 | 212:014540 | 6.85 | 26 | 10.483 | 94 | 37.541 | 10 | 170 | 1.7365 | -9.8481 | 10.478 | 37.540 | Inline 986, Pckmk E. Flank |
| 17 | 212:14:30:00 | 7.49 | 26 | 10.972 | 94 | 37.358 | 15 | 35 | 8.6036 | 12.2873 | 10.979 | 37.353 | Inline 1016, N. of Well |
| 18 | 212:17:50:22 | 6.8 | 26 | 10.871 | 94 | 38.265 | 24 | 273 | -23.9671 | 1.2561 | 10.872 | 38.279 | Inline 1016, West mound pk |
| 19 | 212:21:07:10 | 7.1 | 26 | 10.939 | 94 | 36.757 | 36 | 211 | -18.5414 | -30.8580 | 10.922 | 36.768 | Inline 1016, W. Shldr |
| 20 | 212:23:58:26 | 7.24 | 26 | 11.229 | 94 | 37.466 | 70 | 270 | -70.0000 | 0.0000 | 11.229 | 37.508 | Chemo site from NOAA |
| 21 | 213:14:49:08 | 7.22 | 26 | 10.473 | 94 | 37.632 | 55 | 24 | 22.3705 | 50.2450 | 10.500 | 37.619 | Inline 986, Pckmk |
| 22 | 213:18:35:10 | 4.9 | 26 | 10.985 | 94 | 37.291 | 30 | 12 | 6.2374 | 29.3444 | 11.001 | 37.287 | NE Corner of AC818 |

Sediment headspace methane gas concentrations varied by 7 orders of magnitude within all samples. In general, lower concentrations were found in the shallow core subsamples and higher concentrations in deeper sections (Figure 9). Cores 6, 10, 14, 15, and 21 contained the highest CH₄ concentrations with a range from the limits of detection (LTD) to 21.3 mM. In Core 6, values ranged from 2.2 mM to 21.3 mM CH₄ and the core contained visible gas hydrates. All of these cores were taken near the seismic crossline 13780, on inlines 986 and 1006 in close proximity to the seismic blanking profiles indicative of vertical CH₄ flux and fluid migration (Figures 4 and 5). Sediment headspace methane gas concentrations decreased rapidly away from this region with most cores containing methane concentrations ranging between 8.68×10^{-6} mM to 2.17 mM. Many cores were depleted below 10^{-3} mM through the entire profiles.

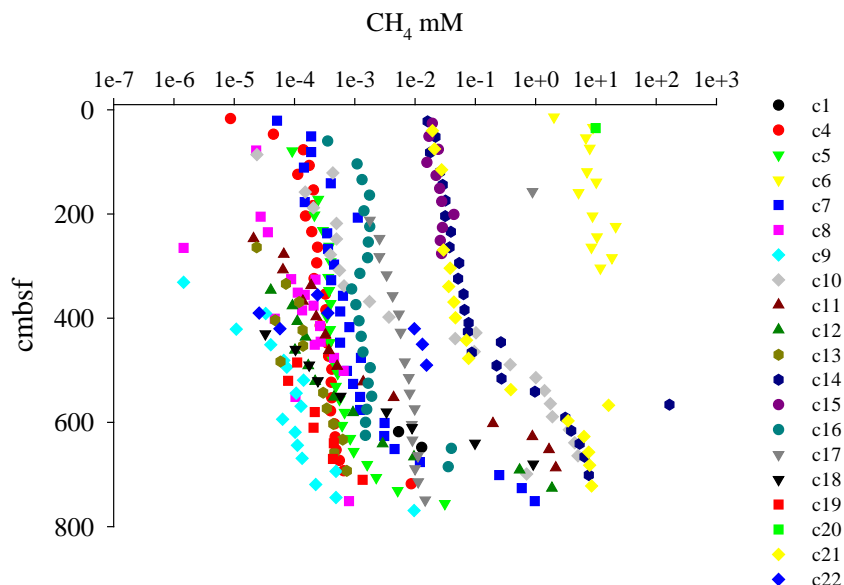


Figure 9: Sediment methane concentration through vertical core profiles.
A spatial description for the variations in concentrations is presented in the text.

Porewater chloride concentrations were generally near the background value of open ocean seawater (559 mM, Figure 10). The control site, core 1, was moderately lower with a range of 522 mM to 541 mM, perhaps resulting from lower coastal ocean salinities nearshore. Core 6 was observed to have substantially lower chloride concentrations with a range of 390 mM to 502 mM. This core contained methane hydrate samples and the lower chloride concentrations are a result of hydrates destabilization during core retrieval and processing. Moderately lower values were also measured in some sections of core 10, with values ranging from 529 mM to 585 mM. This location was found to have high sediment gas methane concentrations and the lower chloride concentrations may represent small amounts of hydrates dissociated during the processing. A key finding of this data set was that porewater chloride concentrations did not significantly exceed seawater background concentrations. In a geochemical survey of another Gulf of Mexico site, Atwater Valley, porewater chloride concentrations as high as 1000 mM were found likely due to the upward migration of deeper, more saline porewaters. This is consistent with reports of abundant salt intrusions and diapirs in the northern Gulf of Mexico (Weimer and Buffler, 1992; Grando and McClay, 2004; Stewart, 2006). Higher salinity has been suggested to decrease hydrate stability resulting in increased deep hydrate dissociation and higher vertical methane diffusion and advection (Coffin et al., 2008).

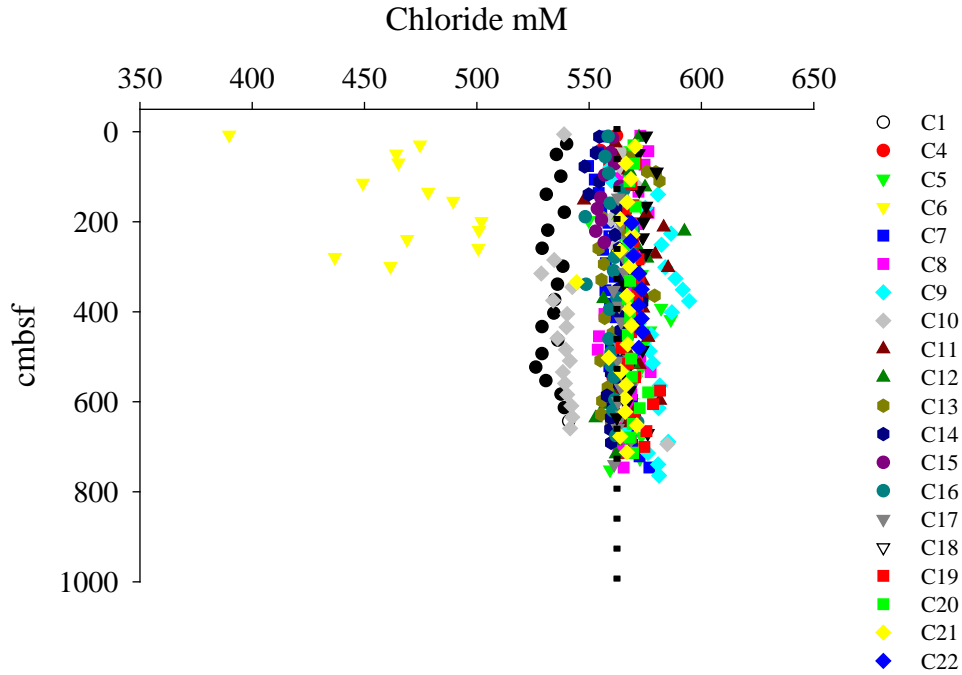


Figure 10: Porewater chloride concentration profiles through piston cores taken on Block 818. The dashed vertical line represents the background seawater chloride concentration of 559 mM.

Sediment porewater sulfate and DIC profiles are presented with a comparison of the inline shallow and deep seismic profiles (Figures 11-16). The primary focus during this expedition was inline 986. Porewater sulfate in the near surface subsamples of the core averaged 26.4 ± 2.3 mM ($n=16$). Core 6 and 15 were not included in the average because shallow porewaters were depleted relative to the over lying seawater due to coring artifacts. There was a large variation in the minimum porewater sulfate concentrations in cores. In cores collected on inline 986 near crossline 13780, minimum sulfate concentrations ranged from 0.62 mM to 1.19 (Figure 11). Cores 17, 22 and 20 located on inlines 1026 and 1046, near crossline 13780, had minimum sulfate concentrations of 9.61 mM, 15.4 mM, and 3.31 mM, respectively. Cores on all of the inlines away from the crossline 13780 had the smallest changes in the porewater sulfate concentrations with a minimum down to 15.83 mM (Figure 16). The SMI depth estimated from these sulfate concentration profiles are presented below. The trends in the sulfate and methane profiles matched the preliminary observations of the seismic data. More shallow sulfate depletion, indicative of more rapid vertical CH_4 fluxes, were observed in regions where shallow sediment and deep seismic profiles were interpreted to be regions of active fluid or gas migration.

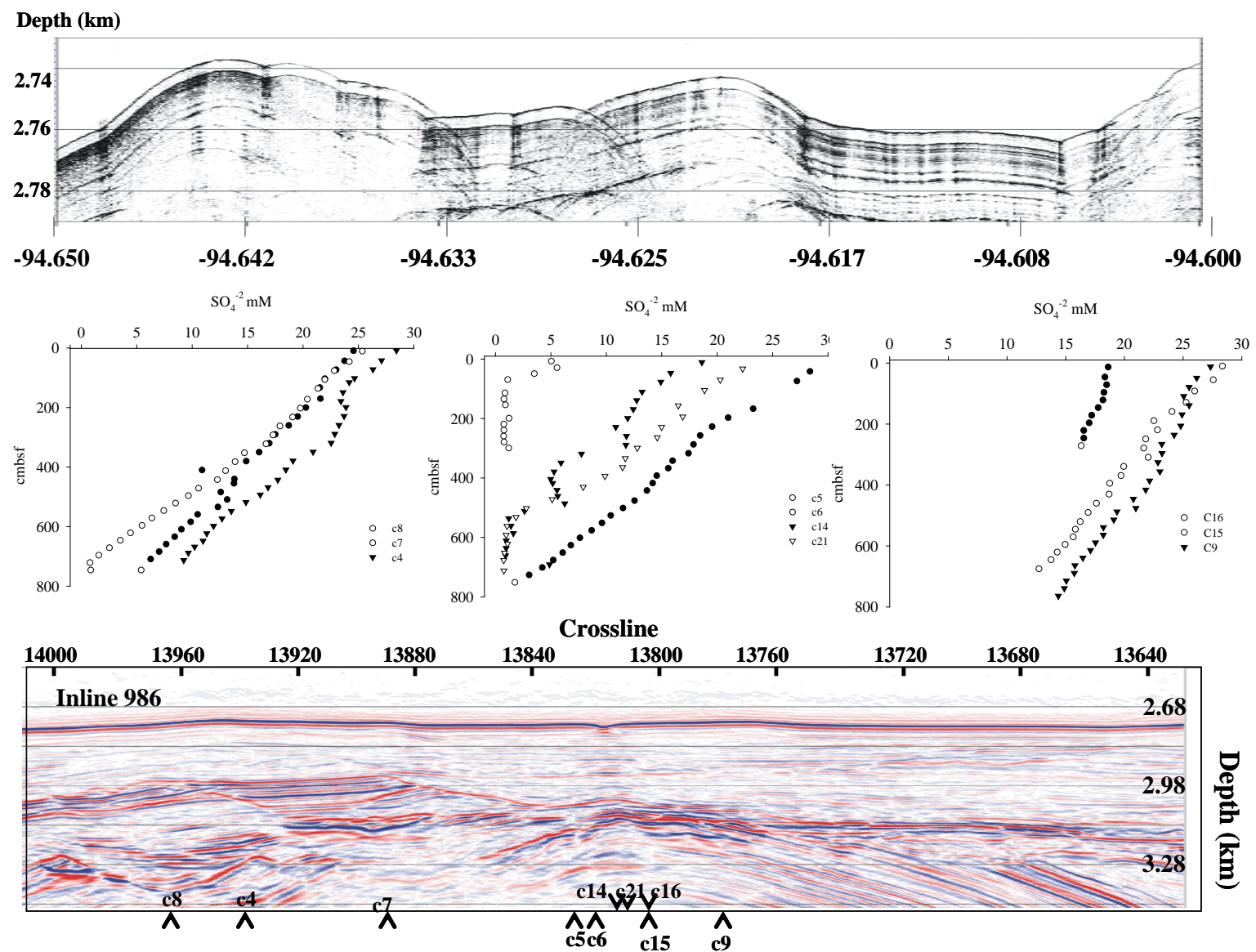


Figure 11: Piston core porewater sulfate profiles compared to shallow 3.5 kHz and deep seismic data. Data in the three plots are separated along inline 986 for western, mid and eastern seismic line data groups.

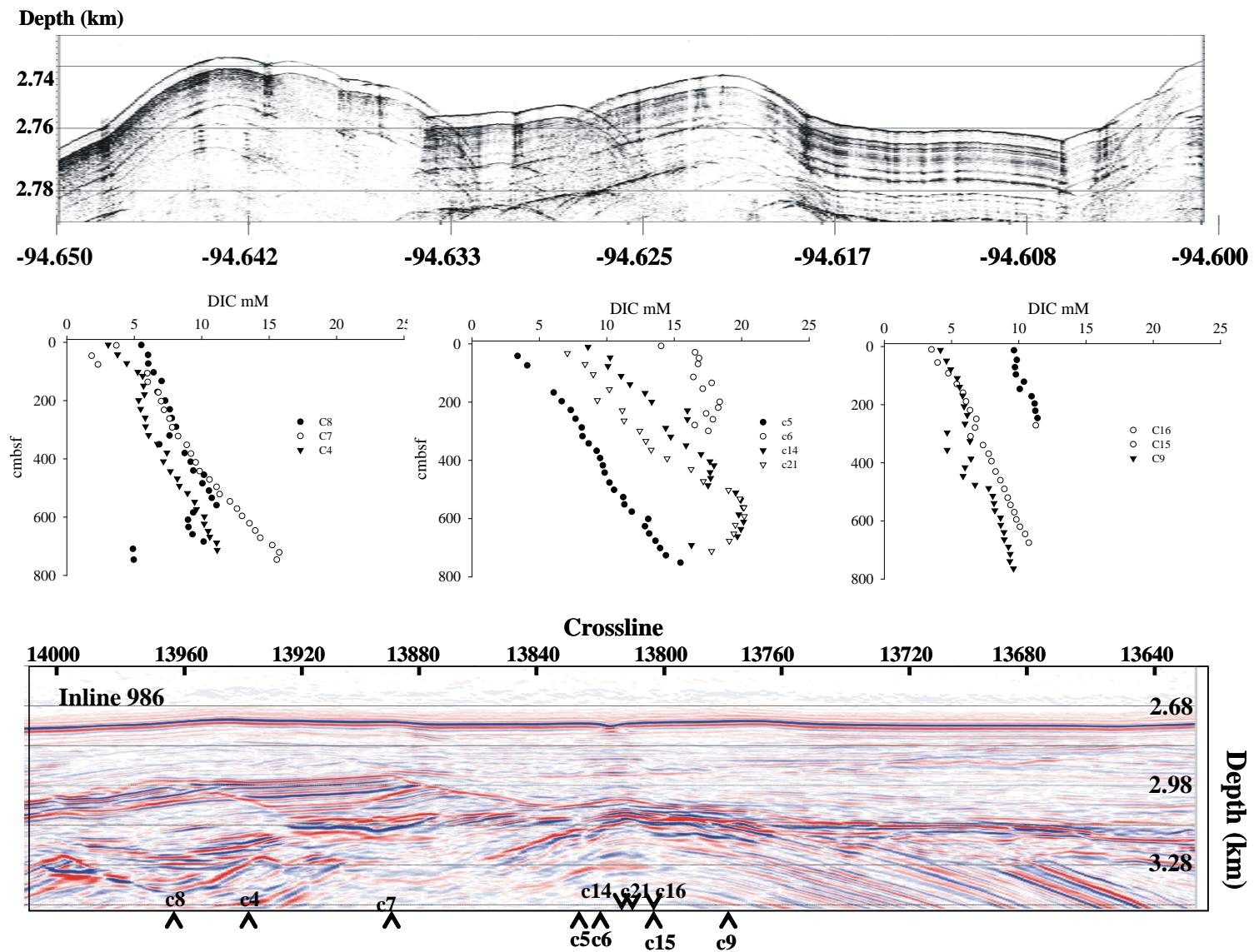


Figure 12: Piston core porewater DIC profiles compared to shallow 3.5 kHz and deep seismic data. Data in the three plots are separated along inline 986 for western, mid and eastern seismic line data groups.

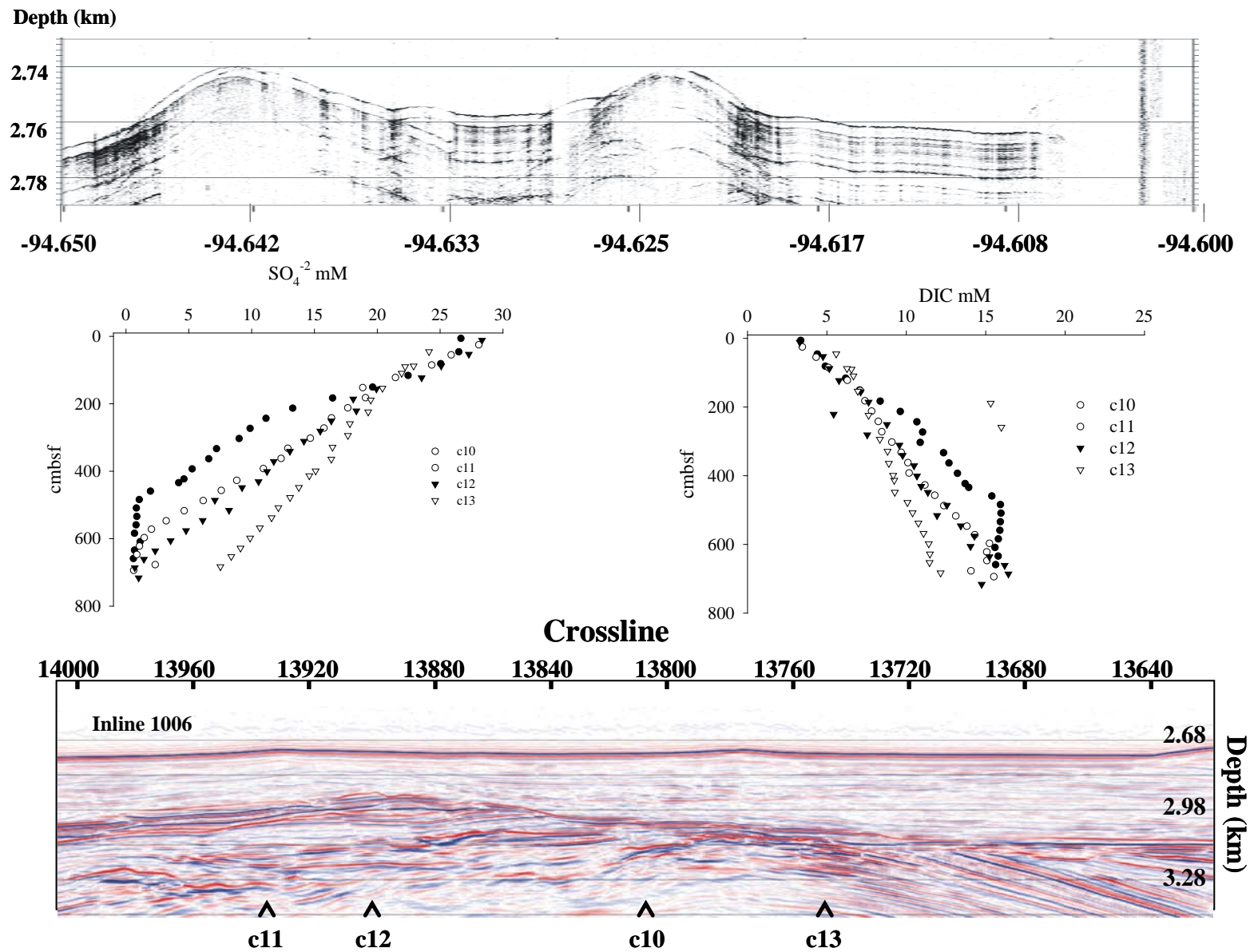


Figure 13: Piston core porewater sulfate and DIC profiles compared to shallow 3.5 kHz and deep inline 1006 seismic data. Porewater data are plotted separately for the sulfate and DIC concentrations.

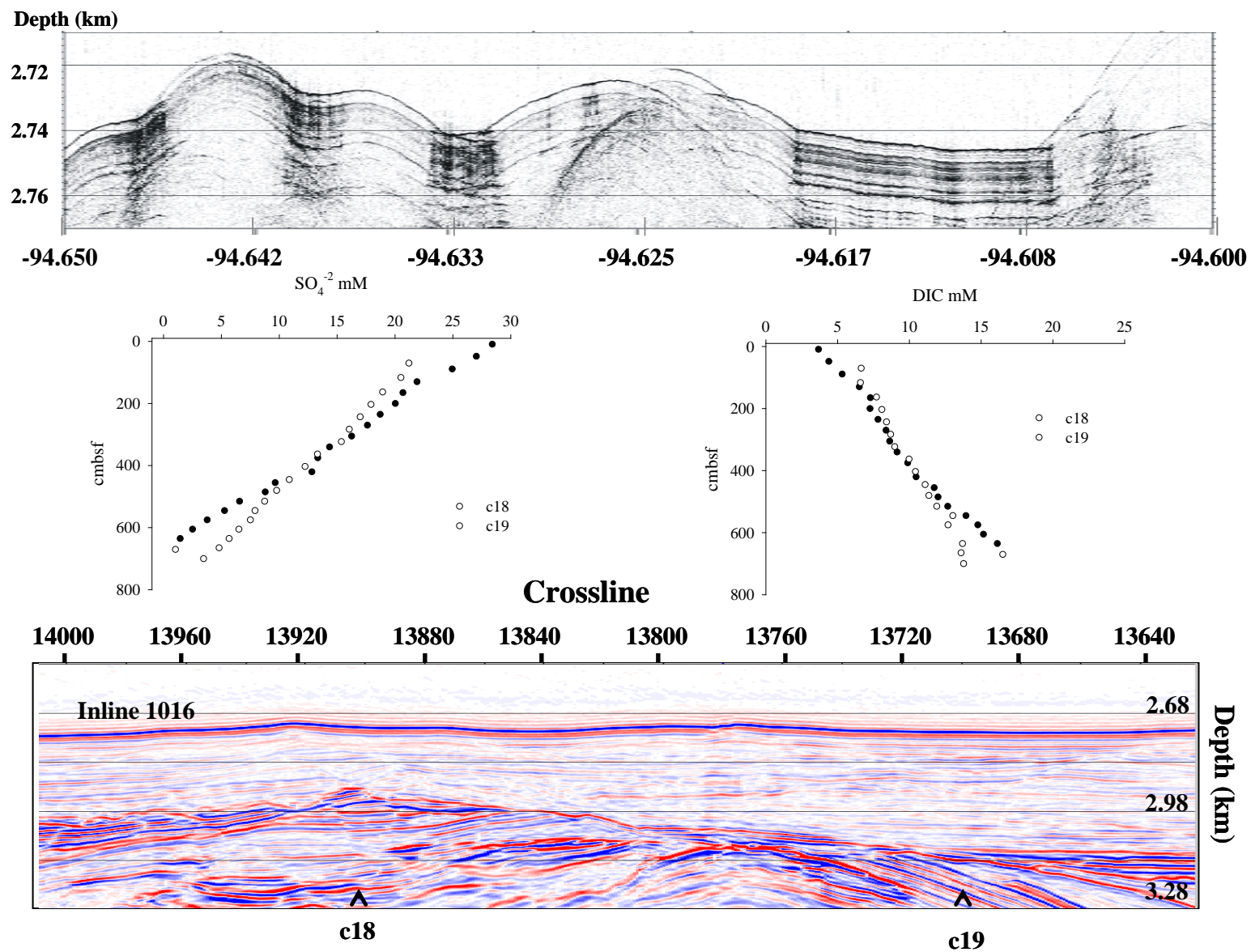


Figure 14: Piston core porewater sulfate and DIC profiles compared to shallow 3.5 kHz and deep inline 1016 seismic data. Porewater data are plotted separately for the sulfate and DIC concentrations.

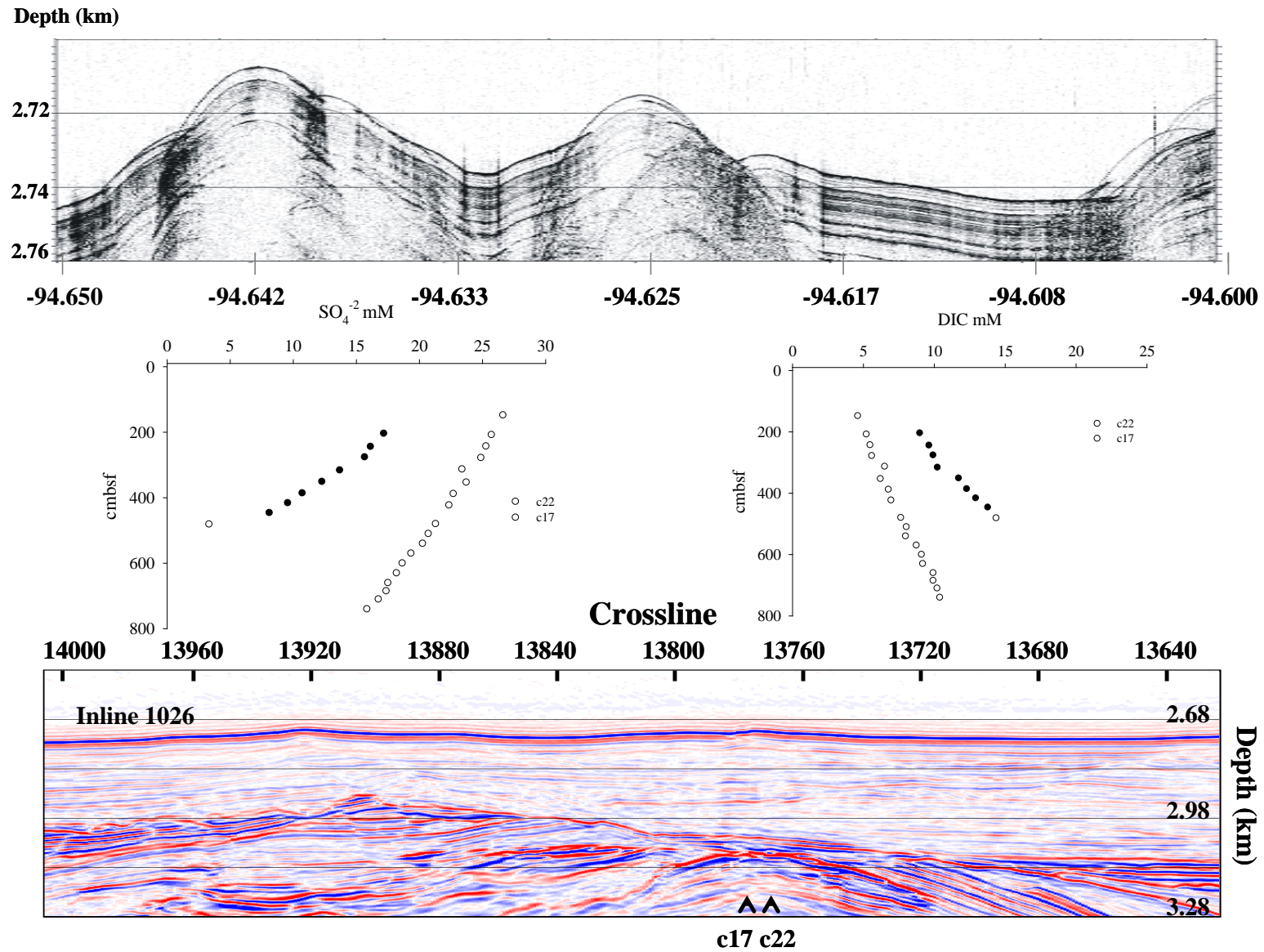


Figure 15: Piston core porewater sulfate and DIC profiles compared to shallow 3.5 kHz and deep inline 1026 seismic data. Porewater data are plotted separately for the sulfate and DIC concentrations.

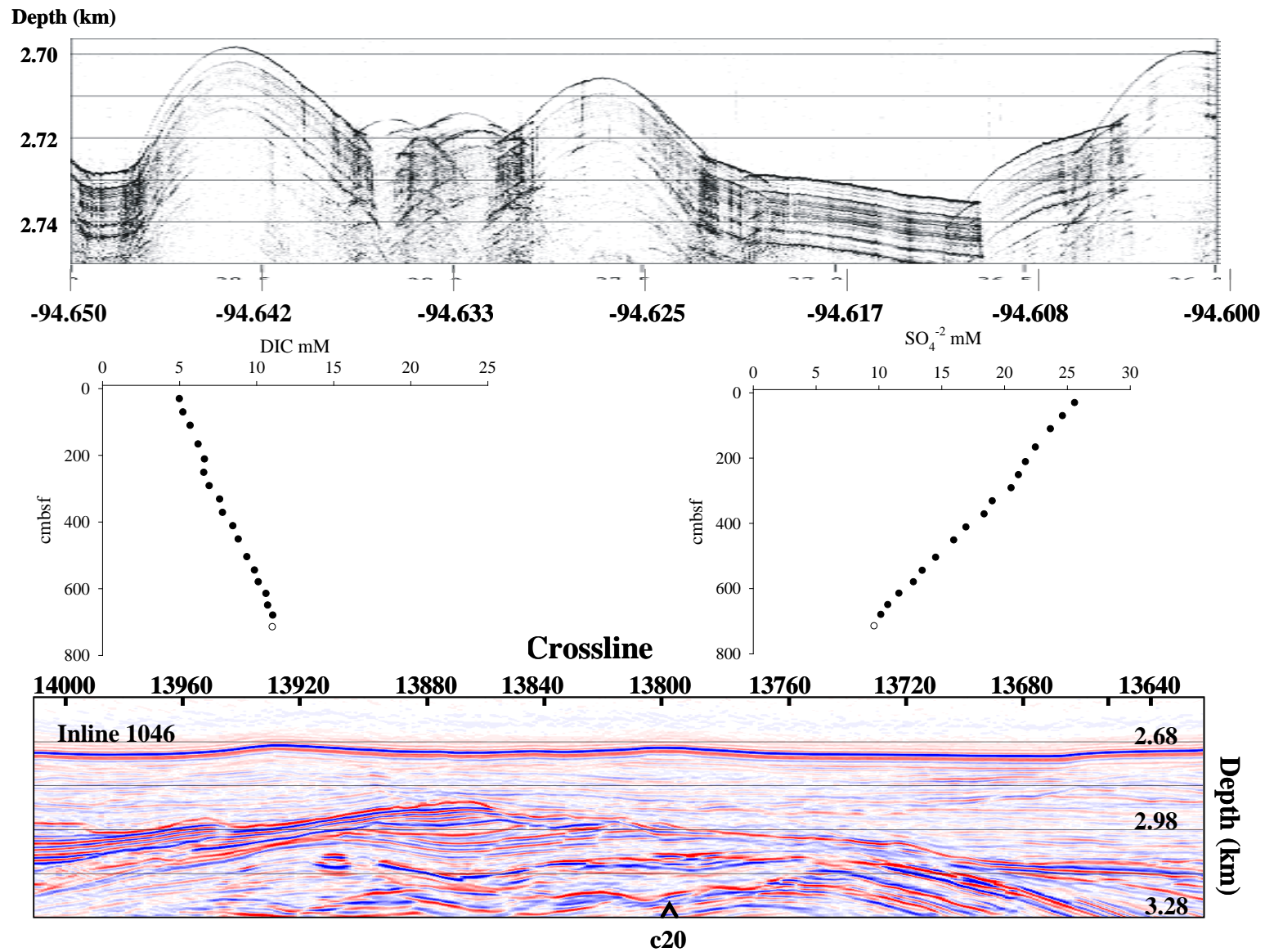


Figure 16: Piston core porewater sulfate and DIC profiles compared to shallow 3.5 kHz and deep inline 1046 seismic data. Porewater data are plotted separately for the sulfate and DIC concentrations.

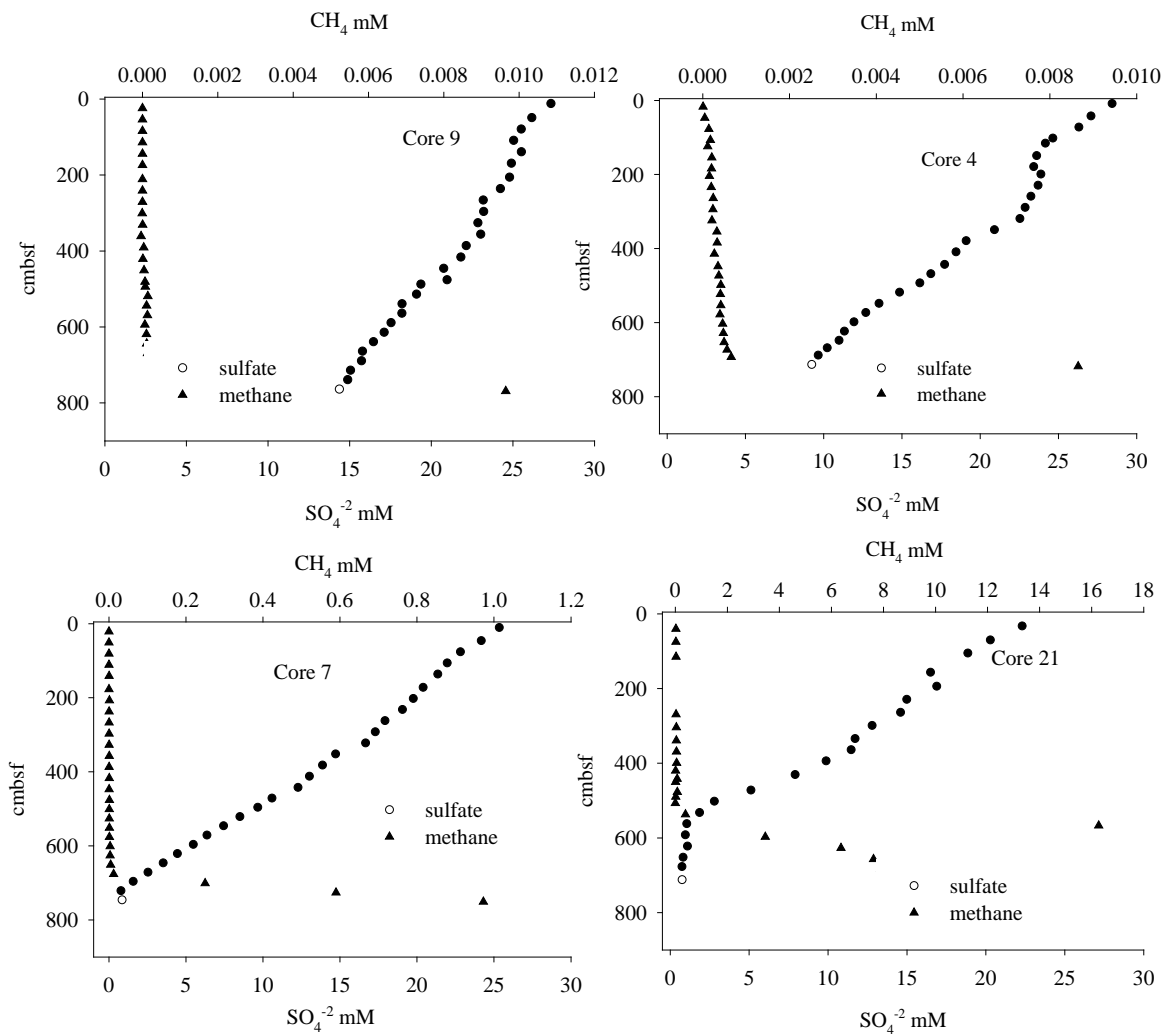
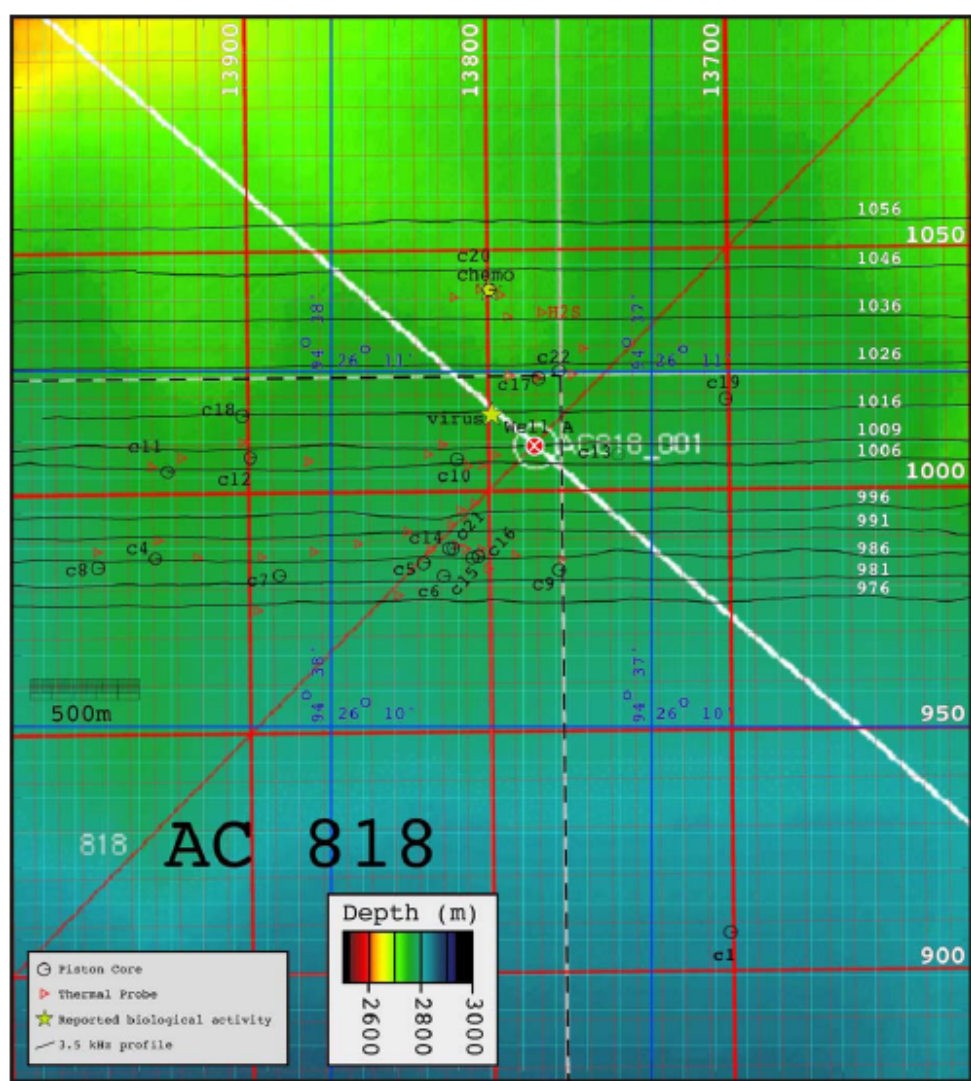


Figure 17: Selected porewater sulfate and sediment methane profiles to provide an overview of the spatial variation in profiles. Note the variation in the scaling of methane concentrations.

An overview of sediment porewater sulfate and methane profiles is presented in Figure 17. Cores taken most distal from the observed seismic blanking on crossline 13780 had the lowest sulfate gradient. In cores 4 and 9 the lowest porewater sulfate concentration was 9.32 mM and 14.4 mM in the deepest core subsample. Sediment headspace methane concentrations showed a slight increase in concentration at the similar depths. Toward crossline 13780, the slope in the sulfate concentration was substantially steeper and observed to have a significant increase in headspace methane concentrations at the depth of sulfate depletion. The concentration gradient profiles are generally linear, with the exception of a couple of potential outliers in mid core depths and a moderately concave down profile observed in core 10. The linear trend in the combined methane and sulfate profiles was used to estimate the SMI depths through the inlines. Where vertical methane diffusion was slower and sharp increases in the methane concentration did not coincide with sharp sulfate gradients, the slope of the sulfate profile was used to extrapolate the depth of sulfate depletion for calculation of the SMI.

A summary of the estimated SMI depths is presented in Figure 18. The SMI depths through the coring region ranged from 1793 cm to 308 cm. Shallow SMIs were measured in two different locations. In one region a shallow SMI was found to transition from west to east between the crosslines 13820 to 13770 and south to north from inlines 986 to 1026 where depths ranges from 308 cm to 589 cm (core 6 and core 22). The SMI in core 6 was an estimate because hydrates retrieved in this core resulted in watered sediments and a large variation in the porewater sulfate and methane profiles. Eastward of this line a rapid deepening of the SMI was observed with values ranging from 828 cm to 1550 cm for cores 19 and 9, respectively. Westward the SMI showed a rapid deep transition, with a value of 1628 cm for core 17, taken close to core 22. The line for predicted high vertical methane flux through the sample region was narrow moving northeast off of inline 986 up to inline 1026. The other region with a shallow SMI was along crossline 13900 where values were measured in a range of 761 cm to 672 cm for cores 7, 12 and 18. Westward from this crossline the SMI deepened with values ranging from 920 cm to 949 cm for cores 4 and 8.



| Core | SMI (cm) | R ² |
|------|----------|----------------|
| C1 | 633 | 0.899 |
| C4 | 920 | 0.981 |
| C5 | 800 | 0.98 |
| C6 | 308 | 0.805 |
| C7 | 761 | 0.993 |
| C8 | 949 | 0.973 |
| C9 | 1550 | 0.972 |
| C10 | 469 | 0.952 |
| C11 | 621 | 0.992 |
| C12 | 672 | 0.981 |
| C13 | 995 | 0.996 |
| C14 | 642 | 0.903 |
| C15 | 1793 | 0.94 |
| C16 | 1242 | 0.989 |
| C17 | 1628 | 0.992 |
| C18 | 679 | 0.994 |
| C19 | 828 | 0.997 |
| C20 | 1107 | 0.995 |
| C21 | 607 | 0.971 |
| C22 | 589 | 0.936 |

Figure 18: Sediment SMI depths calculated from sediment porewater profiles and core sites located on the inline and cross line points. Core 6 contained hydrates and showed a wide variation in the vertical porewater profiles.

C. Heat Flow Data Overview

Alaminos Canyon heat flow data were collected from inline 986 northward up to inline 1047 and from crossline 13960 eastward to crossline 13750 (Figure 19). The data range of vertical heat profiles for this survey was 36.8 mW m^{-2} to 54.6 mW m^{-2} . These data showed similar trends to the porewater shallow SMI with two distinct regions with higher thermal gradients. One elevated region was through on crossline 13900 where a maximum value was measured at 54.6 mW m^{-2} . The other region with an elevated thermal gradient was in the region of crossline 13800 where the values ranged from 48.7 mW m^{-2} to 54.6 mW m^{-2} . Higher heat flow values corresponded to the regions with shallow SMI. However, the range in heat flow data in this regions low relative to the data collected on Atwater Valley in the Gulf of Mexico where values were near 40 mW m^{-2} and maximum data up to 160 mW m^{-2} (Coffin et al., 2008).

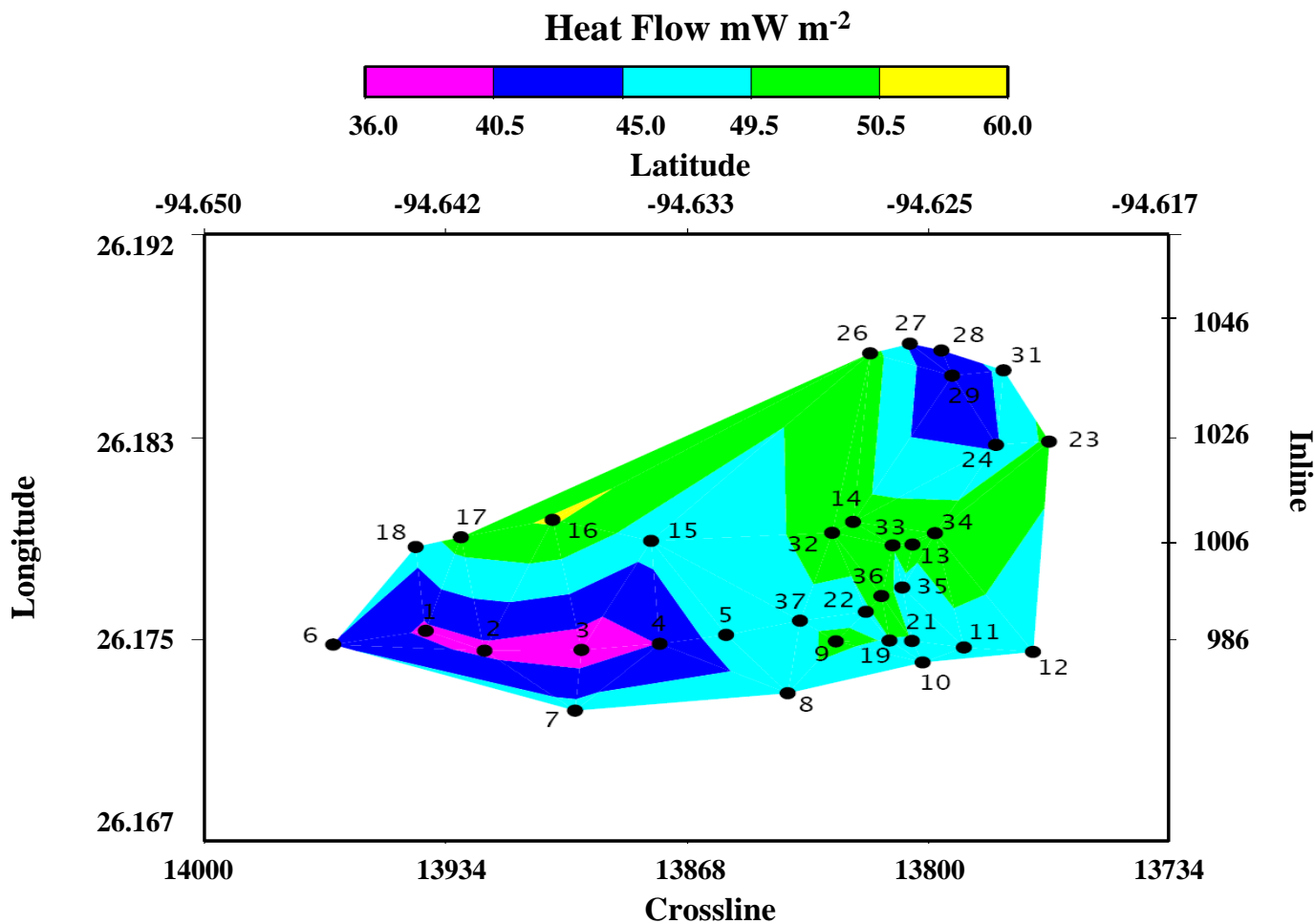


Figure 19: Geothermal gradients measured through crosslines from inline 986 up to inline 1046.

VII. SUMMARY

Geochemical and heat flow data are used to interpret the spatial variation in vertical methane fluxes in Alaminos Canyon Block 818. Goals of this fieldwork were to provide a hydrate pre-drilling data base, further develop calibration of shallow geochemical interpretation of deep seismic surveys of hydrate deposits, and continue basic research on the biogeochemical influence on shallow sediment methane cycling. The following points outline the results of the current data set and plans for further data interpretation.

1. Preliminary estimates of SMI depths for Alaminos Canyon are generally deeper than data collected in the Gulf of Mexico, mid Chilean Margin and off the coast of New Zealand. The water column depth at these other location ranged from 1100 to 1400 meters, while this study site was 2900 to 3000 meters. Further data interpretation of upward methane and downward sulfate gradients will consider the influence of water column depth pressure on the hydrate stability and vertical methane flux. This factor needs calibration for geochemical data interpretation between different coastal regions. Shallow SMI data were observed in regions with elevated heat flow and seismic signatures that indicated possible vertical fluid and/or gas fluxes. Sediment porosity will be analyzed to provide calculations of the vertical methane flux rates through the study region.
2. Heat flow ranged from 36.8 mW m^{-2} to 54.6 mW m^{-2} . These values were in the same range as low background data collected on Atwater Valley in the Gulf of Mexico. Regions with high vertical fluxes up to 160 mW m^{-2} in Atwater Valley were observed on top of a mound where high vertical methane fluxes were believed to result from deep sediment hydrate instability created by salt layers below the methane hydrate stability zone. Lower heat flow data on Atwater Valley were observed across a region off the mound with deep level BSR and deeper SMIs.
3. Stable carbon isotope and gas speciation analysis of porewater and sediment will be conducted to determine the gas source and cycling in this region.
4. Microbial community diversity will be surveyed through varying SMI depths in this study region. These data will be couple with comparisons of microbial community diversity off the coast of Chile, New Zealand and other location in the Gulf of Mexico.
5. Stable carbon isotope analysis in methane, dissolved inorganic carbon, and organic sediment carbon will be coupled with the percent organic carbon in the sediment to survey the contribution of methane to the shallow sediment carbon cycling.
6. A semi-quantitative data analysis will be conducted on the seismic profiles and compared with geochemical and heatflow data to assist in preliminary evaluation of the deep sediment methane hydrate deposits.
7. Future piston coring is being planned to approximately 1 km to the northeast of our study site. This will cover the hydrate drilling location.
8. Deep drill data sets will be compared with this data set for calibration of shallow sediment porewater data interpretation to survey deep sediment hydrate deposits.

Acknowledgements: This fieldwork was supported with funding from ONR Code 33, DOE-NETL, and NRL.

VIII. LITERATURE CITED

- Boehme, S. E., Blair, N. E., Chanton, J. P., Martens, C. S. 1996. A mass balance of ^{13}C and ^{12}C in an organic-rich methane-producing marine sediment. *Geochim. Cosmochim. Acta.* 60:3835-3848.
- Borowski, W. S., C. K. Paull, and W. Ussler III. 1999. Global and local variations of interstitial sulfate gradients in the deep-water, continental margin sediments: Sensitivity to underlying methane and gas hydrates. *Mar. Geol.* 159:131-154.
- Coffin, R. B., L. Hamdan, R. Plummer, J. Smith, J. Gardner, W. T. Wood. 2008. Analysis of Methane and Sulfate Flux in Methane Charged Sediments from the Mississippi Canyon, Gulf of Mexico. *Marine and Petroleum Geology* 25 (2008) 977–987
- Coffin, R B., Pohlman, J. W. Gardner, J., Downer, R., Wood, W., Hamdan, L., Walker, S., Plummer, R., Gettrust, J., Diaz, J. 2007. Methane Hydrate Exploration on the Mid Chilean Coast: A Geochemical and Geophysical Survey. *Am. Chem. Soc., Div. Pet. Chem.* doi:10.1016/j.petro.2006.01.013.
- Coffin, R., L. Hamdan, J. Pohlman, W. Wood, I. Pecher, S. Henrys, J. Greinert, K. Faure. 2007. Geochemical characterization of concentrated gas hydrate deposits on the Hikurangi Margin, New Zealand: Preliminary Geochemical Cruise Report. *NRL/MR/6110—07-9085.*
- Hornbach, M. J., C. Ruppel, and C. L. Van Dover 2007., Three-dimensional structure of fluid conduits sustaining an active deep marine cold seep, *Geophys. Res. Lett.*, 34, L05601, doi:10.1029/2006GL028859
- Meyer, D., L. Zarra. D. Rains, B. Meltz, and T. Hall. 2005. Emergence of the lower tertiary Wilcox Trend in the deepwater Gulf of Mexico. 2005. *Search and Discovery Article #10084.*
- Reeburgh, W. S. 1967. An improved interstitial water sampler. *Limnol. Oceanogr.* 12:163-165.

Appendix 1: Daily activity log.

23 July 2007

1. Researchers arrived to Ingleside Navy Base and started loading equipment on board the RV Cape Hatteras and installing instruments.
2. Labs were well setup by evening hours.
3. Plans were set to leave for Alaminos Canyon by 12:00 AM on 24 July.

24 July 2007

1. RV Cape Hatteras set for Alaminos Canyon by 13:15.
2. Lab instrument calibrations were set and all instruments were operating.
3. Wood and Coffin discussed the preliminary core site selection and steps for the first day on Alaminos Canyon. It was decided to run a preliminary shallow seismic profile on xx line 903 on Block 808 and xx line xxxxx. This would be followed by coring in a region selected for a control site. Heat flow was planned to be run across the same seismic line and correlated with the control geochemical data.
4. Discussions on piston core trigger depth (Bryant, Downer and Coffin) addressed wire stretching concerns to set trigger depth. The decision was made to set the trigger at 15 feet and measure piston core dead space for the next deployment.
5. Wire couple was set up and tested at 11,000 pound pull.
6. Piston core weight, barrels and sleeves were set up for morning use.

25 July 2007

1. On site at approximately 07:30.
2. First operation was a CTD to assist in calibration of heat flow and acoustics profiles. CTD deployed at 07:30.
3. Acoustics run at 12 and 3.5 kHz. These provide shallow sediment profiles over the core area. These data will be coupled with WesternGeco seismic profiles of the same region for a thorough observation of the core location. This selection of the background core was based on the BSR depth and shallow seismic profiles.
4. Piston core (core 1) was dropped at 11:30. Trigger wire was set at 15 ft. Wire was run to 100 meter and the acoustic depth profile was attached to the wire. Deployment was set at 60 m min⁻¹ to 100 m off the sediment floor and the rate was slowed to 10 m min⁻¹. The final core deployment site was set with observation of a relatively deep BSR and a level ocean floor. The deployment depth was in the range of 2800 to 2900 m.
5. Core return started at 12:37 on a 9300 pull out. Core length was 648 cm. Preliminary observation tan with a few black spots mid core depth. No hydrates no gas pockets.
6. Core barrel and liners were replaced and the winch wire was turned over for heat flow probing.
7. Core pulled wire coupling and the coupling had to be reset and tested. The testing held at 14,000 pound pull.
8. Set up for heat flow probing started at 15:00.

9. Seas picked up and stations could not be held for 20 minutes that are required for heat flow. It was decided to pick up on the acoustic profiles while the seas were rough.
10. Under hull bubbles interrupted the acoustic signatures. Activity was cancelled for the day. Plans for the next morning are heat flow if seas are lower. If not piston coring will be conducted.

26 July 2007

1. There were concerns about deploying the heat flow probes in the morning seas.. Piston coring was planned for a new site west of 818 (Core 2 on WG inline 986). During the coring deployment the core trigger was lost and with retrieval to the deck the messenger bar was bent. It was decided to repair the core system and wait for the seas to go down.
2. No further research was conducted on this day. While seas were not exceptionally rough. The crane setting on the back deck was subject to high rises in the raised seas.

27 July 2007

1. Seas still too high to run piston coring, acoustics and heat flow.
2. 12:15 PM seas dropped. Piston core was set up and deployed at 14:30.
3. Core 3 loss messenger mid way through. Upon early retrieval it was observed that the depth finder had been broken off the line. The safety cable saved the pinger. The trip anchor was maintained.
4. 2 80 pound torpedo anchor weights were deployed on the next core (core 4) at the same core location (2 and 3). This core trip with a 9700 lb pull at 7:05. Core was 718 cm. Kelly Rose took on providing geologic observation of the core segment that would not be saved. This was continuation of WG inline 986 and WG crossline 13815 (~).
5. Core 5 over at 9:30. Depth finder/position locator was included with this core.
6. Part of the shallow section of core 5 spilled on the deck. The total surface core section was 132 cm, 60 cm was estimated to be the spill section. This section was the bottom of the core liner. The total core length was 732 cm. Check the deck notes to confirm. The was continuation of WG inline 986 on WG crossline 13817 (~).
7. Core 5 was reported to have higher gas concentrations. The location of the core was off the set station by 250 meters. This station was located on the line and near the vertical seismic pattern. It was decided for core 6 to be on the intended core 5, vertical seismic pattern.
8. The piston core sleeves and barrels were set for the next morning.
9. Heat flow took over at 12:30 and was deployed at 2:00AM.

28 July 2007

1. Heat flow was returned to the deck at 7:30 am with 5 data sites acquired.
2. Piston core was set for core 6 (WG inline 986 and WG crossline 13817 (~)) on the seismic wipe out that was intended for core 5.
3. Core position was over at 10:45. Positioning took a long time a location was off by 50 m. The approach was to deploy the core while positioning and hold the last 10 m until on site. This protocol was not accurate. Ability to position differs between the ship drivers.

4. Core 6 was recovered at 11:45. On core recovery there was a large gas flux coming from the front of the core barrel. With the core sleeve removed on the deepest core section cold spots were felt and hydrates were observed. After cleaning the core sleeve large gas pockets were observed.
5. In addition to the normal porewater and sediment, core pocket gases, hydrates and hydrate gases were sampled.
6. The middle core sleeve collapsed and could not be removed from the core barrel. There was a large amount of compressed plastic in the barrel. The only samples were obtained from the deep core sleeve. No other samples were obtained.
7. Core 6 was located on WG inline 986 WG crossline 13817 (~).
8. The coring system was rebuilt and coring started again.
9. Prior to the next core acoustics was run again.
10. Core 7 went over at 14:00 this site was on the same line on a mound to the west along WG inline 986 WG crossline 13880 (~).
11. Core 7 was retrieved at 15:00. This was one of the longer cores at approximately 7.5 m.
12. The coring system was deployed for Core 8 at 7:00 at a site most western on the same seismic line, WG inline 986 WG crossline 13980 (~).
13. This was the last core for the day.
14. Following the core acoustics was run while the heat flow was prepared.
15. Acoustics was initiated at 23:00.

29 July 2007

1. Heat flow was back on deck and cables transferred for coring at 07:00.
2. Piston core C9 was started on WG inline 986 WG crossline 13765 (~).
3. at 08:30. Pull out 9300 lbs.
4. Piston core C9 out at 10:15. Good core, long grey no gas pockets
5. Piston core C10 over at 11:30 on WG inline 1006 crossline 13810 (~).
6. Core location was near the well 818.
7. Pull out for C10 at 12:35. 9700 lbs pull out.
8. Core 11 was deployed at 15:00 on WG inline 1006 WG crossline 13935 (~).
9. Core 11 pull out was lower at 8750 lb.
10. Core 12 was deployed at 18:30 on WG inline 1006 and crossline 13900 (~).
11. Acoustic profiles were run while the heat flow was set.
12. Heat flow was over at 23:00

30 July 2007

1. Heat flow heat pulse cable was damaged after first probe.
2. Heat flow was back on board by 7:00.
3. Damage to the heat flow probe is being checked for repair.
4. Core 13 was over at 08:30. WG inline 1006 and crossline 13735 (~). This site finishes the inline 1006 coring. Pull out 10406 lb. Over view in preliminary methane data was vertical methane diffusion at a moderate rate with methane profile slopes appearing between 4 and 7 mbsf.
5. Piston core up at 10:30.

6. Piston core 14 over at 11:15. Back on the Core 5 depression area. It is intended to take 2-3 more cores in this region to look at the vertical methane migration.
7. Pull out was above 10,000 lbs.
8. Piston core 14 back up at 13:30. Core contained small granular hydrates. This core was about 50 m away from the focus point where there are depressions on the seismic chart.
9. Piston core 15 was over at 14:30. Extra care was taken to drop the core on the focus point for the seismic chart. Pull out on this core was 10,108
10. This core imploded in the top two cylinders. The sediment retrieved was one barrel and was thought to be intact for this location. Two barrels were damaged beyond use.
11. Acoustic surveys were run during the core repair time.
12. A subsequent core, piston core 16 was taken at a nearby location to complete sampling in this region. This piston core was over at 20:00. Pull out on the core was 9352 lbs.
13. Core 16 was retrieved at 22:00. The core was over 6 m and small fragments of hydrates were observed through the core. In addition to the hydrates there was large vertical tube worms through the core. Discussion with Kelly Rose resulted in a comment that the tube worms had been observed in other cores. This needs to be considered in review of the sulfate profiles for non conservative mixing.
14. Heat flow was deployed at 23:00.

31 July 2007

1. Heat flow was up at 07:00. There was a problem with the data cable and the tow connection. Data was not acquired. This puts a need for rescheduling the cruise for more time on the heat flow probe.
2. Piston core 17 was over at 08:30. The coring region was north of the drill site at WG inline 1016 and crossline 13780 (~) This region was selected for coring because it provides more data around the JIP drill site 818.
3. Core 17 was back on the deck at 10:30. Retrieval of the core found broken liner pieces in the shallow segment. It is suspected that these liners are old and not in good condition.
4. Core 18 was taken at inline 1016, east of core 17 at xxxxxxx. Core over at 11:45.
5. Core 18 back on deck at 13:55. Upper core sleeve broke and needed to be replaced.
6. Core 19 was over at 15:15. It took 45 min to navigate to station. Pull on the retreat was 9300.
7. Core was back on deck at 17:00. High impact on the last segment of the core drop damaged the trigger arm.
8. Core 20 was over at 18:00. Pull on the retreat was 9154.
9. Discussions on the final coring were held and the focus area was decided to be down around Cores 5 and 6.
10. Core 20 was back on the deck at 20:15.
11. Heat flow was setup and deployed at 22:00.

1 August 2007

1. Heat flow was back on the deck at 08:00. Joan Gardner noted hydrogen sulfide odor on the heat flow probe. Changes in coring plan moved the final three cores north of the drill site.

2. Core 21 was deployed at 09:00. Core pull was 10,500 lb.
3. Core was returned to the deck at 11:00.
4. Core 22 site was located in the northeast corner of block 818. This core was set at 13:30.
5. Core 22 pull out was 9357 lbs.
6. Core was returned to the deck at 15:45. The core was collapsed in the second barrel. The core length through the second barrel was measured at 193cm. The collapse in the barrel resulted from poor core liners, aged in the sun.
7. Coring was cancelled at this point because of damage to the coring system and poor core liner quality.
8. Acoustic profiles were taken on new line while attempting to repair the core.
9. Heat flow started at 20:00.

APPENDIX 2: Preliminary porewater data.

| Core | Pore Water Sed Depth (cm) | Chloride (mM) | Sulfate (mM) | DIC (mM) | Gas Sample Sediment Depth (cm) | Gas Sample # | CH ₄ (mM) |
|------|---------------------------------|------------------|-----------------|----------|--------------------------------------|-----------------|----------------------|
| 1 | 643 | 540.9 | 1.13 | 13.98 | 648 | 1 | 0.0129 |
| 1 | 613 | 539.0 | 1.86 | 13.83 | 618 | 2 | 0.0053 |
| 1 | 583 | 537.4 | 8.89 | 11.04 | 588 | 3 | 0.0000 |
| 1 | 553 | 530.7 | 18.12 | 6.34 | 558 | 4 | 0.0000 |
| 1 | 523 | 526.2 | 15.35 | 7.61 | 528 | 5 | 0.0000 |
| 1 | 493 | 529.0 | 18.81 | 7.23 | 498 | 6 | 0.0000 |
| 1 | 463 | 536.0 | 19.85 | 6.87 | 468 | 7 | 0.0000 |
| 1 | 433 | 529.0 | 20.54 | 6.44 | 438 | 8 | 0.0000 |
| 1 | 403 | 534.3 | 21.04 | 6.46 | 408 | 9 | 0.0000 |
| 1 | 373 | 534.7 | 21.46 | 6.22 | 378 | 10 | 0.0000 |
| 1 | 339 | 535.9 | 22.09 | 5.62 | 344 | 11 | 0.0000 |
| 1 | 299 | 538.3 | 23.10 | 5.66 | 304 | 12 | 0.0000 |
| 1 | 259 | 529.0 | 24.04 | 5.10 | 264 | 13 | 0.0000 |
| 1 | 219 | 531.6 | 24.53 | 5.10 | 224 | 14 | 0.0000 |
| 1 | 179 | 538.9 | 25.66 | 4.55 | 184 | 15 | 0.0000 |
| 1 | 139 | 531.0 | 26.14 | 4.14 | 144 | 16 | 0.0000 |
| 1 | 99 | 537.4 | 27.23 | 3.82 | 104 | 17 | 0.0000 |
| 1 | 51 | 535.4 | 28.10 | 3.38 | 64 | 18 | 0.0000 |
| 1 | 27 | 540.0 | 28.57 | 3.23 | 37 | 19 | 0.0000 |
| 4 | 713 | 564.6 | 9.24 | 11.15 | 718 | 20 | 0.0087 |
| 4 | 688 | 561.9 | 9.65 | 11.11 | 693 | 21 | 0.0007 |
| 4 | 668 | 564.9 | 10.22 | 10.60 | 673 | 22 | 0.0006 |
| 4 | 648 | 566.9 | 10.98 | 10.48 | 653 | 23 | 0.0005 |
| 4 | 623 | 561.3 | 11.32 | 10.19 | 628 | 24 | 0.0005 |
| 4 | 598 | 561.0 | 11.93 | 10.20 | 603 | 25 | 0.0005 |
| 4 | 573 | 561.9 | 12.69 | 9.61 | 578 | 26 | 0.0004 |
| 4 | 548 | 560.7 | 13.53 | 9.48 | 553 | 27 | 0.0004 |
| 4 | 518 | 562.4 | 14.85 | 8.95 | 523 | 28 | 0.0004 |
| 4 | 493 | 562.9 | 16.15 | 8.35 | 498 | 29 | 0.0004 |
| 4 | 468 | 562.3 | 16.85 | 8.19 | 473 | 30 | 0.0004 |
| 4 | 443 | 566.9 | 17.73 | 7.68 | 448 | 31 | 0.0004 |
| 4 | 409 | 564.3 | 18.45 | 7.16 | 414 | 32 | 0.0003 |
| 4 | 379 | 570.9 | 19.10 | 7.42 | 384 | 33 | 0.0003 |
| 4 | 349 | 571.7 | 20.91 | 6.72 | 354 | 34 | 0.0003 |
| 4 | 319 | 571.1 | 22.54 | 6.07 | 324 | 35 | 0.0002 |
| 4 | 289 | 570.8 | 22.87 | 5.84 | 294 | 36 | 0.0002 |
| 4 | 259 | 569.9 | 23.24 | 5.81 | 264 | 37 | 0.0002 |
| 4 | 229 | 568.3 | 23.70 | 5.47 | 234 | 38 | 0.0002 |

| | | | | | | | |
|---|-----|-------|-------|-------|-----|----|---------|
| 4 | 199 | 566.9 | 23.88 | 5.33 | 204 | 39 | 0.0002 |
| 4 | 179 | 566.1 | 23.42 | 5.75 | 184 | 40 | 0.0002 |
| 4 | 149 | 565.1 | 23.61 | 5.69 | 154 | 41 | 0.0002 |
| 4 | 116 | 568.0 | 24.17 | 5.62 | 124 | 42 | 0.0001 |
| 4 | 102 | 566.6 | 24.65 | 5.26 | 107 | 43 | 0.0002 |
| 4 | 72 | 559.3 | 26.31 | 4.44 | 77 | 44 | 0.0001 |
| 4 | 42 | 555.1 | 27.08 | 3.76 | 47 | 45 | 0.0000 |
| 4 | 9 | 562.2 | 28.43 | 3.07 | 17 | 46 | 0.0000 |
| 5 | 751 | 559.3 | 1.75 | 15.46 | 756 | 47 | 0.0313 |
| 5 | 726 | 572.6 | 3.04 | 14.38 | 731 | 48 | 0.0052 |
| 5 | 701 | 569.5 | 4.22 | 13.95 | 706 | 49 | 0.0023 |
| 5 | 676 | 573.3 | 5.21 | 13.61 | 681 | 50 | 0.0016 |
| 5 | 651 | 567.4 | 6.07 | 13.14 | 656 | 51 | 0.0010 |
| 5 | 626 | 564.2 | 6.80 | 12.83 | 631 | 52 | 0.0008 |
| 5 | 601 | 569.0 | 7.62 | 13.07 | 606 | 53 | 0.0006 |
| 5 | 576 | 566.4 | 8.67 | 11.85 | 581 | 54 | 0.0007 |
| 5 | 551 | 570.9 | 9.61 | 11.30 | 556 | 55 | 0.0006 |
| 5 | 526 | 573.1 | 10.40 | 11.22 | 531 | 56 | 0.0005 |
| 5 | 501 | 564.4 | 11.50 | 10.54 | 506 | 57 | 0.0005 |
| 5 | 476 | 574.2 | 12.54 | 10.20 | 481 | 58 | 0.0004 |
| 5 | 442 | 577.1 | 13.66 | 9.84 | 447 | 59 | 0.0004 |
| 5 | 417 | 586.4 | 14.18 | 9.71 | 422 | 60 | 0.0004 |
| 5 | 392 | 582.1 | 14.55 | 9.50 | 397 | 61 | 0.0003 |
| 5 | 367 | 575.3 | 15.59 | 9.25 | 372 | 62 | 0.0004 |
| 5 | 342 | 573.1 | 15.98 | 8.66 | 347 | 63 | 0.0004 |
| 5 | 317 | 573.4 | 17.41 | 8.20 | 322 | 64 | 0.0004 |
| 5 | 287 | 572.6 | 17.86 | 8.14 | 292 | 65 | 0.0004 |
| 5 | 257 | 565.9 | 18.47 | 7.68 | 262 | 66 | 0.0004 |
| 5 | 227 | 563.9 | 19.54 | 7.33 | 232 | 67 | 0.0003 |
| 5 | 197 | 549.8 | 20.99 | 6.66 | 202 | 68 | 0.0002 |
| 5 | 167 | 573.2 | 23.24 | 6.06 | 172 | 69 | 0.0002 |
| 5 | 74 | 562.8 | 27.20 | 4.10 | 79 | 70 | 0.0001 |
| 5 | 42 | 566.3 | 28.37 | 3.38 | 49 | 71 | 0.0000 |
| 6 | 299 | 461.6 | 1.19 | 17.53 | 304 | 72 | 11.9115 |
| 6 | 279 | 436.8 | 0.77 | 16.52 | 284 | 73 | 18.5136 |
| 6 | 259 | 500.7 | 0.74 | 17.87 | 264 | 74 | 8.4550 |
| 6 | 239 | 469.0 | 0.76 | 17.36 | 244 | 75 | 10.4520 |
| 6 | 219 | 501.0 | 0.75 | 18.26 | 224 | 76 | 21.3354 |
| 6 | 199 | 502.1 | 1.22 | 18.37 | 204 | 77 | 8.8222 |
| 6 | 154 | 489.5 | 0.89 | 17.11 | 159 | 78 | 5.1528 |
| 6 | 134 | 478.3 | 0.77 | 17.78 | 139 | 79 | 10.1720 |
| 6 | 114 | 449.2 | 0.87 | 16.42 | 119 | 80 | 7.1275 |

| | | | | | | | |
|---|-----|-------|-------|-------|-----|-----|--------|
| 6 | 69 | 465.1 | 1.11 | 16.76 | 74 | 81 | 7.9333 |
| 6 | 49 | 464.1 | 3.50 | 16.84 | 54 | 82 | 6.8548 |
| 6 | 29 | 474.7 | 5.55 | 16.54 | 34 | 83 | 8.9910 |
| 6 | 7 | 389.7 | 5.04 | 14.03 | 14 | 84 | 2.0176 |
| 7 | 746 | 576.8 | 0.85 | 15.57 | 751 | 85 | 0.9724 |
| 7 | 721 | 572.5 | 0.78 | 15.75 | 726 | 86 | 0.5898 |
| 7 | 696 | 569.1 | 1.57 | 15.23 | 701 | 87 | 0.2496 |
| 7 | 671 | 567.4 | 2.54 | 14.34 | 676 | 88 | 0.0120 |
| 7 | 646 | 570.4 | 3.52 | 13.97 | 651 | 89 | 0.0046 |
| 7 | 621 | 567.7 | 4.44 | 13.54 | 626 | 90 | 0.0031 |
| 7 | 596 | 569.0 | 5.47 | 12.99 | 601 | 91 | 0.0031 |
| 7 | 571 | 565.2 | 6.36 | 12.62 | 576 | 92 | 0.0012 |
| 7 | 546 | 564.4 | 7.44 | 12.09 | 551 | 93 | 0.0012 |
| 7 | 521 | 559.0 | 8.50 | 11.33 | 526 | 94 | 0.0009 |
| 7 | 496 | 562.1 | 9.66 | 11.10 | 501 | 95 | 0.0007 |
| 7 | 471 | 559.7 | 10.58 | 10.57 | 476 | 96 | 0.0013 |
| 7 | 442 | 566.7 | 12.27 | 9.85 | 447 | 97 | 0.0006 |
| 7 | 412 | 561.8 | 13.01 | 9.55 | 417 | 98 | 0.0008 |
| 7 | 382 | 559.3 | 13.87 | 9.20 | 387 | 99 | 0.0006 |
| 7 | 352 | 557.3 | 14.71 | 8.89 | 357 | 100 | 0.0006 |
| 7 | 322 | 561.4 | 16.66 | 8.25 | 327 | 101 | 0.0004 |
| 7 | 292 | 557.4 | 17.29 | 7.81 | 297 | 102 | 0.0005 |
| 7 | 262 | 556.2 | 17.92 | 7.61 | 267 | 103 | 0.0004 |
| 7 | 232 | 559.0 | 19.05 | 7.21 | 237 | 104 | 0.0003 |
| 7 | 202 | 558.6 | 19.76 | 6.99 | 207 | 105 | 0.0011 |
| 7 | 172 | 555.4 | 20.39 | 6.79 | 177 | 106 | 0.0001 |
| 7 | 136 | 554.3 | 21.35 | 6.00 | 141 | 107 | 0.0004 |
| 7 | 106 | 552.5 | 21.96 | 5.97 | 111 | 108 | 0.0001 |
| 7 | 76 | 549.5 | 22.82 | 2.31 | 81 | 109 | 0.0002 |
| 7 | 46 | 554.1 | 24.17 | 1.84 | 51 | 110 | 0.0002 |
| 7 | 11 | 556.9 | 25.35 | 3.67 | 21 | 111 | 0.0001 |
| 8 | 746 | 565.3 | 5.40 | 4.96 | 751 | 112 | 0.0008 |
| 8 | 709 | 563.0 | 6.26 | 4.90 | 576 | 113 | 0.0000 |
| 8 | 684 | 563.7 | 7.02 | 10.14 | 551 | 114 | 0.0001 |
| 8 | 659 | 562.5 | 7.65 | 9.32 | 526 | 115 | 0.0000 |
| 8 | 634 | 570.4 | 8.42 | 9.02 | 501 | 116 | 0.0007 |
| 8 | 609 | 567.2 | 9.03 | 8.98 | 476 | 117 | 0.0005 |
| 8 | 584 | 568.8 | 9.86 | 9.37 | 451 | 118 | 0.0002 |
| 8 | 559 | 568.5 | 10.49 | 11.10 | 426 | 119 | 0.0000 |
| 8 | 534 | 577.3 | 12.32 | 10.75 | 401 | 120 | 0.0000 |
| 8 | 509 | 572.8 | 13.15 | 10.54 | 376 | 121 | 0.0002 |
| 8 | 484 | 553.9 | 12.57 | 10.05 | 351 | 122 | 0.0001 |

| | | | | | | | |
|---|-----|-------|-------|-------|-----|-----|--------|
| 8 | 455 | 554.4 | 13.77 | 10.17 | 326 | 123 | 0.0002 |
| 8 | 440 | 556.8 | 13.81 | 9.38 | 445 | 124 | 0.0003 |
| 8 | 410 | 568.6 | 10.89 | 9.18 | 415 | 125 | 0.0003 |
| 8 | 380 | 570.0 | 14.88 | 8.74 | 385 | 126 | 0.0001 |
| 8 | 350 | 570.4 | 16.04 | 6.85 | 355 | 127 | 0.0001 |
| 8 | 320 | 569.4 | 16.96 | 7.61 | 325 | 128 | 0.0001 |
| 8 | 290 | 572.5 | 17.50 | 8.10 | 295 | 129 | 0.0000 |
| 8 | 260 | 568.5 | 18.71 | 7.78 | 265 | 130 | 0.0000 |
| 8 | 230 | 569.0 | 19.52 | 7.63 | 235 | 131 | 0.0000 |
| 8 | 200 | 571.6 | 20.25 | 7.29 | 205 | 132 | 0.0000 |
| 8 | 170 | 576.5 | 21.57 | 6.72 | 175 | 133 | 0.0000 |
| 8 | 133 | 572.0 | 21.52 | 7.03 | 138 | 134 | 0.0000 |
| 8 | 103 | 562.9 | 21.98 | 6.43 | 108 | 135 | 0.0000 |
| 8 | 73 | 574.7 | 22.99 | 6.04 | 78 | 136 | 0.0000 |
| 8 | 43 | 576.4 | 23.75 | 6.02 | 48 | 137 | 0.0000 |
| 8 | 9 | 572.8 | 24.55 | 5.52 | 18 | 138 | 0.0000 |
| 9 | 764 | 581.2 | 14.37 | 9.61 | 769 | 139 | 0.0096 |
| 9 | 739 | 580.7 | 14.88 | 9.34 | 744 | 140 | 0.0005 |
| 9 | 714 | 576.2 | 15.05 | 9.36 | 719 | 141 | 0.0002 |
| 9 | 689 | 585.2 | 15.73 | 9.23 | 694 | 142 | 0.0005 |
| 9 | 664 | 565.5 | 15.78 | 8.92 | 669 | 143 | 0.0001 |
| 9 | 639 | 569.7 | 16.46 | 8.90 | 644 | 144 | 0.0001 |
| 9 | 614 | 580.9 | 17.11 | 8.66 | 619 | 145 | 0.0001 |
| 9 | 589 | 579.5 | 17.54 | 8.64 | 594 | 146 | 0.0001 |
| 9 | 564 | 581.5 | 18.20 | 8.22 | 569 | 147 | 0.0001 |
| 9 | 539 | 565.9 | 18.21 | 8.16 | 544 | 148 | 0.0001 |
| 9 | 514 | 578.4 | 19.09 | 8.07 | 519 | 149 | 0.0001 |
| 9 | 488 | 576.9 | 19.37 | 7.76 | 494 | 150 | 0.0001 |
| 9 | 476 | 577.5 | 20.97 | 6.75 | 481 | 151 | 0.0001 |
| 9 | 446 | 572.1 | 20.76 | 5.86 | 451 | 152 | 0.0000 |
| 9 | 416 | 586.9 | 21.82 | 6.00 | 421 | 153 | 0.0000 |
| 9 | 386 | 594.5 | 22.14 | 6.44 | 391 | 154 | 0.0000 |
| 9 | 356 | 591.7 | 23.03 | 4.67 | 361 | 155 | 0.0000 |
| 9 | 326 | 588.5 | 22.86 | 6.37 | 331 | 156 | 0.0000 |
| 9 | 296 | 583.9 | 23.21 | 4.67 | 301 | 157 | 0.0000 |
| 9 | 266 | 569.0 | 23.18 | 6.00 | 271 | 158 | 0.0000 |
| 9 | 236 | 582.2 | 24.24 | 6.17 | 241 | 159 | 0.0000 |
| 9 | 206 | 586.5 | 24.79 | 5.93 | 211 | 160 | 0.0000 |
| 9 | 169 | 575.0 | 24.91 | 5.83 | 174 | 161 | 0.0000 |
| 9 | 139 | 580.7 | 25.52 | 5.60 | 144 | 162 | 0.0000 |
| 9 | 109 | 559.9 | 25.05 | 5.42 | 114 | 163 | 0.0000 |
| 9 | 79 | 559.5 | 25.51 | 4.93 | 84 | 164 | 0.0000 |

| | | | | | | | |
|----|-----|-------|-------|-------|-----|-----|--------|
| 9 | 49 | 560.1 | 26.15 | 4.62 | 54 | 165 | 0.0000 |
| 9 | 12 | 571.3 | 27.33 | 4.17 | 24 | 166 | 0.0000 |
| 10 | 694 | 584.8 | 0.62 | 15.51 | 699 | 167 | 0.7100 |
| 10 | 659 | 541.6 | 0.59 | 15.63 | 664 | 168 | 5.0524 |
| 10 | 634 | 542.5 | 0.68 | 15.79 | 639 | 169 | 4.4507 |
| 10 | 609 | 542.1 | 1.12 | 15.59 | 614 | 170 | 3.6210 |
| 10 | 584 | 540.2 | 0.68 | 15.80 | 589 | 171 | 1.8999 |
| 10 | 559 | 539.2 | 0.80 | 15.89 | 564 | 172 | 1.7553 |
| 10 | 534 | 538.3 | 0.86 | 15.92 | 539 | 173 | 1.4108 |
| 10 | 509 | 541.4 | 0.83 | 15.96 | 514 | 174 | 1.0109 |
| 10 | 484 | 539.6 | 1.06 | 15.93 | 489 | 175 | 0.3789 |
| 10 | 459 | 535.9 | 1.95 | 15.39 | 464 | 176 | 0.0962 |
| 10 | 434 | 539.9 | 4.19 | 13.93 | 439 | 177 | 0.0465 |
| 10 | 423 | 540.2 | 4.62 | 13.70 | 428 | 178 | 0.1025 |
| 10 | 393 | 534.0 | 5.27 | 13.22 | 398 | 179 | 0.0037 |
| 10 | 363 | 542.5 | 6.59 | 12.69 | 368 | 180 | 0.0018 |
| 10 | 333 | 528.7 | 7.21 | 12.35 | 338 | 181 | 0.0007 |
| 10 | 303 | 534.5 | 9.00 | 10.88 | 308 | 182 | 0.0006 |
| 10 | 273 | 561.3 | 9.88 | 11.03 | 278 | 183 | 0.0004 |
| 10 | 243 | 561.8 | 11.14 | 10.67 | 248 | 184 | 0.0005 |
| 10 | 213 | 559.7 | 13.27 | 9.62 | 218 | 185 | 0.0005 |
| 10 | 183 | 561.3 | 16.45 | 8.36 | 188 | 186 | 0.0002 |
| 10 | 151 | 564.5 | 19.63 | 7.07 | 158 | 187 | 0.0002 |
| 10 | 116 | 570.4 | 22.45 | 6.18 | 121 | 188 | 0.0004 |
| 10 | 81 | 564.7 | 25.05 | 4.90 | 86 | 189 | 0.0000 |
| 10 | 46 | 564.5 | 26.49 | 4.40 | 51 | 190 | 0.0000 |
| 10 | 6 | 538.8 | 26.65 | 3.35 | 11 | 191 | 0.0000 |
| 11 | 677 | 561.8 | 2.33 | 14.07 | 687 | 192 | 2.1652 |
| 11 | 647 | 567.1 | 0.86 | 15.08 | 652 | 193 | 1.6734 |
| 11 | 622 | 570.0 | 1.07 | 15.07 | 627 | 194 | 0.8856 |
| 11 | 597 | 581.5 | 1.45 | 15.24 | 602 | 195 | 0.1962 |
| 11 | 572 | 561.6 | 2.03 | 14.31 | 577 | 196 | 0.0000 |
| 11 | 547 | 562.5 | 3.20 | 13.81 | 552 | 197 | 0.0044 |
| 11 | 517 | 572.5 | 4.64 | 13.12 | 522 | 198 | 0.0014 |
| 11 | 487 | 567.1 | 6.15 | 12.37 | 492 | 199 | 0.0005 |
| 11 | 457 | 576.3 | 7.58 | 11.79 | 462 | 200 | 0.0004 |
| 11 | 427 | 566.7 | 8.82 | 11.17 | 432 | 201 | 0.0003 |
| 11 | 392 | 574.0 | 10.93 | 10.18 | 397 | 202 | 0.0002 |
| 11 | 362 | 574.1 | 12.35 | 10.10 | 367 | 203 | 0.0001 |
| 11 | 332 | 574.0 | 12.88 | 9.68 | 337 | 204 | 0.0002 |
| 11 | 302 | 585.2 | 14.67 | 9.09 | 307 | 205 | 0.0001 |
| 11 | 272 | 579.5 | 15.76 | 8.46 | 277 | 206 | 0.0001 |

| | | | | | | | |
|----|-----|-------|-------|-------|-----|-----|---------|
| 11 | 242 | 568.2 | 16.36 | 8.24 | 247 | 207 | 0.0000 |
| 11 | 212 | 583.2 | 17.65 | 7.82 | 217 | 208 | 0.0000 |
| 11 | 182 | 575.5 | 19.06 | 7.40 | 187 | 209 | 0.0000 |
| 11 | 152 | 547.7 | 18.84 | 7.10 | 157 | 210 | 0.0000 |
| 11 | 122 | 568.3 | 21.45 | 6.29 | 127 | 211 | 0.0000 |
| 11 | 85 | 567.4 | 24.33 | 5.10 | 90 | 212 | 0.0000 |
| 11 | 55 | 562.0 | 25.88 | 4.32 | 60 | 213 | 0.0000 |
| 11 | 25 | 561.7 | 28.08 | 3.45 | 30 | 214 | 0.0000 |
| 12 | 716 | 561.9 | 1.01 | 14.75 | 726 | 215 | 1.8659 |
| 12 | 686 | 561.7 | 0.70 | 16.43 | 691 | 216 | 0.5440 |
| 12 | 661 | 560.5 | 1.43 | 16.20 | 666 | 217 | 0.0096 |
| 12 | 636 | 552.9 | 2.33 | 15.23 | 641 | 218 | 0.0029 |
| 12 | 606 | 557.2 | 3.55 | 14.05 | 611 | 219 | -0.0011 |
| 12 | 576 | 559.4 | 4.78 | 14.29 | 581 | 220 | 0.0009 |
| 12 | 546 | 566.3 | 6.11 | 13.43 | 551 | 221 | 0.0005 |
| 12 | 516 | 569.7 | 8.21 | 11.94 | 521 | 222 | 0.0002 |
| 12 | 486 | 560.8 | 7.07 | 12.56 | 491 | 223 | 0.0002 |
| 12 | 449 | 560.3 | 9.24 | 11.36 | 461 | 224 | 0.0001 |
| 12 | 431 | 569.6 | 10.55 | 10.94 | 436 | 225 | 0.0002 |
| 12 | 401 | 568.6 | 11.22 | 10.67 | 406 | 226 | 0.0001 |
| 12 | 371 | 556.4 | 11.76 | 10.49 | 376 | 227 | 0.0001 |
| 12 | 341 | 572.0 | 13.05 | 9.77 | 346 | 228 | 0.0000 |
| 12 | 311 | 567.2 | 14.16 | 9.57 | 316 | 229 | 0.0000 |
| 12 | 281 | 575.8 | 15.46 | 7.54 | 286 | 230 | 0.0000 |
| 12 | 251 | 571.0 | 16.34 | 8.78 | 256 | 231 | 0.0000 |
| 12 | 221 | 592.4 | 18.33 | 5.43 | 226 | 232 | 0.0000 |
| 12 | 186 | 563.1 | 18.09 | 7.63 | 191 | 233 | 0.0000 |
| 12 | 156 | 562.6 | 19.94 | 7.13 | 161 | 234 | 0.0000 |
| 12 | 123 | 574.9 | 23.53 | 5.77 | 128 | 235 | 0.0000 |
| 12 | 88 | 568.1 | 25.08 | 5.16 | 93 | 236 | 0.0000 |
| 12 | 53 | 568.3 | 27.29 | 4.76 | 58 | 237 | 0.0000 |
| 12 | 12 | 572.2 | 28.34 | 3.29 | 23 | 238 | 0.0000 |
| 13 | 683 | 568.5 | 7.52 | 12.16 | 693 | 239 | 0.0007 |
| 13 | 653 | 559.7 | 8.38 | 11.47 | 658 | 240 | 0.0005 |
| 13 | 628 | 555.4 | 9.11 | 11.49 | 633 | 241 | 0.0006 |
| 13 | 598 | 555.8 | 9.88 | 11.42 | 603 | 242 | 0.0004 |
| 13 | 568 | 558.3 | 10.65 | 11.09 | 573 | 243 | 0.0003 |
| 13 | 538 | 566.2 | 11.59 | 10.76 | 543 | 244 | 0.0003 |
| 13 | 508 | 555.0 | 12.13 | 10.40 | 513 | 245 | 0.0000 |
| 13 | 478 | 565.6 | 13.06 | 10.07 | 483 | 246 | 0.0001 |
| 13 | 448 | 560.5 | 13.76 | 9.28 | 453 | 247 | 0.0001 |
| 13 | 414 | 556.9 | 14.59 | 9.24 | 423 | 248 | 0.0001 |

| | | | | | | | |
|----|-----|-------|-------|-------|--------|-----|----------|
| 13 | 399 | 563.8 | 15.09 | 9.17 | 404 | 249 | 0.0000 |
| 13 | 364 | 579.1 | 16.34 | 8.90 | 369 | 250 | 0.0001 |
| 13 | 329 | 555.5 | 16.44 | 8.82 | 334.00 | 251 | 0.0001 |
| 13 | 294 | 556.6 | 17.67 | 8.34 | 299.00 | 252 | 0.0000 |
| 13 | 259 | 554.2 | 17.82 | 15.99 | 264 | 253 | 0.0000 |
| 13 | 224 | 566.9 | 19.28 | 7.63 | 229 | 254 | 0.0000 |
| 13 | 189 | 555.5 | 19.48 | 15.32 | 194 | 255 | 0.0000 |
| 13 | 154 | 564.6 | 20.41 | 6.95 | 159 | 256 | 0.0000 |
| 13 | 110 | 581.3 | 21.94 | 6.67 | 124 | 257 | 0.0000 |
| 13 | 90 | 579.7 | 22.22 | 6.55 | 95 | 258 | 0.0000 |
| 13 | 88 | 575.8 | 22.89 | 6.27 | 93 | 259 | 0.0000 |
| 13 | 46 | 569.3 | 24.12 | 5.59 | 58.00 | 260 | 0.0000 |
| 14 | 691 | 559.8 | 4.87 | 16.28 | 701.00 | 261 | 7.6381 |
| 14 | 661 | 559.5 | 0.92 | 19.68 | 666 | 262 | 6.4755 |
| 14 | 636 | 559.7 | 0.96 | 19.94 | 641 | 263 | 5.3893 |
| 14 | 611 | 560.5 | 0.97 | 20.14 | 616 | 264 | 3.8975 |
| 14 | 586 | 558.0 | 1.61 | 19.79 | 591 | 265 | 3.1084 |
| 14 | 561 | 563.3 | 1.40 | 20.09 | 566 | 266 | 166.5352 |
| 14 | 536 | 559.7 | 1.20 | 19.94 | 541 | 267 | 0.9762 |
| 14 | 511 | 563.8 | 2.61 | 19.56 | 516 | 268 | 0.2725 |
| 14 | 486 | 561.7 | 6.25 | 17.51 | 491 | 269 | 0.2258 |
| 14 | 461 | 565.9 | 5.62 | 17.70 | 466 | 270 | 0.0873 |
| 14 | 441 | 564.0 | 5.55 | 17.66 | 446 | 271 | 0.2656 |
| 14 | 418 | 565.3 | 5.17 | 17.95 | 426 | 272 | 0.0755 |
| 14 | 404 | 563.9 | 4.98 | 17.65 | 409 | 273 | 0.0776 |
| 14 | 379 | 573.7 | 5.29 | 16.99 | 384 | 274 | 0.0662 |
| 14 | 349 | 563.2 | 5.91 | 15.88 | 354 | 275 | 0.0639 |
| 14 | 319 | 565.0 | 7.76 | 14.74 | 324 | 276 | 0.0519 |
| 14 | 289 | 566.4 | 11.77 | 14.37 | 294 | 277 | 0.0541 |
| 14 | 259 | 563.3 | 11.81 | 15.98 | 264 | 278 | 0.0374 |
| 14 | 229 | 561.5 | 10.85 | 15.98 | 234 | 279 | 0.0393 |
| 14 | 199 | 567.2 | 11.93 | 13.33 | 204 | 280 | 0.0317 |
| 14 | 169 | 562.1 | 12.43 | 12.84 | 174 | 281 | 0.0319 |
| 14 | 139 | 549.8 | 12.74 | 11.72 | 144 | 282 | 0.0288 |
| 14 | 111 | 554.4 | 13.22 | 11.06 | 119 | 283 | 0.0260 |
| 14 | 77 | 548.0 | 14.92 | 10.09 | 82 | 284 | 0.0177 |
| 14 | 47 | 553.0 | 15.81 | 10.25 | 52 | 285 | 0.0218 |
| 14 | 11 | 554.5 | 18.62 | 8.61 | 22 | 286 | 0.0162 |
| 15 | 271 | 562.4 | 16.32 | 11.26 | 276 | 287 | 0.0276 |
| 15 | 246 | 556.7 | 16.54 | 11.39 | 251 | 288 | 0.0263 |
| 15 | 221 | 552.9 | 16.53 | 11.23 | 226 | 289 | 0.0285 |
| 15 | 196 | 555.5 | 16.99 | 11.18 | 201 | 290 | 0.0441 |

| | | | | | | | |
|----|-----|-------|-------|-------|-----|-----|--------|
| 15 | 171 | 553.7 | 17.21 | 10.95 | 176 | 291 | 0.0277 |
| 15 | 146 | 555.1 | 17.76 | 10.07 | 151 | 292 | 0.0256 |
| 15 | 121 | 563.7 | 18.17 | 10.38 | 126 | 293 | 0.0223 |
| 15 | 96 | 556.9 | 18.25 | 9.78 | 101 | 294 | 0.0158 |
| 15 | 71 | 561.4 | 18.48 | 9.72 | 76 | 295 | 0.0244 |
| 15 | 46 | 559.4 | 18.34 | 9.85 | 51 | 296 | 0.0170 |
| 15 | 13 | 560.4 | 18.62 | 9.64 | 26 | 297 | 0.0194 |
| 16 | 675 | 561.9 | 12.72 | 10.74 | 685 | 298 | 0.0356 |
| 16 | 645 | 571.6 | 13.75 | 10.47 | 650 | 299 | 0.0401 |
| 16 | 620 | 560.6 | 14.27 | 10.08 | 625 | 300 | 0.0015 |
| 16 | 595 | 561.5 | 14.95 | 9.82 | 600 | 301 | 0.0015 |
| 16 | 570 | 567.9 | 15.63 | 9.67 | 575 | 302 | 0.0016 |
| 16 | 545 | 561.1 | 15.82 | 9.38 | 550 | 303 | 0.0019 |
| 16 | 520 | 559.8 | 16.23 | 9.17 | 525 | 304 | 0.0017 |
| 16 | 490 | 559.8 | 16.90 | 8.93 | 495 | 305 | 0.0018 |
| 16 | 460 | 558.8 | 17.61 | 8.63 | 465 | 306 | 0.0014 |
| 16 | 430 | 570.8 | 18.70 | 8.27 | 435 | 307 | 0.0013 |
| 16 | 395 | 559.1 | 18.75 | 7.97 | 405 | 308 | 0.0012 |
| 16 | 369 | 562.4 | 19.70 | 7.76 | 374 | 309 | 0.0010 |
| 16 | 339 | 548.7 | 19.94 | 7.34 | 344 | 310 | 0.0009 |
| 16 | 309 | 560.8 | 22.03 | 6.41 | 314 | 311 | 0.0012 |
| 16 | 279 | 561.3 | 21.64 | 6.75 | 284 | 312 | 0.0016 |
| 16 | 249 | 568.9 | 21.81 | 6.84 | 254 | 313 | 0.0017 |
| 16 | 219 | 569.6 | 22.81 | 6.37 | 224 | 314 | 0.0018 |
| 16 | 189 | 548.3 | 22.51 | 6.07 | 194 | 315 | 0.0014 |
| 16 | 159 | 559.4 | 24.05 | 5.85 | 164 | 316 | 0.0018 |
| 16 | 129 | 565.5 | 25.25 | 5.39 | 134 | 317 | 0.0013 |
| 16 | 92 | 558.7 | 25.98 | 4.76 | 104 | 318 | 0.0011 |
| 16 | 55 | 557.1 | 27.57 | 3.96 | 60 | 319 | 0.0004 |
| 16 | 10 | 558.5 | 28.35 | 3.51 | 20 | 320 | 0.0000 |
| 17 | 739 | 561.1 | 15.83 | 10.38 | 749 | 321 | 0.0147 |
| 17 | 709 | 569.8 | 16.73 | 10.19 | 714 | 322 | 0.0113 |
| 17 | 684 | 568.6 | 17.35 | 9.91 | 689 | 323 | 0.0100 |
| 17 | 659 | 562.8 | 17.49 | 9.91 | 664 | 324 | 0.0112 |
| 17 | 629 | 564.6 | 18.17 | 9.17 | 634 | 325 | 0.0091 |
| 17 | 599 | 562.9 | 18.63 | 9.09 | 604 | 326 | 0.0088 |
| 17 | 569 | 564.1 | 19.31 | 8.72 | 574 | 327 | 0.0099 |
| 17 | 539 | 564.5 | 20.23 | 7.96 | 544 | 328 | 0.0082 |
| 17 | 509 | 562.9 | 20.69 | 8.02 | 514 | 329 | 0.0079 |
| 17 | 479 | 563.7 | 21.26 | 7.63 | 484 | 330 | 0.0068 |
| 17 | 422 | 564.3 | 22.33 | 6.94 | 427 | 331 | 0.0058 |
| 17 | 387 | 563.4 | 22.67 | 6.75 | 392 | 332 | 0.0054 |

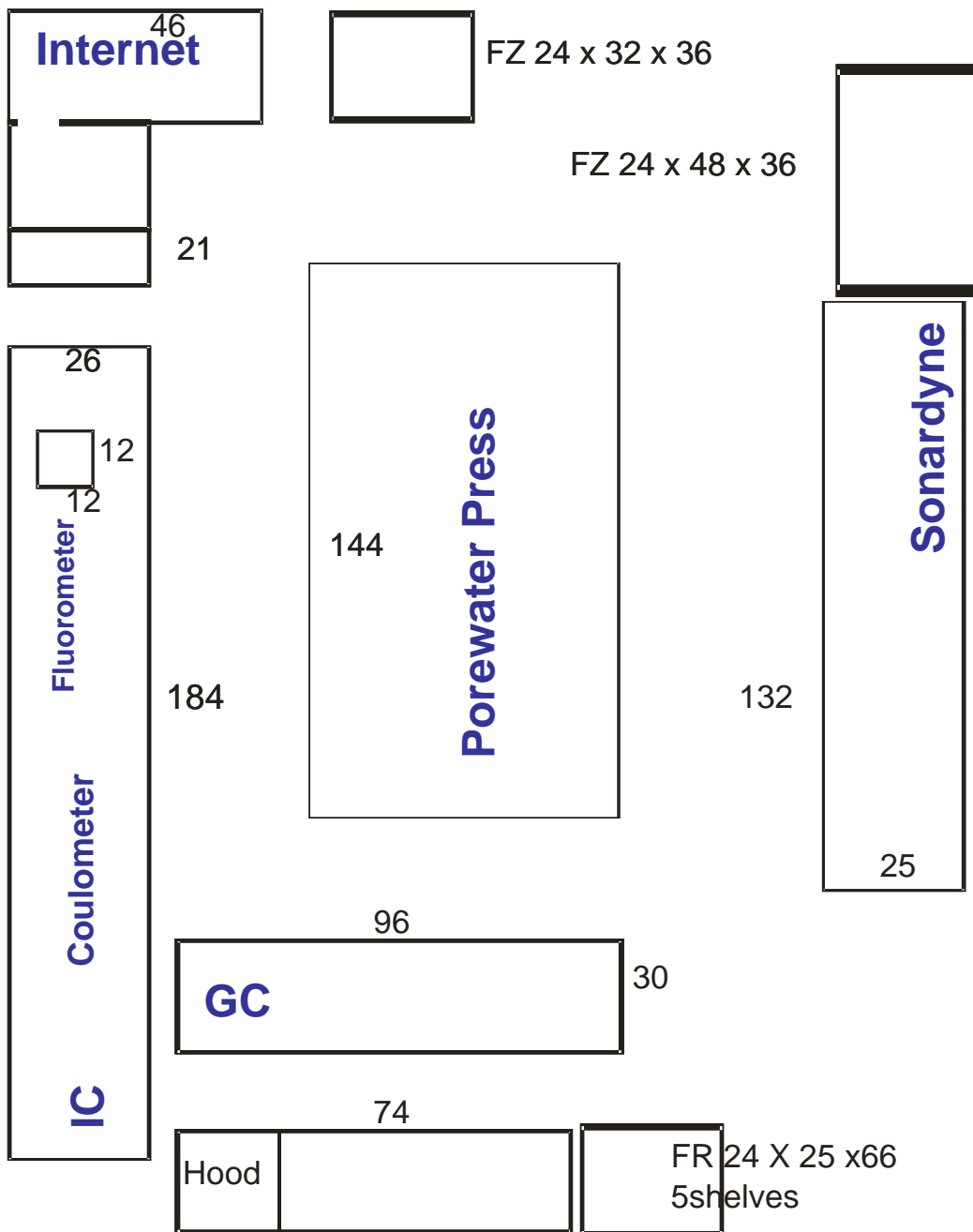
| | | | | | | | |
|----|-----|-------|-------|-------|-----|-----|--------|
| 17 | 352 | 560.9 | 23.69 | 6.19 | 357 | 333 | 0.0043 |
| 17 | 312 | 565.8 | 23.36 | 6.49 | 317 | 334 | 0.0034 |
| 17 | 277 | 565.2 | 24.86 | 5.58 | 282 | 335 | 0.0026 |
| 17 | 242 | 567.3 | 25.26 | 5.46 | 247 | 336 | 0.0026 |
| 17 | 207 | 564.3 | 25.70 | 5.20 | 212 | 337 | 0.0018 |
| 17 | 147 | 562.9 | 26.61 | 4.59 | 157 | 338 | 0.8872 |
| 18 | 670 | 576.1 | 1.03 | 16.51 | 680 | 339 | 0.9123 |
| 18 | 635 | 562.4 | 1.44 | 16.13 | 640 | 340 | 0.0988 |
| 18 | 605 | 566.5 | 2.51 | 15.16 | 610 | 341 | 0.0089 |
| 18 | 575 | 568.0 | 3.77 | 14.77 | 580 | 342 | 0.0034 |
| 18 | 545 | 566.3 | 5.27 | 13.94 | 550 | 343 | 0.0006 |
| 18 | 515 | 568.7 | 6.57 | 12.67 | 520 | 344 | 0.0002 |
| 18 | 485 | 573.7 | 8.79 | 12.00 | 490 | 345 | 0.0002 |
| 18 | 455 | 568.2 | 9.65 | 11.73 | 460 | 346 | 0.0001 |
| 18 | 420 | 571.6 | 12.82 | 10.47 | 430 | 347 | 0.0000 |
| 18 | 375 | 568.4 | 13.32 | 9.88 | 380 | 348 | 0.0000 |
| 18 | 340 | 565.9 | 14.34 | 9.14 | 345 | 349 | 0.0000 |
| 18 | 305 | 569.9 | 16.25 | 8.63 | 310 | 350 | 0.0000 |
| 18 | 270 | 575.3 | 17.61 | 8.37 | 275 | 351 | 0.0000 |
| 18 | 235 | 573.9 | 18.72 | 7.81 | 240 | 352 | 0.0000 |
| 18 | 200 | 574.3 | 20.03 | 7.26 | 205 | 353 | 0.0000 |
| 18 | 165 | 575.4 | 20.68 | 7.28 | 170 | 354 | 0.0000 |
| 18 | 130 | 572.3 | 21.90 | 6.51 | 135 | 355 | 0.0000 |
| 18 | 89 | 580.1 | 24.95 | 5.32 | 100 | 356 | 0.0000 |
| 18 | 48 | 572.1 | 27.03 | 4.39 | 53 | 357 | 0.0000 |
| 18 | 9 | 575.3 | 28.40 | 3.67 | 18 | 358 | 0.0000 |
| 19 | 700 | 574.6 | 3.46 | 13.78 | 710 | 359 | 0.0014 |
| 19 | 665 | 575.5 | 4.80 | 13.60 | 670 | 360 | 0.0004 |
| 19 | 635 | 570.1 | 5.67 | 13.70 | 640 | 361 | 0.0005 |
| 19 | 605 | 578.4 | 6.51 | | 610 | 362 | 0.0002 |
| 19 | 575 | 581.6 | 7.51 | 12.69 | 580 | 363 | 0.0002 |
| 19 | 545 | 570.5 | 7.91 | 13.03 | 550 | 364 | 0.0000 |
| 19 | 515 | 567.4 | 8.74 | 11.91 | 520 | 365 | 0.0001 |
| 19 | 480 | 564.5 | 9.77 | 11.36 | 485 | 366 | 0.0001 |
| 19 | 445 | 568.8 | 10.86 | 11.10 | 450 | 367 | 0.0000 |
| 19 | 403 | 571.8 | 12.23 | 10.42 | 408 | 368 | 0.0000 |
| 19 | 363 | 571.3 | 13.30 | 9.98 | 368 | 369 | 0.0000 |
| 19 | 323 | 572.1 | 15.36 | 8.98 | 328 | 370 | 0.0000 |
| 19 | 283 | 572.0 | 16.05 | 8.70 | 288 | 371 | 0.0000 |
| 19 | 243 | 569.5 | 16.99 | 8.41 | 248 | 372 | 0.0000 |
| 19 | 203 | 568.5 | 17.92 | 8.08 | 208 | 373 | 0.0000 |
| 19 | 163 | 569.8 | 18.93 | 7.71 | 168 | 374 | 0.0000 |

| | | | | | | | |
|----|-----|-------|-------|-------|-----|-----|---------|
| 19 | 117 | 568.9 | 20.51 | 6.59 | 128 | 375 | 0.0000 |
| 19 | 70 | 570.7 | 21.20 | 6.64 | 75 | 376 | 0.0000 |
| 20 | 714 | 569.6 | 9.61 | 11.01 | 724 | 377 | 0.0000 |
| 20 | 679 | 568.0 | 10.15 | 11.04 | 684 | 378 | 0.0000 |
| 20 | 649 | 569.4 | 10.70 | 10.71 | 654 | 379 | 0.0000 |
| 20 | 614 | 572.5 | 11.59 | 10.60 | 619 | 380 | 0.0000 |
| 20 | 579 | 576.3 | 12.74 | 10.10 | 584 | 381 | 0.0000 |
| 20 | 544 | 569.0 | 13.44 | 9.86 | 549 | 382 | 0.0000 |
| 20 | 504 | 568.7 | 14.51 | 9.36 | 514 | 383 | 0.0000 |
| 20 | 451 | 567.2 | 15.95 | 8.80 | 458 | 384 | 0.0000 |
| 20 | 411 | 568.2 | 16.92 | 8.45 | 416 | 385 | 0.0000 |
| 20 | 371 | 567.2 | 18.37 | 7.78 | 376 | 386 | 0.0000 |
| 20 | 331 | 568.3 | 19.02 | 7.60 | 336 | 387 | 0.0000 |
| 20 | 291 | 568.3 | 20.52 | 6.92 | 296 | 388 | 0.0000 |
| 20 | 251 | 567.4 | 21.10 | 6.57 | 256 | 389 | 0.0000 |
| 20 | 211 | 569.1 | 21.66 | 6.61 | 216 | 390 | 0.0000 |
| 20 | 166 | 570.6 | 22.45 | 6.20 | 176 | 391 | 0.0000 |
| 20 | 110 | 568.0 | 23.64 | 5.68 | 115 | 392 | 0.0000 |
| 20 | 70 | 570.1 | 24.61 | 5.21 | 75 | 393 | 0.0000 |
| 20 | 30 | 569.8 | 25.57 | 4.98 | 35 | 394 | 9.9194 |
| 21 | 712 | 566.8 | 0.75 | 17.77 | 722 | 395 | 8.5063 |
| 21 | 677 | 563.8 | 0.74 | 19.08 | 682 | 396 | 7.8952 |
| 21 | 652 | 571.2 | 0.81 | 19.42 | 657 | 397 | 7.6172 |
| 21 | 622 | 566.2 | 1.09 | 19.53 | 627 | 398 | 6.3649 |
| 21 | 592 | 565.9 | 0.96 | 20.20 | 597 | 399 | 3.4578 |
| 21 | 562 | 566.5 | 1.04 | 20.17 | 567 | 400 | 16.2701 |
| 21 | 532 | 564.2 | 1.86 | 19.86 | 537 | 401 | 0.3881 |
| 21 | 502 | 558.8 | 2.79 | 19.03 | 507 | 402 | -0.0004 |
| 21 | 472 | 567.2 | 5.12 | 17.16 | 477 | 403 | 0.0774 |
| 21 | 431 | 568.9 | 7.91 | 16.25 | 442 | 404 | 0.0714 |
| 21 | 394 | 568.2 | 9.88 | 14.47 | 399 | 405 | 0.0470 |
| 21 | 364 | 566.9 | 11.47 | 13.29 | 369 | 406 | 0.0442 |
| 21 | 334 | 544.4 | 11.71 | 12.89 | 339 | 407 | 0.0362 |
| 21 | 299 | 568.1 | 12.79 | 12.44 | 304 | 408 | 0.0382 |
| 21 | 264 | 563.8 | 14.60 | 11.28 | 269 | 409 | 0.0297 |
| 21 | 229 | 569.3 | 14.98 | 11.15 | 115 | 410 | 0.0276 |
| 21 | 194 | 563.8 | 16.89 | 9.30 | 75 | 411 | 0.0210 |
| 21 | 157 | 566.9 | 16.49 | 10.19 | 40 | 412 | 0.0194 |
| 21 | 105 | 568.6 | 18.86 | 9.00 | 490 | 413 | 0.0156 |
| 21 | 70 | 566.4 | 20.28 | 8.39 | 450 | 414 | 0.0133 |
| 21 | 33 | 570.4 | 22.30 | 7.08 | 420 | 415 | 0.0097 |
| 22 | 480 | 572.1 | 3.31 | 14.35 | 390 | 416 | 0.0004 |

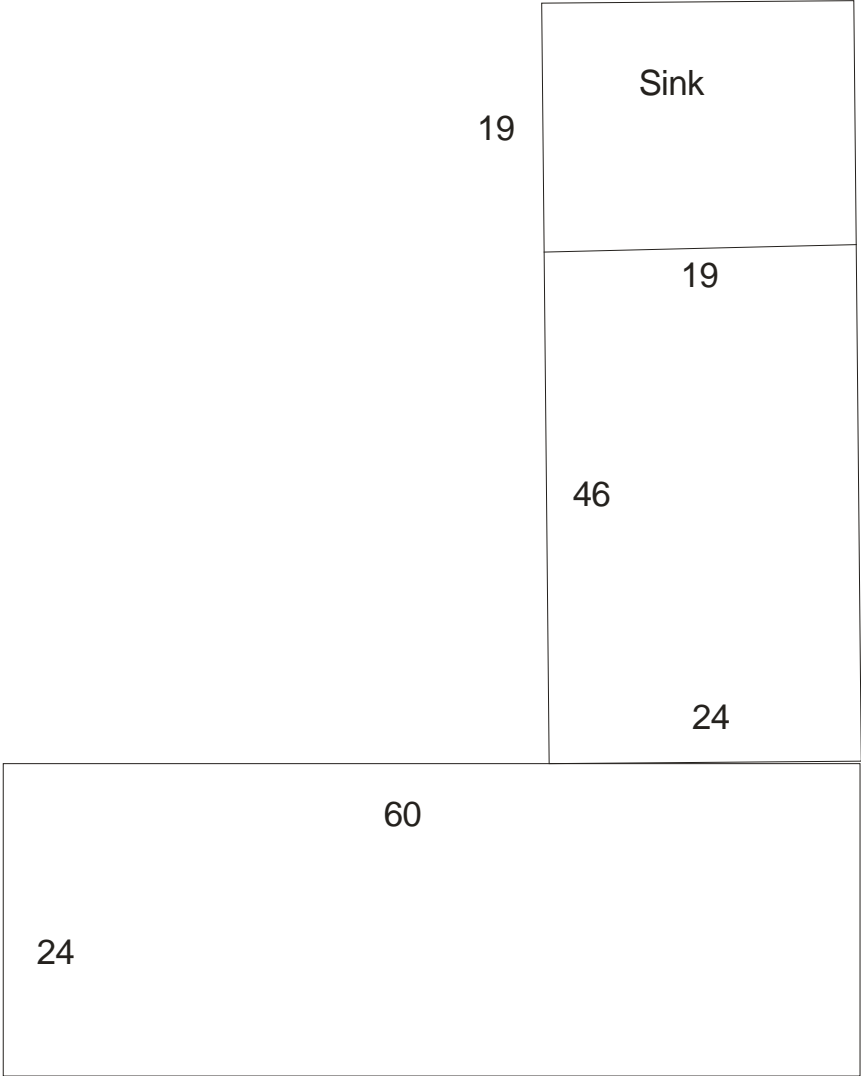
| | | | | | | | |
|-----------|-----|-------|-------|-------|-----|-----|--------|
| 22 | 445 | 573.8 | 8.08 | 13.76 | 355 | 417 | 0.0002 |
| 22 | 415 | 573.4 | 9.54 | 12.91 | 420 | 418 | 0.0001 |
| 22 | 385 | 572.0 | 10.70 | 12.27 | 390 | 419 | 0.0000 |
| 22 | 350 | 573.4 | 12.25 | 11.70 | 355 | 420 | 0.0000 |
| 22 | 315 | 572.3 | 13.66 | 10.21 | 320 | 421 | 0.0000 |
| 22 | 275 | 569.8 | 15.64 | 9.90 | 280 | 422 | 0.0000 |
| 22 | 243 | 568.5 | 16.11 | 9.61 | 248 | 423 | 0.0000 |
| 22 | 203 | 568.9 | 17.15 | 8.96 | 213 | 424 | 0.0000 |

Appendix 3: On board Chemistry Lab lay out.

Lab space (inches) and instrument layout (including freezers FZ and refrigerator FR) for the main lab.



WET LAB *Units for the lab space is in inches*



Appendix 4: Core Descriptions

| Core | Section | Length (cm) | Pore water distance from top of core (cm) | | Average cmb/sf | Sample Thickness | Sample # | Lithology | Color | Fossils bivalves, gastropod, forams, other | Diagenesis rare, Common, Abundant | Bioturbation | Disturbance | Clay Consistency | Other | Sample Photos | Written Descriptions | | |
|--|---------|----------------|---|--------|-------------------|---------------------|----------|--|--------------------------------------|---|--|--------------|-------------|---------------------|--|------------------|---|----|------------|
| | | | top | bottom | | | | | | | | | | | | | | cm | clay, sand |
| | | | | | | | | | | | | | | | | | | | |
| No description for Core 1, Cores 2 & 3 were failed pulls | | | | | | | | | | | | | | | | | | | |
| 4 | I | 304 | 693 | 708 | 701 | 15 | KR4 01 | clay | very light gray | Foram bearing | FeS mottling rare | | | | | | Very light gray, foram bearing clay, rare FeS mottling throughout | | |
| 4 | I | 304 | 673 | 683 | 678 | 10 | KR4 02 | clay | very light gray | Foram bearing | FeS mottling rare | | | | | | Very light gray, foram bearing clay, rare FeS mottling throughout | | |
| 4 | I | 304 | 653 | 663 | 658 | 10 | KR4 03 | clay | light gray | Foram bearing | FeS mottling common | | | | | | Light gray, foram bearing clay with common FeS mottling throughout | | |
| 4 | I | 304 | 628 | 643 | 636 | 15 | KR4 04 | clay | light gray | Foram bearing | FeS mottling common | | | | | | Light gray, foram bearing clay with common FeS mottling throughout | | |
| 4 | I | 304 | 603 | 618 | 611 | 15 | KR4 05 | clay | light gray | Foram bearing | FeS mottling common | | | | | | Light gray, foram bearing clay with common FeS mottling throughout | | |
| 4 | I | 304 | 578 | 593 | 586 | 15 | KR4 06 | clay | light gray | Foram bearing | FeS mottling common | | | | | | Light gray, foram bearing clay with common FeS mottling throughout | | |
| 4 | I | 304 | 553 | 568 | 561 | 15 | KR4 07 | >4cm thick rich quartz sand layer, bounded by clay | sand, lt gray clay, light gray | Foram bearing | FeS mottling common | | | | | | >4cm medium grained, moderately well sorted, well rounded, quartz rich sand layer; Surrounded by light gray, foram bearing clay with common FeS mottling throughout | | |
| 4 | I | 304 | 523 | 538 | 531 | 15 | KR4 08 | clay | light gray | Foram bearing | FeS mottling common | | | | | | Light gray, foram bearing clay with common FeS mottling throughout | | |
| 4 | I | 304 | 498 | 513 | 506 | 15 | KR4 09 | clay | light gray | Foram bearing | FeS mottling rare | | | | | | Light gray, foram bearing clay, FeS mottling rare throughout | | |
| 4 | I | 304 | 473 | 488 | 481 | 15 | KR4 10 | >5cm thick rich quartz sand layer, bounded by clay | sand, lt gray clay, light gray | Foram bearing | FeS mottling rare | | | | | | >5cm medium grained, moderately well sorted, well rounded, quartz rich sand layer; Surrounded by light gray, foram bearing clay with rare FeS mottling throughout | | |
| 4 | I | 304 | 448 | 463 | 456 | 15 | KR4 11 | clay | light gray | Foram bearing | FeS mottling rare | | | | | | Light gray, foram bearing clay, FeS mottling rare throughout | | |
| 4 | I | 304 | 414 | 438 | 426 | 24 | KR4 12 | clay | light gray | Foram bearing | FeS mottling rare | | | | | | Light gray, foram bearing clay, FeS mottling rare throughout | | |
| 4 | II | 307 | 384 | 404 | 394 | 20 | KR4 13 | clay | very dark gray | Foram bearing | FeS mottling rare | | | | | | Dark gray, foram bearing clay, FeS mottling rare throughout | | |
| 4 | II | 307 | 354 | 374 | 364 | 20 | KR4 14 | clay | very dark gray | Foram bearing | FeS mottling common | | | | | | Dark gray, foram bearing clay, FeS mottling common throughout | | |
| 4 | II | 307 | 324 | 344 | 334 | 20 | KR4 15 | clay w/ 2cm diameter sand pocket | sand, lt gray clay, vry dk gray | Foram bearing | FeS mottling common | | | | | | 2cm diameter, medium grained, quartz rich sand pocket; Surrounded by dark gray, foram bearing clay, FeS mottling common throughout | | |
| 4 | II | 307 | 294 | 314 | 304 | 20 | KR4 16 | clay | very dark gray | Foram bearing | FeS mottling common | | | | | | Dark gray, foram bearing clay, FeS mottling common throughout | | |
| 4 | II | 307 | 264 | 284 | 274 | 20 | KR4 17 | quartz rich sand layer, bounded by clay | sand white/lt gray; clay vry dk gray | Foram bearing | FeS mottling common | | | | | | >10cm thick, medium grained, quartz rich sand layer ("also was present in porewater sample Sec. 2, 150T). Clay same as sample KR18 | | |
| 4 | II | 307 | 234 | 254 | 244 | 20 | KR4 18 | clay | very dark gray | Foram bearing | FeS mottling common | | | | | | Dark gray, foram bearing clay, FeS mottling common throughout | | |
| 4 | II | 307 | 204 | 224 | 214 | 20 | KR4 19 | clay | very dark gray | Foram bearing | FeS mottling common | | | | | | Dark gray, foram bearing clay, FeS mottling common throughout | | |
| 4 | II | 307 | 184 | 194 | 189 | 10 | KR4 20 | clay | very dark gray | Foram bearing | FeS mottling rare | | | | | | Dark gray, foram bearing clay, FeS mottling rare throughout | | |
| 4 | II | 307 | 154 | 174 | 164 | 20 | KR4 21 | clay | light gray | Foram bearing | FeS mottling rare | | | | | | Light gray, foram bearing clay; FeS mottling rare throughout | | |
| 4 | II | 307 | 124 | 144 | 134 | 20 | KR4 22 | clay | light gray | Foram bearing | FeS mottling rare | | | | | | Light gray, foram bearing clay; FeS mottling rare throughout | | |
| 4 | III | 107 | 77 | 97 | 87 | 20 | KR4 23 | clay | light gray | Foram bearing | FeS mottling rare | | | | | | Light gray, foram bearing clay; FeS mottling rare throughout | | |
| 4 | III | 107 | 47 | 67 | 57 | 20 | KR4 24 | clay | light gray | Foram bearing | | | | | | | Light gray, foram bearing clay; FeS mottling rare throughout | | |
| 4 | III | 107 | 17 | 37 | 27 | 20 | KR4 25 | clay | light gray | | | | | watery | | | Light gray-brown, foram bearing clay; FeS mottling rare throughout; Top of sample very wet/malleable | | |
| 5 | I | 309 | 731 | 746 | 739 | 15 | KR5 01 | clay | light brown-gray | Foram bearing | FeS mottling rare | | | firm | | | Light brown-gray, foram bearing, clay; solid/firm consistency; Rare FeS mottling | | |
| 5 | I | 309 | 706 | 721 | 714 | 15 | KR5 02 | silt/sand pockets, <1cm | light brown-gray | Foram bearing | FeS mottling rare | | | firm | | | Light brown-gray, foram bearing, clay; with <1cm diameter silt/very fine grained sand pockets; Rare FeS mottling | | |
| 5 | I | 309 | 681 | 696 | 689 | 15 | KR5 03 | clay | light brown-gray | Foram bearing | FeS mottling rare | | | firm | | | Light gray-brown, foram bearing clay with Rare FeS mottling | | |
| 5 | I | 309 | 656 | 671 | 664 | 15 | KR5 04 | clay | light brown-gray | Foram bearing | FeS mottling rare | | | | | | Light gray-brown, foram bearing clay with Rare FeS mottling | | |
| 5 | I | 309 | 631 | 646 | 639 | 15 | KR5 05 | clay | light brown-gray | Foram bearing Shell fragments (bivalve); | FeS mottling rare | | | | or FeS nodules, sampled, <1/4cm diameter | X | Light gray-brown, foram bearing clay with Rare FeS mottling; <1/4cm diameter carbonate or gray siltstone nodules (Sampled) | | |
| 5 | I | 309 | 606 | 621 | 614 | 15 | KR5 06 | clay | light gray | Foram bearing | FeS mottling rare | | | | | X | Light gray, foram bearing clay; Rare FeS mottling; fragments of bivalve shell present (Sampled) | | |

| | | | | | | | | | | | | | | |
|---|------|-----|-----|-----|-----|-----|--------|----------------------------|------------------------------|--|--|----------------|--------|---|
| 5 | I | 309 | 531 | 546 | 539 | 15 | KR5 09 | clay | light gray | Foram bearing | FeS mottling rare | | | Light gray, foram bearing clay; Rare FeS mottling |
| 5 | I | 309 | 506 | 521 | 514 | 15 | KR5 10 | clay | light gray | Foram bearing | FeS mottling rare | | | Light gray, foram bearing clay; Rare FeS mottling |
| 5 | I | 309 | 481 | 496 | 489 | 15 | KR5 11 | clay | light gray | Foram bearing | FeS mottling rare | | | Light gray, foram bearing clay; Rare FeS mottling |
| 5 | I | 309 | 547 | 471 | 509 | -76 | KR5 12 | clay | light gray | Foram bearing | FeS mottling rare | | | Light gray, foram bearing clay; Rare FeS mottling |
| 5 | II | 308 | 422 | 437 | 430 | 15 | KR5 13 | clay | light gray | Foram bearing | FeS mottling rare | | | Light gray, foram bearing clay; Rare FeS mottling |
| 5 | II | 308 | 397 | 412 | 405 | 15 | KR5 14 | clay | light gray | Foram bearing | FeS mottling rare | | | Light gray, foram bearing clay; Rare FeS mottling |
| 5 | II | 308 | 372 | 387 | 380 | 15 | KR5 15 | clay | light gray | Foram bearing | FeS mottling rare | | | Light gray, foram bearing clay; Rare FeS mottling |
| 5 | II | 308 | 347 | 362 | 355 | 15 | KR5 16 | clay | light gray | Foram bearing | FeS mottling rare | | | Light gray, foram bearing clay; Rare FeS mottling |
| 5 | II | 308 | 322 | 337 | 330 | 15 | KR5 17 | clay | light gray | Foram bearing | FeS mottling rare | | | Light gray, foram bearing clay; Rare FeS mottling |
| 5 | II | 308 | 292 | 312 | 302 | 20 | KR5 18 | clay | light gray | Foram bearing | FeS mottling rare | | | Light gray, foram bearing clay; Rare FeS mottling |
| 5 | II | 308 | 262 | 282 | 272 | 20 | KR5 19 | clay | light gray | Foram bearing | FeS mottling rare | | | Light gray, foram bearing clay; Rare FeS mottling |
| 5 | II | 308 | 232 | 252 | 242 | 20 | KR5 20 | silt/sand pockets, <1cm | light gray | Shell fragments (sampled); Foram bearing | FeS mottling rare | | X | Light gray, foram bearing clay; Rare FeS mottling; small sand pockets, <1cm diameter; shell fragment (Sampled) |
| 5 | II | 308 | 202 | 222 | 212 | 20 | KR5 21 | clay | light gray | Foram bearing | FeS mottling rare | | | Light gray, foram bearing clay; Rare FeS mottling |
| 5 | II | 308 | 172 | 192 | 182 | 20 | KR5 22 | clay | light gray | Foram bearing | FeS mottling rare | | | Light gray, foram bearing clay; Rare FeS mottling |
| 5 | II | 308 | 139 | 162 | 151 | 23 | KR5 23 | clay | light gray | Foram bearing | FeS mottling rare | | | Light gray, foram bearing clay; Rare FeS mottling |
| 5 | III* | 139 | 109 | 129 | 119 | 20 | KR5 24 | clay | light gray | Foram bearing | FeS mottling rare | | | Light gray, foram bearing clay; Rare FeS mottling |
| 6 | I | 304 | 284 | 294 | 289 | 10 | KR6 01 | clay | light gray | Foram bearing | FeS mottling rare | Salmon texture | watery | |
| 6 | I | 304 | 264 | 274 | 269 | 10 | KR6 02 | clay | light gray | Foram bearing | FeS mottling rare | Salmon texture | | |
| 6 | I | 304 | 244 | 254 | 249 | 10 | KR6 03 | clay | light gray | Foram bearing | FeS mottling rare | Salmon texture | | |
| 6 | I | 304 | 224 | 234 | 229 | 10 | KR6 04 | clay | light gray | Foram bearing | FeS mottling rare | Salmon texture | | |
| 6 | I | 304 | 204 | 214 | 209 | 10 | KR6 05 | ~1cm sand pocket with | light gray | Foram bearing | FeS mottling rare | | | ~1cm oil stain |
| 6 | I | 304 | 159 | 194 | 177 | 35 | KR6 06 | clay | light gray | Forams rare | FeS mottling rare | | | void, ~10+cm |
| 6 | I | 304 | 139 | 149 | 144 | 10 | KR6 07 | clay | light gray | Forams rare | FeS mottling rare | | | |
| 6 | I | 304 | 119 | 129 | 124 | 10 | KR6 08 | clay | light gray | Forams rare | FeS mottling rare | | | stain |
| 6 | I | 304 | 74 | 109 | 92 | 35 | KR6 09 | clay | light gray | Forams rare | FeS mottling rare | | | void |
| 6 | I | 304 | 54 | 64 | 59 | 10 | KR6 10 | clay; small sand/silt lens | light gray | Foram bearing | FeS mottling rare | | | |
| 6 | I | 304 | 34 | 44 | 39 | 10 | KR6 11 | clay | light gray | Foram bearing | FeS mottling rare | | | |
| 6 | I | 304 | 14 | 24 | 19 | 10 | KR6 12 | clay | light gray | Foram bearing | FeS mottling rare | | | light oil stain? |
| 7 | I | 304 | 726 | 741 | 734 | 15 | KR7 01 | clay | light green-gray | Foram bearing | FeS mottling rare; visible pyrite, <1mm; copper colored streaks/mottling rare; visible; copper colored | | | light green, foram bearing clay; FeS mottling rare throughout, <1mm diameter pyrite grains present?; Copper colored mottling rare throughout |
| 7 | I | 306 | 701 | 716 | 709 | 15 | KR7 02 | clay | light green-gray | Foram bearing | FeS mottling rare; visible; copper colored streaks/mottling rare; visible; copper colored | | | light green, foram bearing clay; FeS mottling rare throughout, <1mm diameter pyrite grains present?; Copper colored mottling rare throughout |
| 7 | I | 306 | 676 | 691 | 684 | 15 | KR7 03 | clay | light green-gray | Foram bearing | FeS mottling rare; visible; copper colored streaks/mottling rare; 2cm long nodule within FeS patch | | X | light green, foram bearing clay; FeS mottling rare throughout, <1mm diameter pyrite grains present?; Copper colored mottling rare throughout; 2cm long, narrow nodule within FeS pocket (Sampled) |
| 7 | I | 306 | 651 | 666 | 659 | 15 | KR7 04 | clay | light green-brown | Foram bearing | FeS mottling rare; pyrite grains <1mm | | | light green, foram bearing clay; FeS mottling rare throughout, <1mm diameter pyrite grains present?; Copper colored mottling rare throughout |
| 7 | I | 306 | 626 | 641 | 634 | 15 | KR7 05 | clay | light brown-flesh-green clay | Foram bearing | FeS mottling rare; pyrite grains <1mm | | | light brown-flesh-green colored, foram bearing clay; rare FeS mottling and pyrite grains throughout |
| 7 | I | 306 | 601 | 616 | 609 | 15 | KR7 06 | clay | light brown-flesh-green clay | Foram bearing | FeS mottling rare; pyrite grains <1mm | | | light brown-flesh-green, foram bearing clay; Distinct FeS patches which are semi-cohesive |
| 7 | I | 306 | 576 | 591 | 584 | 15 | KR7 07 | clay | light brown-flesh-green clay | Foram bearing | FeS mottling rare; pyrite grains <1mm | | | light brown-flesh-green colored, foram bearing clay; rare FeS mottling and pyrite grains throughout |

| | | | | | | | | | | | | |
|---|-----|-----|-----|-----|-----|----|--------|---|------------------------------|---------------|---|---|
| 7 | I | 306 | 601 | 616 | 609 | 15 | KR7 06 | clay | light brown-flesh-green clay | Foram bearing | FeS mottles rare; pyrite grains <1mm | light brown-flesh-green, foram bearing clay; Distinct FeS patches which are semi-cohesive |
| 7 | I | 306 | 576 | 591 | 584 | 15 | KR7 07 | clay | light brown-flesh-green clay | Foram bearing | FeS mottles rare; pyrite grains <1mm | light brown-flesh-green colored, foram bearing clay; rare FeS mottling and pyrite grains throughout |
| 7 | I | 306 | 551 | 566 | 559 | 15 | KR7 08 | clay; 1cm thick, FeS stained quartz rich sand layer | light brown-flesh-green clay | Foram bearing | FeS mottling rare | light brown-flesh-green colored, foram bearing clay; rare FeS mottling and pyrite grains throughout; FeS stained, fine grained, quartz rich sand layer ~1cm thick |
| 7 | I | 306 | 526 | 541 | 534 | 15 | KR7 09 | clay | light brown-flesh-green clay | Foram bearing | FeS mottling rare | light brown-flesh-green colored, foram bearing clay; rare FeS mottling and pyrite grains throughout |
| 7 | I | 306 | 501 | 516 | 509 | 15 | KR7 10 | clay | light brown-flesh-green clay | Foram bearing | FeS mottling rare | light brown-flesh-green colored, foram bearing clay; rare FeS mottling and pyrite grains throughout |
| 7 | I | 306 | 476 | 491 | 484 | 15 | KR7 11 | clay | light brown-flesh-green clay | Foram bearing | FeS mottling rare | light brown-flesh-green colored, foram bearing clay; rare FeS mottling and pyrite grains throughout |
| 7 | I | 306 | 445 | 466 | 456 | 21 | KR7 12 | clay; <1cm thick, fine grained sand layer | light brown-flesh-green clay | Foram bearing | FeS mottling rare | light brown-flesh-green colored, foram bearing clay; rare FeS mottling and pyrite grains throughout; 1cm thick, fine grained, quartz rich sand layer |
| 7 | II | 306 | 417 | 437 | 427 | 20 | KR7 13 | clay | light brown-flesh-green clay | Foram rich | FeS mottling rare | light brown-flesh-green colored, foram rich clay; rare FeS mottling and pyrite grains throughout |
| 7 | II | 306 | 387 | 407 | 397 | 20 | KR7 14 | clay; ~1cm diameter sand pocket | light brown-flesh-green clay | Foram rich | FeS mottling rare | light brown-flesh-green colored, foram rich clay; rare FeS mottling and pyrite grains throughout |
| 7 | II | 306 | 357 | 377 | 367 | 20 | KR7 15 | clay | light brown-flesh-green clay | Foram rich | FeS mottling rare | light brown-flesh-green colored, foram rich clay; rare FeS mottling and pyrite grains throughout |
| 7 | II | 306 | 327 | 347 | 337 | 20 | KR7 16 | clay | light brown-flesh-green clay | Foram bearing | FeS mottling rare | light brown-flesh-green colored, foram bearing clay; rare FeS mottling and pyrite grains throughout |
| 7 | II | 306 | 297 | 317 | 307 | 20 | KR7 17 | clay | light brown-flesh-green clay | Foram bearing | FeS mottling rare | light brown-flesh-green colored, foram bearing clay; rare FeS mottling and pyrite grains throughout; clay is moister/more watery |
| 7 | II | 306 | 267 | 287 | 277 | 20 | KR7 18 | clay | light brown-flesh-green clay | Foram bearing | FeS mottling rare | light brown-flesh-green colored, foram bearing clay; rare FeS mottling; clay is moister/more watery |
| 7 | II | 306 | 237 | 257 | 247 | 20 | KR7 19 | clay; ~1cm diameter sand pocket | light brown-flesh-green clay | Foram bearing | FeS mottling rare | light brown-flesh-green colored, foram bearing clay; rare FeS mottling and pyrite grains throughout; clay is moister/more watery |
| 7 | II | 306 | 207 | 227 | 217 | 20 | KR7 20 | clay | light brown-flesh-green clay | Foram bearing | FeS mottling rare | |
| 7 | II | 306 | 177 | 197 | 187 | 20 | KR7 21 | clay | light brown-flesh-green clay | Foram bearing | FeS mottling rare | |
| 7 | II | 306 | 141 | 167 | 154 | 26 | KR7 22 | clay | light brown-flesh-green clay | Foram bearing | FeS mottling rare | |
| 7 | III | 141 | 111 | 131 | 121 | 20 | KR7 23 | diameter sand pocket | light brown-flesh-green clay | Foram bearing | FeS mottling rare | |
| 7 | III | 141 | 81 | 101 | 91 | 20 | KR7 24 | clay | light brown-flesh-green clay | Foram bearing | FeS mottling rare | |
| 7 | III | 141 | 51 | 71 | 61 | 20 | KR7 25 | clay | light brown-flesh-green clay | Foram bearing | FeS mottling rare | |
| 7 | III | 141 | 21 | 41 | 31 | 20 | KR7 26 | clay | light brown-flesh-green clay | Foram bearing | FeS mottling rare | |
| 8 | I | 304 | 714 | 729 | 722 | 15 | KR8 01 | clay | light brown | Foram bearing | FeS mottling rare; faint copper colored rare; faint copper colored | firm |
| 8 | I | 304 | 689 | 704 | 697 | 15 | KR8 02 | clay | light brown | Foram bearing | FeS mottling rare; faint copper colored rare; faint copper colored | firm |
| 8 | I | 304 | 664 | 679 | 672 | 15 | KR8 03 | clay | light brown | Foram bearing | FeS mottling rare; faint copper colored rare; bold copper colored rare; bold copper colored | firm |
| 8 | I | 304 | 639 | 654 | 647 | 15 | KR8 04 | clay | light brown | Foram bearing | FeS mottling rare; bold copper colored rare; bold copper colored | firm |
| 8 | I | 304 | 614 | 629 | 622 | 15 | KR8 05 | clay | light brown | Foram bearing | FeS mottling rare; bold copper colored rare; bold copper colored | malleable |
| 8 | I | 304 | 589 | 604 | 597 | 15 | KR8 06 | clay | light brown | Foram bearing | FeS mottling rare; bold copper colored rare; bold copper colored | malleable |
| 8 | I | 304 | 564 | 579 | 572 | 15 | KR8 07 | clay | light brown | Foram bearing | FeS mottling rare; bold copper colored rare; bold copper colored | malleable |
| 8 | I | 304 | 539 | 554 | 547 | 15 | KR8 08 | clay | light brown | Foram bearing | FeS mottling rare; bold copper colored rare; bold copper colored | malleable |
| 8 | I | 304 | 514 | 529 | 522 | 15 | KR8 09 | clay | light brown | Foram bearing | FeS mottling rare; bold copper colored rare; bold copper colored | malleable |

increased moisture content from KR7 17 to surface

| | | | | | | | | | | | | | | |
|---|-----|-----|-----|-----|-----|----|--------|---|---|---------------|--------------------------------------|---|--|-----|
| 8 | III | 138 | 18 | 38 | 28 | 20 | KR8 25 | clay | light gray | Foram rich | common; copper colored mottling rare | Sands patches, up to 2cm diameter t-out | extremely malleable | |
| 9 | I | 288 | 744 | 769 | 757 | 25 | KR9 01 | clay | light green-gray-flesh/brown | Foram bearing | rare; flesh colored mottling rare | | firm | |
| 9 | I | 288 | 719 | 734 | 727 | 15 | KR9 02 | clay | light green-gray-flesh/brown | Foram bearing | rare; flesh colored mottling rare | | firm | |
| 9 | I | 288 | 694 | 709 | 702 | 15 | KR9 03 | clay | light green-gray-with flesh/brown patches | Foram bearing | rare; flesh colored mottling rare | | malleable | |
| 9 | I | 288 | 669 | 684 | 677 | 15 | KR9 04 | clay | light green-gray | Foram bearing | rare; flesh colored mottling rare | | malleable | |
| 9 | I | 288 | 644 | 659 | 652 | 15 | KR9 05 | clay | light green-gray | Foram bearing | FeS mottling common | | malleable | |
| 9 | I | 288 | 619 | 634 | 627 | 15 | KR9 06 | clay | light green-gray | Foram bearing | flesh colored mottling rare | | malleable | |
| 9 | I | 288 | 594 | 609 | 602 | 15 | KR9 07 | clay | light green-gray | Foram bearing | FeS mottling common | | malleable | |
| 9 | I | 288 | 569 | 584 | 577 | 15 | KR9 08 | medium grained, quartz rich sand pockets | light green-gray | Foram bearing | flesh colored mottling rare | | malleable | X X |
| 9 | I | 288 | 544 | 559 | 552 | 15 | KR9 09 | clay | light green-gray-with flesh/brown patches | Foram bearing | rare; flesh colored mottling rare | | firm | |
| 9 | I | 288 | 519 | 534 | 527 | 15 | KR9 10 | thick, medium grained, quartz rich sand layer | light green-gray | Foram bearing | FeS mottling common | | malleable | |
| 9 | I | 288 | 494 | 509 | 502 | 15 | KR9 11 | clay | light green-gray | Foram bearing | flesh colored mottling rare | | very malleable | |
| 9 | II | 307 | 451 | 471 | 461 | 20 | KR9 12 | clay; 1 quartz rich sand pocket 1cm diameter | light green-gray | Foram bearing | FeS mottling common | | very malleable | |
| 9 | II | 307 | 421 | 441 | 431 | 20 | KR9 13 | clay | light green-gray | Foram bearing | flesh colored mottling rare | | very malleable and increasing moisture | |
| 9 | II | 307 | 391 | 411 | 401 | 20 | KR9 14 | clay | light green-gray | Foram bearing | FeS mottling common | | very malleable and increasing moisture | |
| 9 | II | 307 | 361 | 381 | 371 | 20 | KR9 15 | clay | light green-gray | Foram bearing | flesh colored mottling rare | | very malleable and increasing moisture | |
| 9 | II | 307 | 331 | 351 | 341 | 20 | KR9 16 | clay | light green-gray | Foram bearing | FeS mottling common | | very malleable and increasing moisture | |
| 9 | II | 307 | 301 | 321 | 311 | 20 | KR9 17 | clay | light green-gray | Foram bearing | flesh colored mottling rare | | very malleable and increasing moisture | |
| 9 | II | 307 | 271 | 291 | 281 | 20 | KR9 18 | clay | light green-gray | Foram bearing | FeS mottling common | | very malleable and increasing moisture | |
| 9 | II | 307 | 241 | 261 | 251 | 20 | KR9 19 | clay | light green-gray | Foram bearing | flesh colored mottling rare | | very malleable and increasing moisture | |
| 9 | II | 307 | 211 | 231 | 221 | 20 | KR9 20 | clay | light green-gray | Foram rich | FeS mottling common | vertical worm burrows rare throughout | very malleable and increasing moisture | |
| 9 | II | 307 | 174 | 201 | 188 | 27 | KR9 21 | clay | light green-gray | Foram rich | FeS mottling common | vertical worm burrows rare throughout | very malleable and increasing moisture | |
| 9 | III | 174 | 144 | 164 | 154 | 20 | KR9 22 | clay | light green-gray | Foram rich | FeS mottling common | vertical worm burrows common throughout | extremely malleable and moisture | |

| | | | | | | | | | | | | | | | | |
|----|-----|-----|-----|-----|-----|----|---------|---|------------------------|----------------|---|---|-----------|---|---|---|
| | | | | | | | | | | | FeS mottling common flesh colored mottling rare | | | | very malleable and increasing moisture | |
| 9 | II | 307 | 241 | 261 | 251 | 20 | KR9 19 | clay | light green-gray | Foram bearing | | | | | | |
| 9 | II | 307 | 211 | 231 | 221 | 20 | KR9 20 | clay | light green-gray | Foram rich | FeS mottling common | vertical worm burrows rare throughout | | | very malleable and increasing moisture | |
| 9 | II | 307 | 174 | 201 | 188 | 27 | KR9 21 | clay | light green-gray | Foram rich | FeS mottling common | vertical worm burrows rare throughout | | | very malleable and increasing moisture | |
| 9 | III | 174 | 144 | 164 | 154 | 20 | KR9 22 | clay | light green-gray | Foram rich | FeS mottling common flesh colored mottling rare | vertical worm burrows common throughout | | | extremely malleable and moisture | |
| 9 | III | 174 | 114 | 134 | 124 | 20 | KR9 23 | clay | light green-gray | Foram rich | FeS mottling common flesh colored mottling rare | vertical worm burrows common throughout | | | extremely malleable and moisture | |
| 9 | III | 174 | 84 | 104 | 94 | 20 | KR9 24 | clay | light green-gray | Foram rich | FeS mottling common flesh colored mottling rare | vertical worm burrows common throughout | | | extremely malleable and moisture | |
| 9 | III | 174 | 54 | 74 | 64 | 20 | KR9 25 | clay | light green-gray | Foram rich | FeS mottling common flesh colored mottling rare | vertical worm burrows common throughout | | | extremely malleable and moisture | |
| 9 | III | 174 | 24 | 44 | 34 | 20 | KR9 26 | clay | light green-gray | Foram rich | FeS mottling common flesh colored mottling rare | | | very malleable and increasing moisture | silt dispersed in clay matrix | |
| 10 | I | 289 | 682 | 697 | 690 | 15 | KR10 01 | clay | light green-gray | Forams bearing | FeS mottling rare | gas cracks common t-out | Firm | | one gas crack | |
| 10 | I | 289 | 657 | 672 | 665 | 15 | KR10 02 | clay | light green-gray | Forams bearing | FeS mottling rare | gas cracks common t-out | Firm | | | |
| 10 | I | 289 | 632 | 647 | 640 | 15 | KR10 03 | clay | light green-gray | Forams bearing | FeS mottling rare | gas cracks common t-out | Firm | | | |
| 10 | I | 289 | 607 | 622 | 615 | 15 | KR10 04 | clay | light green-gray | Forams bearing | FeS mottling rare; rare flesh/copper colored | gas cracks rare t-out | Firm | | | |
| 10 | I | 289 | 582 | 597 | 590 | 15 | KR10 05 | clay | light green-gray | Forams bearing | FeS mottling rare; rare flesh/copper colored | gas cracks rare t-out | Firm | | | |
| 10 | I | 289 | 557 | 572 | 565 | 15 | KR10 06 | clay | light green-gray | Forams bearing | FeS mottling common; Flesh/copper colored | gas cracks rare t-out | Firm | | | |
| 10 | I | 289 | 532 | 547 | 540 | 15 | KR10 07 | clay | light green-gray | Forams bearing | FeS mottling common; Flesh/copper colored | gas cracks rare t-out | malleable | oil streaks? | | |
| 10 | I | 289 | 507 | 522 | 515 | 15 | KR10 08 | clay | light green-gray | Forams bearing | FeS mottling common; Flesh/copper colored | gas cracks rare t-out | malleable | oil streaks? | | |
| 10 | I | 289 | 482 | 497 | 490 | 15 | KR10 09 | clay | light green-gray | Forams bearing | FeS mottling common; Flesh/copper colored | gas cracks rare t-out | malleable | oil streaks? H2S odor | | |
| 10 | I | 289 | 457 | 472 | 465 | 15 | KR10 10 | clay | light green-gray | Forams bearing | FeS mottling common; Flesh/copper colored | gas cracks rare t-out | malleable | oil streaks? H2S odor | | |
| 10 | I | 289 | 428 | 447 | 438 | 19 | KR10 11 | clay | light green-gray | Forams bearing | FeS mottling common patches common | gas cracks rare t-out | malleable | common oil or iron streaks? | | X |
| 10 | II | 307 | 398 | 418 | 408 | 20 | KR10 12 | clay | light brown-flesh-gray | Foram bearing | FeS mottling rare | | | very malleable | | |
| 10 | II | 307 | 368 | 388 | 378 | 20 | KR10 13 | clay | light brown-flesh-gray | Foram bearing | FeS mottling rare | | | very malleable | | |
| 10 | II | 307 | 338 | 358 | 348 | 20 | KR10 14 | thick, medium grained, quartz rich sand layer | light brown-flesh-gray | Foram bearing | FeS mottling rare | | | very malleable | | |
| 10 | II | 307 | 308 | 328 | 318 | 20 | KR10 15 | clay | light brown-flesh-gray | Foram bearing | FeS mottling rare | | | very malleable, increased moisture | | |
| 10 | II | 307 | 278 | 298 | 288 | 20 | KR10 16 | clay | light brown-flesh-gray | Foram bearing | FeS mottling rare | | | very malleable, increased moisture | | |

| | | | | | | | | | | | | | |
|----|-----|-----|-----|-----|-----|----|---------|---------------------------------------|------------------------|------------------------------------|---|---------------------------------------|------------------------------------|
| 10 | II | 307 | 248 | 268 | 258 | 20 | KR10 17 | <1cm diameter, FeS stained sand | light brown-flesh-gray | Foram bearing | FeS mottling rare | | very malleable, increased moisture |
| 10 | II | 307 | 218 | 238 | 228 | 20 | KR10 18 | clay | light brown-flesh-gray | Foram bearing | FeS mottling rare | | very malleable, increased moisture |
| 10 | II | 307 | 188 | 208 | 198 | 20 | KR10 19 | clay | light brown-flesh-gray | Foram bearing | FeS mottling rare | rare worm burrows throughout | very malleable, increased moisture |
| 10 | II | 307 | 158 | 178 | 168 | 20 | KR10 20 | Small, FeS stained sand pockets t-out | light brown-flesh-gray | Foram rich | FeS mottling rare | common worm burrows throughout | very malleable, increased moisture |
| 10 | II | 307 | 121 | 143 | 132 | 22 | KR10 21 | Small, FeS stained sand pockets t-out | light brown-flesh-gray | Foram rich | FeS mottling rare | common worm burrows throughout | very malleable, increased moisture |
| 10 | III | 121 | 86 | 111 | 99 | 25 | KR10 22 | Small, FeS stained sand pockets t-out | light brown-flesh-gray | Foram rich | FeS mottling rare | common worm burrows throughout | very malleable, increased moisture |
| 10 | III | 121 | 51 | 76 | 64 | 25 | KR10 23 | Small, FeS stained sand pockets t-out | light brown-flesh-gray | Foram rich | FeS mottling rare | common worm burrows throughout | very malleable, increased moisture |
| 10 | III | 121 | 11 | 41 | 26 | 30 | KR10 24 | Small, FeS stained sand pockets t-out | light brown-flesh-gray | Foram rich | FeS mottling rare | common worm burrows throughout | very malleable, increased moisture |
| 11 | I | 290 | 652 | 667 | 660 | 15 | KR11 01 | clay | light green-gray | Foram bearing | rare | | firm |
| 11 | I | 290 | 627 | 642 | 635 | 15 | KR11 02 | clay | light green-gray | Foram bearing | rare | | firm |
| 11 | I | 290 | 602 | 617 | 610 | 15 | KR11 03 | clay | light green-gray | Foram bearing | common; copper color mottles rare abundant; | | firm |
| 11 | I | 290 | 577 | 592 | 585 | 15 | KR11 04 | clay | light green-gray | Foram bearing | common; copper color mottles rare | | firm |
| 11 | I | 290 | 552 | 567 | 560 | 15 | KR11 05 | FeS stained sand pocket ~2cm | light green-gray | Foram bearing | common; copper color mottles rare | | firm |
| 11 | I | 290 | 522 | 542 | 532 | 20 | KR11 06 | clay | light green-gray | Foram bearing | common; copper color mottles rare | | malleable |
| 11 | I | 290 | 492 | 512 | 502 | 20 | KR11 07 | clay | light green-gray | Foram bearing | rare | | malleable |
| 11 | I | 290 | 462 | 482 | 472 | 20 | KR11 08 | clay; 1cm sand lens | light green-gray | Foram bearing | ~1-2cm diameter and 1mm thick | vertical worm burrow? | malleable |
| 11 | I | 290 | 432 | 452 | 442 | 20 | KR11 09 | clay; 1 FeS stained sand lens | light green-gray | Foram bearing | ~1-2cm diameter and 1mm thick | | malleable |
| 11 | I | 290 | 397 | 422 | 410 | 25 | KR11 10 | clay; 11/2cm sand lens | light green-gray | Foram rich | rare t-out FeS lenses rare | | very malleable |
| 11 | II | 307 | 367 | 387 | 377 | 20 | KR11 11 | clay; sand lens 1cm diameter | light green-gray | Foram bearing | ~1-2cm diameter and 1mm thick | | very malleable |
| 11 | II | 307 | 337 | 357 | 347 | 20 | KR11 12 | clay | light green-gray | Foram bearing | rare t-out | | very malleable |
| 11 | II | 307 | 307 | 327 | 317 | 20 | KR11 13 | thick sand layer | light green-gray | Foram bearing | FeS mottling rare | | very malleable |
| 11 | II | 307 | 277 | 297 | 287 | 20 | KR11 14 | clay | light green-gray | Foram bearing | FeS mottling rare | | very malleable & moist |
| 11 | II | 307 | 247 | 267 | 257 | 20 | KR11 15 | clay | light green-gray | Foram bearing | FeS mottling rare | | very malleable & moist |
| 11 | II | 307 | 217 | 237 | 227 | 20 | KR11 16 | clay | light green-gray | Foram bearing | FeS mottling common | | very malleable & moist |
| 11 | II | 307 | 187 | 207 | 197 | 20 | KR11 17 | clay | light green-gray | Foram bearing | FeS mottling common | vertical worm burrows rare throughout | very malleable & moist |
| 11 | II | 307 | 157 | 177 | 167 | 20 | KR11 18 | clay | light green-gray | Foram bearing | common; copper color mottles rare | vertical worm burrows rare throughout | very malleable & moist |
| 11 | II | 307 | 127 | 147 | 137 | 20 | KR11 19 | clay | light green-gray | Foram bearing | common; copper color mottles rare | vertical worm burrows rare throughout | very malleable & moist |
| 11 | II | 307 | 90 | 117 | 104 | 27 | KR11 20 | clay | light brown | Foram rich | common; copper color mottles rare | vertical worm burrows rare throughout | very malleable & moist |
| 11 | III | 90 | 60 | 80 | 70 | 20 | KR11 21 | clay | light brown | Foram rich | common; copper color mottles rare | vertical worm burrows rare throughout | very malleable & moist |
| 11 | III | 90 | 30 | 50 | 40 | 20 | KR11 22 | clay | light brown-flesh clay | Foram rich | common | vertical worm burrows rare throughout | very malleable & moist |
| 11 | III | 90 | 0 | 20 | 10 | 20 | KR11 23 | clay | Iron-red-brown | Foram-rich; shell fragments common | No distinct FeS apparent | vertical worm burrows rare throughout | X |

| | | | | | | | | | | | | | |
|----|-----|-----|-----|-----|-----|----|---------|--|------------------|---------------|---|---|---------------------------|
| 12 | I | 290 | 691 | 706 | 699 | 15 | KR12 01 | clay | light green-gray | Foram bearing | common; 1/4cm diameter pyritized common; copper colored mottling rare | malleable & moist | |
| 12 | I | 290 | 666 | 681 | 674 | 15 | KR12 02 | clay | light green-gray | Foram bearing | common; copper colored mottling rare | malleable & moist | |
| 12 | I | 290 | 641 | 656 | 649 | 15 | KR12 03 | clay | light green-gray | Foram bearing | common; copper colored mottling rare | malleable & moist | |
| 12 | I | 290 | 611 | 631 | 621 | 20 | KR12 04 | clay | light gray-brown | Foram bearing | rare | malleable | |
| 12 | I | 290 | 581 | 601 | 591 | 20 | KR12 05 | clay | light gray-brown | Foram bearing | rare | malleable | |
| 12 | I | 290 | 551 | 571 | 561 | 20 | KR12 06 | clay | light gray-brown | Foram bearing | rare | malleable | |
| 12 | I | 290 | 521 | 541 | 531 | 20 | KR12 07 | thick, medium grained, quartz rich sand layer sand patches t-out | light gray-brown | Foram bearing | FeS mottling rare | malleable & moist | |
| 12 | I | 290 | 491 | 511 | 501 | 20 | KR12 08 | sand patches t-out | light gray-brown | Foram bearing | FeS mottling rare | malleable & moist | |
| 12 | I | 290 | 461 | 481 | 471 | 20 | KR12 09 | sand patches t-out | light gray-brown | Foram bearing | FeS mottling rare | malleable & moist | |
| 12 | I | 290 | 696 | 716 | 706 | 20 | KR12 10 | sand patches t-out | light gray-brown | Foram rich | FeS mottling rare | very wet and malleable | 1cm gas crack? |
| 12 | II | 308 | 376 | 396 | 386 | 20 | KR12 11 | sand patches t-out | light gray-brown | Foram bearing | FeS mottling rare | malleable & moist | |
| 12 | II | 308 | 346 | 366 | 356 | 20 | KR12 12 | sand patches t-out | light gray-brown | Foram bearing | FeS mottling rare | malleable & moist | |
| 12 | II | 308 | 316 | 336 | 326 | 20 | KR12 13 | clay; rare sand patches t-out | light gray-brown | Foram bearing | 5cm long, 2cm wide, FeS stained, foram rich burrow | malleable & moist | |
| 12 | II | 308 | 286 | 306 | 296 | 20 | KR12 14 | clay; rare sand patches t-out | light gray-brown | Foram bearing | 3cm long, 1cm wide, FeS stained, foram rich burrow | malleable & moist | |
| 12 | II | 308 | 256 | 276 | 266 | 20 | KR12 15 | sand patches t-out | light gray-brown | Foram bearing | FeS mottling rare | very malleable & moist | |
| 12 | II | 308 | 226 | 246 | 236 | 20 | KR12 16 | deck, no sample | | | | | |
| 12 | II | 308 | 191 | 216 | 204 | 25 | KR12 17 | clay | light gray-brown | Foram bearing | FeS mottling common | malleable & moist | X X |
| 12 | II | 308 | 161 | 181 | 171 | 20 | KR12 18 | clay | light gray-brown | Foram rich | FeS mottling abundant | vertical worm burrows rare throughout | very malleable & moist |
| 12 | II | 308 | 128 | 151 | 140 | 23 | KR12 19 | clay | light gray-brown | Foram rich | FeS mottling abundant | vertical worm burrows rare throughout | very malleable & moist |
| 12 | III | 128 | 93 | 118 | 106 | 25 | KR12 20 | clay | light gray-brown | Foram rich | FeS mottling rare | vertical worm burrows abundant throughout | extremely wet & malleable |
| 12 | III | 128 | 58 | 83 | 71 | 25 | KR12 21 | clay | light gray-brown | Foram rich | FeS mottling rare | vertical worm burrows abundant throughout | extremely wet & malleable |
| 12 | III | 128 | 23 | 48 | 36 | 25 | KR12 22 | clay | light gray-brown | Foram rich | FeS mottling rare | vertical worm burrows abundant throughout | extremely wet & malleable |

| | | | | | | | | | | | | | | |
|----|-----|-----|-----|-----|-----|----|---------|---|------------------------|--|---|------------------------|---------------------------------------|-----|
| 13 | I | 289 | 658 | 673 | 666 | 15 | KR13 01 | clay | light green-brown-gray | Foram bearing | FeS mottling rare; copper mottling rare; rare; copper mottling common | malleable | | |
| 13 | I | 289 | 633 | 648 | 641 | 15 | KR13 02 | clay | light green-brown-gray | Foram bearing; Shell fragments rare | FeS mottling rare; copper mottling common | malleable | faint oil streak and H2S odor | X |
| 13 | I | 289 | 603 | 623 | 613 | 20 | KR13 03 | clay | light green-brown-gray | Foram bearing; Shell fragments rare | FeS mottling rare; copper mottling common | malleable | faint oil streak and H2S odor | |
| 13 | I | 289 | 573 | 593 | 583 | 20 | KR13 04 | clay | light green-brown-gray | Foram bearing; Shell fragments rare | FeS mottling rare; copper mottling common | malleable | shell and FeS rich layer, including 1 | X X |
| 13 | I | 289 | 543 | 563 | 553 | 20 | KR13 05 | clay | light green-brown-gray | Foram bearing; Shell fragments concentrated in 1cm layer | FeS mottling rare; copper mottling common | malleable | | |
| 13 | I | 289 | 513 | 533 | 523 | 20 | KR13 06 | clay | light green-brown-gray | Foram bearing; Shell fragments concentrated in 1cm layer | FeS mottling rare; copper mottling common; pyrite grains, mm size, rare t-out | malleable | | |
| 13 | I | 289 | 483 | 503 | 493 | 20 | KR13 07 | clay | light green-brown-gray | Foram bearing | FeS mottling rare; copper mottling common; pyrite grains, mm size, rare t-out | malleable | | |
| 13 | I | 289 | 453 | 473 | 463 | 20 | KR13 08 | clay | light green-brown-gray | Foram bearing; Shell fragments concentrated in 1cm layer | FeS mottling rare; copper mottling rare | malleable & moist | | |
| 13 | I | 289 | 423 | 443 | 433 | 20 | KR13 09 | clay | light green-brown-gray | Foram bearing; Shell fragments concentrated in 1cm layer | FeS mottling rare; copper mottling rare | malleable & moist | | |
| 13 | II | 309 | 369 | 394 | 382 | 25 | KR13 10 | clay | light green-brown-gray | Foram bearing; Shell fragments concentrated in 1cm layer | FeS mottling rare; copper mottling rare | malleable & moist | | |
| 13 | II | 309 | 334 | 359 | 347 | 25 | KR13 11 | clay | light green-brown-gray | Foram bearing; Shell fragments concentrated in 1cm layer | FeS mottling rare; copper mottling rare | malleable & moist | | |
| 13 | II | 309 | 299 | 324 | 312 | 25 | KR13 12 | stained sand pocket, ~2cm diameter | light gray | foram bear | FeS mottling moderate | very malleable & moist | | |
| 13 | II | 309 | 264 | 289 | 277 | 25 | KR13 13 | clay | light gray | foram rich | FeS mottling moderate | very malleable & moist | | |
| 13 | II | 309 | 229 | 254 | 242 | 25 | KR13 14 | clay | light gray | foram rich | FeS mottling moderate | very malleable & moist | | |
| 13 | II | 309 | 194 | 219 | 207 | 25 | KR13 15 | clay | light gray | foram rich | FeS mottling moderate | very malleable & moist | | |
| 13 | II | 309 | 159 | 184 | 172 | 25 | KR13 16 | clay | light gray | foram rich | FeS mottling moderate | very malleable & moist | | |
| 13 | II | 309 | 124 | 149 | 137 | 25 | KR13 17 | clay | light gray | foram rich | FeS mottling moderate | very malleable & moist | | |
| 13 | III | 95 | 60 | 85 | 73 | 25 | KR13 18 | thick, medium grained, quartz rich sand layer; <1cm diameter sand | light gray | foram rich | FeS mottling moderate; copper color mottling rare t-out | very malleable & moist | | |
| 13 | III | 95 | 25 | 50 | 38 | 25 | KR13 19 | clay; <1cm diameter sand pockets rare t-out | light gray | foram rich | FeS mottling moderate; copper color mottling moderate t-out | very malleable & moist | | |

| | | | | | | | | | | | | | | | | |
|----|-----|-----|-----|-----|-----|----|---------|---------------------------------------|------------------|---|-------------------------|---|--|---|--------------------------------------|-----|
| 14 | I | 292 | 666 | 681 | 674 | 15 | KR14 01 | clay | light green-gray | foram bearing; shell fragments rare t-out | FeS mottling rare | | Salmon texture | dry, firm | H2S odor, visible hydrate | |
| 14 | I | 292 | 641 | 656 | 649 | 15 | KR14 02 | clay | light green-gray | shell fragments including 1 large piece rare t-out | FeS mottling rare | slime, gooney, snot like substance ??? Dead worm??? | Salmon texture / Gas cracks | dry, firm | H2S odor, visible hydrate | X X |
| 14 | I | 292 | 616 | 631 | 624 | 15 | KR14 03 | clay | light green-gray | foram bearing; shell fragments rare t-out | FeS mottling rare | | Salmon texture rare / 3cm diameter moussey pocket with oil stain | dry, firm | H2S odor | X |
| 14 | I | 292 | 591 | 606 | 599 | 15 | KR14 04 | clay | light green-gray | foram bearing; shell fragments rare t-out | FeS mottling rare | | Salmon texture rare / 4cm x 2cm diameter moussey pocket | dry, firm | H2S odor, oil pocket ~1/2cm diameter | X |
| 14 | I | 292 | 566 | 581 | 574 | 15 | KR14 05 | clay | light green-gray | foram bearing | rare | | | maileable | | |
| 14 | I | 292 | 541 | 556 | 549 | 15 | KR14 06 | clay | light green-gray | foram bearing | rare | | | maileable | | |
| 14 | I | 292 | 516 | 531 | 524 | 15 | KR14 07 | clay | light green-gray | foram bearing | FeS mottling rare | | 2 small moussey pockets, <2cm diameter | maileable | | |
| 14 | I | 292 | 491 | 506 | 499 | 15 | KR14 08 | clay | light green-gray | foram bearing; shell fragments rare t-out | FeS mottling rare | | | maileable | | |
| 14 | I | 292 | 466 | 481 | 474 | 15 | KR14 09 | clay | light green-gray | foram bearing; shell fragments rare t-out | FeS mottling rare | rare; possible <1cm diameter authigenic carbonate | small moussey pocket near shell fragments, 1cm diameter | maileable | | |
| 14 | I | 292 | 446 | 456 | 451 | 10 | KR14 10 | medium grained, quartz rich sand lens | light green-gray | foram bearing; shell hash abundant at sand pocket | FeS mottling rare t-out | | | maileable; shell hash/sand area was wet | | |
| 14 | I | 292 | 426 | 436 | 431 | 10 | KR14 11 | clay | light green-gray | 2cm thick shell hash-clay interval with whole gastropod | FeS mottling rare | | small moussey pocket near shell fragments, <2cm diameter | maileable; shell has area was wet | | X |
| 14 | II | 307 | 384 | 399 | 392 | 15 | KR14 12 | clay | light green-gray | foram bearing; 2cm thick shell hash-clay interval | FeS mottling rare | | small moussey pocket near shell fragments, <2cm diameter | maileable; shell has area was wet | | X |
| 14 | II | 307 | 354 | 374 | 364 | 20 | KR14 13 | clay | light gray | foram bearing | FeS mottling rare | | | maileable & moist | | |
| 14 | II | 307 | 324 | 344 | 334 | 20 | KR14 14 | clay | light gray | foram bearing | FeS mottling rare | | | very maileable & moist | | |
| 14 | II | 307 | 294 | 314 | 304 | 20 | KR14 15 | clay | light gray | foram bearing | FeS mottling rare | | | very maileable & moist | | |
| 14 | II | 307 | 264 | 284 | 274 | 20 | KR14 16 | clay | light gray | foram bearing | rare; copper colored | | | very maileable & moist | I2S odor t-out | |
| 14 | II | 307 | 234 | 254 | 244 | 20 | KR14 17 | clay | light gray | foram bearing | mottling rare | colored | | very maileable & moist | I2S odor t-out | |
| 14 | II | 307 | 204 | 224 | 214 | 20 | KR14 18 | clay | light green-gray | foram rich | FeS mottling rare | pockets of concentrated forams | | very maileable & moist | | |
| 14 | II | 307 | 174 | 194 | 184 | 20 | KR14 19 | clay | light green-gray | foram rich | FeS mottling rare | pockets of concentrated forams | | very maileable & moist | | |
| 14 | II | 307 | 144 | 164 | 154 | 20 | KR14 20 | clay | light green-gray | foram rich | FeS mottling rare | pockets of concentrated forams | | very maileable & moist | | |
| 14 | II | 307 | 119 | 134 | 127 | 15 | KR14 21 | clay | light green-gray | foram rich | FeS mottling rare | vertical worm burrows densely/complete ly packed with forams | | very maileable & moist | | |
| 14 | III | 102 | 82 | 102 | 92 | 20 | KR14 22 | clay | light green-gray | foram rich | FeS mottling rare | vertical worm burrows densely/complete ly packed with forams | | very maileable & moist | | |
| 14 | III | 102 | 52 | 72 | 62 | 20 | KR14 23 | clay | light green-gray | foram rich | FeS mottling rare | vertical worm burrows densely containing foram "nodules"/burrow casts | | very maileable & moist | | |

| | | | | | | | | | | | | | | | | |
|----|----|-----|-----|-----|-----|----|---------|------|-------------------------------------|---|-------------------|--|---|------------------------|-------------------------|---|
| 15 | I | 276 | 251 | 266 | 259 | 15 | KR15 01 | clay | light gray | foram bearing | FeS mottling rare | vertical burrow lined sparsely with forams | 2cm wide x 6cm long soupy vug in middle of sample | firm | H2S odor | |
| 15 | I | 276 | 226 | 241 | 234 | 15 | KR15 02 | clay | light gray | foram bearing | FeS mottling rare | | | firm | H2S odor | X |
| 15 | I | 276 | 201 | 216 | 209 | 15 | KR15 03 | clay | light gray | foram bearing to rich | FeS mottling rare | | | malleable | | |
| 15 | I | 276 | 176 | 191 | 184 | 15 | KR15 04 | clay | light gray | foram bearing to rich | FeS mottling rare | | | malleable | | |
| 15 | I | 276 | 151 | 166 | 159 | 15 | KR15 05 | clay | light gray | to rich; intact bivalve shells, 3 of them | FeS mottling rare | vertical burrows rare t-out | 2cm diameter soupy void near shells | malleable | | |
| 15 | I | 276 | 126 | 141 | 134 | 15 | KR15 06 | clay | light gray | foram bearing to rich; shell fragments t-out | FeS mottling rare | | | moist & malleable | | |
| 15 | I | 276 | 101 | 116 | 109 | 15 | KR15 07 | clay | light gray | foram bearing to rich; shell fragments and bivalve shells t-out | FeS mottling rare | | soupy voids with higher concentrations of forams | moist & malleable | | |
| 15 | I | 276 | 76 | 91 | 84 | 15 | KR15 08 | clay | light gray | foram bearing to rich; shell fragments and bivalve shells t-out | FeS mottling rare | vertical burrows rare t-out | soupy voids with higher concentrations of forams | moist & malleable | | |
| 15 | I | 276 | 51 | 66 | 59 | 15 | KR15 09 | clay | light gray | shell fragments rare | FeS mottling rare | vertical burrows abundant t-out | | very wet and malleable | | |
| 15 | I | 276 | 26 | 41 | 34 | 15 | KR15 10 | clay | light gray | shell fragments rare | FeS mottling rare | vertical burrows abundant t-out | | very wet and malleable | | |
| 16 | I | 301 | 857 | 872 | 865 | 15 | KR16 01 | clay | light brown-flesh-gray mottled clay | forams rare t-out | FeS mottling rare | | | moist but firm | | |
| 16 | I | 301 | 832 | 847 | 840 | 15 | KR16 02 | clay | light brown-flesh-gray mottled clay | forams rare t-out | FeS mottling rare | | | moist but firm | | |
| 16 | I | 301 | 807 | 822 | 815 | 15 | KR16 03 | clay | light brown-flesh-gray mottled clay | forams rare t-out | FeS mottling rare | | | moist but firm | | |
| 16 | I | 301 | 782 | 797 | 790 | 15 | KR16 04 | clay | light brown-flesh-gray mottled clay | forams rare t-out | FeS mottling rare | | | moist but firm | mottling of clay colors | |
| 16 | I | 301 | 757 | 772 | 765 | 15 | KR16 05 | clay | light gray-brown | forams rare t-out | FeS mottling rare | | | malleable & moist | | |
| 16 | I | 301 | 732 | 747 | 740 | 15 | KR16 06 | clay | light gray-brown | forams rare t-out | FeS mottling rare | | | malleable & moist | | |
| 16 | I | 301 | 702 | 722 | 712 | 20 | KR16 07 | clay | light gray-brown | forams rare t-out | FeS mottling rare | | | malleable & moist | | |
| 16 | I | 301 | 672 | 692 | 682 | 20 | KR16 08 | clay | light gray-brown | forams rare t-out | FeS mottling rare | | | malleable & moist | | |
| 16 | I | 301 | 642 | 662 | 652 | 20 | KR16 09 | clay | light gray-brown | forams rare t-out | FeS mottling rare | | | malleable & moist | | |
| 16 | I | 301 | 612 | 632 | 622 | 20 | KR16 10 | clay | light gray-brown | forams rare t-out | FeS mottling rare | | | malleable & moist | | |
| 16 | II | 304 | 580 | 590 | 585 | 10 | KR16 11 | clay | light gray-brown | forams rare t-out | FeS mottling rare | | vertical fracture through entire sample, interior is soupy | malleable & moist | | |
| 16 | II | 304 | 550 | 570 | 560 | 20 | KR16 12 | clay | light gray-brown | forams rare t-out | FeS mottling rare | | vertical fracture through entire sample, aperture of 2cm, interior is soupy | malleable & moist | | X |
| 16 | II | 304 | 520 | 540 | 530 | 20 | KR16 13 | clay | light gray-brown | forams rare t-out | FeS mottling rare | | vertical fracture through entire sample, aperture of 2cm, interior is soupy | malleable & moist | | X |
| 16 | II | 304 | 490 | 510 | 500 | 20 | KR16 14 | clay | light gray-brown | forams rare t-out | FeS mottling rare | | vertical fracture through entire sample, aperture of 2cm, interior is soupy | malleable & moist | | X |
| 16 | II | 304 | 460 | 480 | 470 | 20 | KR16 15 | clay | light gray-brown | forams rare t-out | FeS mottling rare | | vertical fracture through entire sample, aperture of 2cm, interior is soupy | malleable & moist | | |
| 16 | II | 304 | 430 | 450 | 440 | 20 | KR16 16 | clay | light gray-brown | forams rare t-out | FeS mottling rare | | vertical fracture through entire sample, aperture is narrowing, interior is soupy | very moist & malleable | | |

| | | | | | | | | | | | | | | | | | |
|----|-----|-----|-----|-----|-----|-----|---------|-----------------------|------------------|---|--|--|-------------------|-----------------|---|---|---|
| 17 | I* | 302 | 714 | 729 | 722 | 15 | KR17 01 | clay | light gray | small <1cm length calcareous worm | FeS mottling rare | | firm | H2S odor | X | X | *Section III was not sampled but was measured at 137cm total length |
| 17 | I | 302 | 689 | 704 | 697 | 15 | KR17 02 | clay | light gray | foram bearing | rare; light brown mottles, <1cm | | firm | H2S odor | | | *Section 1 top liner overlapped by 20cm with section 2 liner so 20cm added to section 1 sample depths |
| 17 | I | 302 | 664 | 679 | 672 | 15 | KR17 03 | clay | light gray | foram bearing | FeS mottling rare; light brown mottles, <1cm | | moist but firm | H2S odor faint | | | |
| 17 | I | 302 | 634 | 654 | 644 | 20 | KR17 04 | clay | light gray | foram bearing; 1 small pocket of shell hash | FeS mottles common | small pockets of forams rare t-out | moist but firm | | | | Section 2 at base of section interval is very fluid |
| 17 | I | 302 | 604 | 624 | 614 | 20 | KR17 05 | clay | light gray | foram bearing; 1 small pocket of shell hash | FeS mottles common | small pockets of forams common t-out | moist but firm | | | | Sample 125 taken but porewater sample acquired but volume was not recorded/forgotten |
| 17 | I | 302 | 574 | 594 | 584 | 20 | KR17 06 | clay | light gray | foram bearing; 1 small pocket of shell hash | light green mottling rare t-out | small pockets of forams common t-out | moist & malleable | | | | |
| 17 | I | 302 | 544 | 564 | 554 | 20 | KR17 07 | clay | light green-gray | foram bearing | FeS mottling rare | | moist & malleable | | | | |
| 17 | I | 302 | 514 | 534 | 524 | 20 | KR17 08 | clay | light green-gray | foram bearing | FeS mottling rare | | moist & malleable | | | | |
| 17 | I | 302 | 484 | 504 | 494 | 20 | KR17 09 | clay disturbed sample | light green-gray | foram bearing | FeS mottling rare | vertical, FeS stained burrow, 1/2 cm diameters and 20 cm long, shell casement from worm is lining the burrow | moist & malleable | | X | | |
| 17 | I | 302 | 447 | 474 | 461 | 27 | KR17 10 | | | | | | | | | | |
| 17 | II | 290 | 412 | 437 | 425 | 25 | KR17 11 | clay | light green-gray | foram bearing | FeS mottling abundant | burrows abundant | soupy & wet t-out | | | | |
| 17 | II | 290 | 377 | 402 | 390 | 25 | KR17 12 | clay | light green-gray | foram bearing | FeS mottling abundant | burrows abundant | soupy & wet t-out | | | | |
| 17 | II | 290 | 337 | 367 | 352 | 30 | KR17 13 | clay | light green-gray | foram bearing | FeS mottling abundant | burrows abundant | soupy & wet t-out | liner cracked | | | |
| 17 | II | 290 | 302 | 327 | 315 | 25 | KR17 14 | clay | light green-gray | foram bearing | FeS mottling abundant | burrows abundant | soupy & wet t-out | | | | |
| 17 | II | 290 | 267 | 292 | 280 | 25 | KR17 15 | clay | light green-gray | foram bearing | FeS mottling abundant | burrows abundant | soupy & wet t-out | | | | |
| 17 | II | 290 | 232 | 257 | 245 | 25 | KR17 16 | clay | light green-gray | foram bearing | FeS mottling abundant | burrows abundant | soupy & wet t-out | dropped on deck | | | |
| 17 | II | 290 | 197 | 222 | 210 | 25 | KR17 17 | clay | light green-gray | foram bearing | FeS mottling abundant | burrows abundant | soupy & wet t-out | dropped on deck | | | |
| 17 | II | 290 | 177 | 197 | 187 | 20 | KR17 18 | clay | light green-gray | foram bearing | FeS mottling abundant | burrows abundant | soupy & wet t-out | | | | sample dropped on deck but preserved |
| 17 | III | 137 | 0 | 137 | 69 | 137 | KR17 19 | clay | light green-gray | foram bearing | FeS mottling abundant | burrows abundant | soupy & wet t-out | | | | liner cracked, only part of sample available for analysis |

| | | | | | | | | | | | | | |
|----|-----|-----|-----|-----|-----|----|---------|--|-------------------|---------------------------|---|--|--|
| 18 | I | 300 | 640 | 660 | 650 | 20 | KR18 01 | clay | light gray | foram bearing | FeS mottling abundant | bioturbation moderate; FeS stained, foram concentrated pockets | moist & malleable |
| 18 | I | 300 | 610 | 630 | 620 | 20 | KR18 02 | clay | light gray | foram bearing; shell hash | FeS mottling abundant; flesh colored patches rare | bioturbation moderate; FeS stained, foram concentrated pockets | moist & malleable |
| 18 | I | 300 | 580 | 600 | 590 | 20 | KR18 03 | clay | light gray | foram bearing; shell hash | FeS mottling abundant; patches abundant | bioturbation moderate; FeS stained, foram concentrated pockets | moist & malleable |
| 18 | I | 300 | 550 | 570 | 560 | 20 | KR18 04 | clay | light gray | foram bearing to rich | FeS mottling rare | | malleable |
| 18 | I | 300 | 520 | 540 | 530 | 20 | KR18 05 | thick, FeS stained sand | light gray | foram bearing to rich | FeS mottling common | | malleable |
| 18 | I | 300 | 490 | 510 | 500 | 20 | KR18 06 | clay | light gray | foram bearing | FeS mottling rare | | malleable |
| 18 | I | 300 | 460 | 480 | 470 | 20 | KR18 07 | thick sand lens/pocket | light gray | foram bearing | FeS mottling rare | | malleable |
| 18 | I | 300 | 430 | 450 | 440 | 20 | KR18 08 | clay | light gray | foram bearing | FeS mottling rare | | malleable |
| 18 | I | 300 | 380 | 410 | 395 | 30 | KR18 09 | FeS stained sand lens; rare sand pockets <1cm clay; rare sand pockets <1cm t-out | light gray | foram rich | FeS mottling rare; flesh colored mottling rare | bioturbation/wor m burrows rare t-out | moist & malleable |
| 18 | II | 302 | 345 | 370 | 358 | 25 | KR18 10 | | light gray | foram rich | FeS mottling rare; flesh colored mottling rare | bioturbation/wor m burrows rare t-out | moist & malleable |
| 18 | II | 302 | 310 | 335 | 323 | 25 | KR18 11 | clay | light brown -gray | foram rich | FeS mottling abundant | bioturbation/wor m burrows common t-out containing forams and sand | moist & malleable |
| 18 | II | 302 | 275 | 300 | 288 | 25 | KR18 12 | clay | light brown -gray | foram rich | FeS mottling abundant | bioturbation/wor m burrows common t-out containing forams and sand | moist & malleable |
| 18 | II | 302 | 240 | 265 | 253 | 25 | KR18 13 | clay | light brown -gray | foram rich | FeS mottling abundant | bioturbation/wor m burrows common t-out containing forams and sand | very moist & malleable |
| 18 | II | 302 | 205 | 230 | 218 | 25 | KR18 14 | clay | light brown -gray | foram rich | FeS mottling abundant | bioturbation/wor m burrows common t-out containing forams and sand | very moist & malleable |
| 18 | II | 302 | 170 | 195 | 183 | 25 | KR18 15 | clay | light brown -gray | foram rich | FeS mottling abundant | bioturbation/wor m burrows common t-out containing forams and sand | very moist & malleable |
| 18 | II | 302 | 135 | 160 | 148 | 25 | KR18 16 | clay | light brown -gray | foram rich | FeS mottling abundant | bioturbation/wor m burrows common t-out containing forams and sand | very moist & malleable |
| 18 | II | 302 | 100 | 125 | 113 | 25 | KR18 17 | clay | light brown -gray | foram rich | FeS mottling abundant | bioturbation/wor m burrows common t-out containing forams and sand | coring related disturbance extremely moist & malleable |
| 18 | III | 78 | 53 | 78 | 66 | 25 | KR18 18 | clay | light brown -gray | foram rich | FeS mottling abundant | bioturbation/wor m burrows common t-out containing forams and sand | coring related disturbance extremely moist & malleable |
| 18 | III | 78 | 18 | 43 | 31 | 25 | KR18 19 | clay | light brown -gray | foram rich | FeS mottling abundant | bioturbation/wor m burrows common t-out containing forams and sand | coring related disturbance extremely moist & malleable |

| | | | | | | | | | | | | | |
|----|------|-----|-----|-----|-----|----|---------|-------------------------------------|------------------------------------|---|--|--------------------------------|--|
| 19 | I | 302 | 669 | 689 | 679 | 20 | KR19 01 | clay | light brown-flesh | foram bearing rare shell fragments (<mm size) t- out | common and in small patches FeS mottling common and in small patches | firm | |
| 19 | I | 302 | 639 | 659 | 649 | 20 | KR19 02 | clay | light brown-flesh | rare shell fragments (<mm size) t- out | FeS mottling common and in small patches | firm | |
| 19 | I | 302 | 609 | 629 | 619 | 20 | KR19 03 | clay | light brown-flesh | rare shell fragments (<mm size) t- out | FeS mottling common and in small patches | firm | |
| 19 | I | 302 | 579 | 599 | 589 | 20 | KR19 04 | clay | light brown-flesh | rare shell fragments (<mm size) t- out | FeS mottling common and in small patches | firm | |
| 19 | I | 302 | 549 | 569 | 559 | 20 | KR19 05 | clay | light brown-flesh | rare shell fragments (<mm size) t- out | FeS mottling common and in small patches | firm | |
| 19 | I | 302 | 519 | 539 | 529 | 20 | KR19 06 | clay | light brown-flesh | rare shell fragments (<mm size) t- out | FeS mottling rare; light gray mottles rare t-out | malleable | |
| 19 | I | 302 | 484 | 509 | 497 | 25 | KR19 07 | clay | light brown-flesh | rare shell fragments (<mm size) t- out | FeS mottling rare; light gray mottles rare t-out | malleable | |
| 19 | I | 302 | 449 | 474 | 462 | 25 | KR19 08 | clay | light brown-flesh | rare shell fragments (<mm size) t- out | FeS mottling rare; light gray mottles rare t-out | moist & malleable | |
| 19 | I | 302 | 407 | 439 | 423 | 32 | KR19 09 | clay | light brown flesh to light gray | rare shell fragments (<mm size) t- out | FeS mottling rare; light gray mottles rare t-out | moist & malleable | |
| 19 | II | 303 | 367 | 397 | 382 | 30 | KR19 10 | clay | light gray | foram bearing; rare shell fragments (<mm size) t- out | common and in small patches; flesh colored mottles rare t- | moist & malleable | |
| 19 | II | 303 | 327 | 357 | 342 | 30 | KR19 11 | FeS stained sand pockets -1cm | light gray | foram bearing | FeS mottling rare | moist & malleable | |
| 19 | II | 303 | 287 | 317 | 302 | 30 | KR19 12 | clay | light gray | foram bearing | FeS mottling rare | moist & malleable | |
| 19 | II | 303 | 247 | 277 | 262 | 30 | KR19 13 | clay | light gray | foram bearing | FeS mottling rare | moist & malleable | |
| 19 | II | 303 | 207 | 237 | 222 | 30 | KR19 14 | clay | light gray | foram bearing | FeS mottling rare | moist & malleable | |
| 19 | II | 303 | 167 | 197 | 182 | 30 | KR19 15 | clay | light gray | foram bearing | FeS mottling rare moderate bioturbation/vertic al burrows | very moist & malleable | |
| 19 | II | 303 | 127 | 157 | 142 | 30 | KR19 16 | clay | light gray | foram bearing | FeS mottling rare moderate bioturbation/vertic al burrows | very moist & malleable | |
| 19 | III* | 105 | 75 | 105 | 90 | 30 | KR19 17 | clay | light gray | foram bearing | FeS mottling rare one large vertical burrow lined with forams | extremely moist & malleable | top 65cm of liner cracked, no samples taken |

| | | | | | | | | | | | | | | |
|----|-----|-----|-----|-----|-----|----|---------|------|------------------------|---|---|---|-----------------------------|---|
| 20 | I | 308 | 684 | 704 | 694 | 20 | KR20 01 | clay | light brown-flesh clay | foram rare | FeS mottling common | | malleable | |
| 20 | I | 308 | 654 | 674 | 664 | 20 | KR20 02 | clay | light brown-flesh clay | foram bearing | FeS mottling common; patches up to 1cm diameter | pods of forams and shell hash rare t-out up to 1cm diameter | malleable | |
| 20 | I | 308 | 619 | 644 | 632 | 25 | KR20 03 | clay | light brown-flesh clay | foram bearing | FeS mottling common; patches up to 1cm diameter | pods of forams and shell hash rare t-out up to 1cm diameter | malleable | |
| 20 | I | 308 | 584 | 609 | 597 | 25 | KR20 04 | clay | light brown-flesh clay | foram bearing | cohesive FeS patches up to 2cm diameter | pods of forams and shell hash rare t-out up to 1cm diameter | moist & malleable | |
| 20 | I | 308 | 549 | 574 | 562 | 25 | KR20 05 | clay | light brown-flesh clay | foram bearing | cohesive FeS patches up to 2cm diameter | pods of forams and shell hash rare t-out up to 1cm diameter | moist & malleable | |
| 20 | I | 308 | 514 | 539 | 527 | 25 | KR20 06 | clay | light gray | foram bearing | rare; pyrite grains <1mm | | malleable | |
| 20 | I | 308 | 458 | 494 | 476 | 36 | KR20 07 | clay | light gray | foram bearing | FeS mottles rare; faint flesh and teal colored mottles rare t-rare; faint flesh and teal colored mottles rare t-rare; | pods of forams and sand t-out up to 3cm diameter | malleable | |
| 20 | I | 308 | 416 | 444 | 430 | 28 | KR20 08 | clay | light gray | foram bearing | flesh and teal colored mottles rare t-rare; faint flesh and teal colored mottles rare t-rare; | foram pockets rare t-out | moist & malleable | |
| 20 | II | 301 | 376 | 406 | 391 | 30 | KR20 09 | clay | light gray | foram bearing | flesh and teal colored mottles rare t-rare; Cohesive FeS patches, up to 2cm diameter, rare; | foram pockets rare t-out | moist & malleable | |
| 20 | II | 301 | 336 | 366 | 351 | 30 | KR20 10 | clay | light gray-brown | foram bearing | Cohesive FeS patches, up to 2cm diameter, rare; | <1cm diameter foram pods | moist & malleable | |
| 20 | II | 301 | 296 | 326 | 311 | 30 | KR20 11 | clay | light gray-brown | foram bearing | Cohesive FeS patches, up to 2cm diameter, FeS mottling rare | <1cm diameter foram pods | moist & malleable | |
| 20 | II | 301 | 256 | 286 | 271 | 30 | KR20 12 | clay | light gray-brown | foram bearing | FeS mottling rare; 2cm thick FeS stained granular layer that may be carbonate precipitate, seems | <1cm diameter foram pods | moist & malleable | |
| 20 | II | 301 | 216 | 246 | 231 | 30 | KR20 13 | clay | light gray-brown | foram bearing | FeS mottling rare | 1 worm burrow, vertical and foram lined | moist & malleable | |
| 20 | II | 301 | 176 | 206 | 191 | 30 | KR20 14 | clay | light gray-brown | foram bearing; small whole bivalve (clam) shell | FeS mottling rare | vertical burrows t-out with concentration of forams within | very moist & malleable | X |
| 20 | II | 301 | 115 | 156 | 136 | 41 | KR20 15 | clay | light gray-brown | foram bearing | FeS mottling rare | vertical burrows t-out with concentration of forams within | very moist & malleable | |
| 20 | III | 115 | 75 | 105 | 90 | 30 | KR20 16 | clay | light gray-brown | foram bearing | FeS mottling rare | concentration of forams within | very moist & malleable | |
| 20 | III | 115 | 35 | 65 | 50 | 30 | KR20 17 | clay | light gray-brown | foram rich | FeS mottling rare | abundant vertical burrows t-out with concentration of forams within | extremely moist & malleable | |
| 20 | III | 115 | 0 | 25 | 13 | 25 | KR20 18 | clay | light gray-brown | foram rich | FeS mottling rare | abundant vertical burrows t-out with concentration of forams within | extremely moist & malleable | |

| | | | | | | | | | | | | | | | |
|----|-----|-----|-----|-----|-----|----|---------|------|--|--|---|-----------------------------|-------------------|---------------------------|----------------------------------|
| 21 | I | 303 | 722 | 732 | 710 | 10 | KR21 01 | clay | gray | up to 3cm diameter bivalve shells whole and fragments FeS mottling abundant | | | very dry and firm | X | sample is from core cutting shoe |
| 21 | I | 303 | 682 | 702 | 678 | 20 | KR21 02 | clay | gray | foram bearing; shell fragments common t-out FeS mottling common t-out | gas cracks; salmon texture | dry, firm | | | |
| 21 | I | 303 | 657 | 672 | 651 | 15 | KR21 03 | clay | gray | foram bearing; shell fragments common t-out FeS mottling common t-out | gas cracks; salmon texture | firm | | | |
| 21 | I | 303 | 627 | 647 | 622 | 20 | KR21 04 | clay | gray | foram bearing; shell fragments common t-out FeS mottling common t-out | 3 soupy pockets ~3cm diameter; salmon texture; gas cracks t-out | moist but firm | | | |
| 21 | I | 303 | 597 | 617 | 592 | 20 | KR21 05 | clay | light gray | foram bearing; shell fragments common t-out FeS mottling common t-out | soupy pockets t-out; salmon texture; gas cracks t-out | moist but firm | X | | |
| 21 | I | 303 | 567 | 587 | 562 | 20 | KR21 06 | clay | light gray | foram bearing FeS mottling common t-out | 1-3cm gas pockets rare t-out with soupy interiors | dry, firm | X | | |
| 21 | I | 303 | 537 | 557 | 532 | 20 | KR21 07 | clay | light gray | foram bearing FeS mottling rare | 1 gas pocket/crack | malleable | | | |
| 21 | I | 303 | 507 | 527 | 502 | 20 | KR21 08 | clay | light gray | foram bearing; 1 shell hash lens ~1/2cm FeS mottling rare | | moist & malleable | | | |
| 21 | I | 303 | 477 | 497 | 471 | 20 | KR21 09 | clay | light gray | foram rich ~2cm thick; foram bearing t-out FeS mottling rare; light flesh color | 1-2cm wide, 8cm long vertical burrow, soupy interior | moist & malleable | | | |
| 21 | I | 303 | 442 | 467 | 583 | 25 | KR21 10 | clay | light gray | foram bearing t-out mottling rare t-out | vertical burrows, 1cm diameter, common t-out | moist & malleable | | | |
| 21 | II | 304 | 399 | 419 | 394 | 20 | KR21 11 | clay | light gray | foram bearing t-out mottling rare t-out | vertical burrows common t-out | moist & malleable | | | |
| 21 | II | 304 | 369 | 389 | 364 | 20 | KR21 12 | clay | light gray | shell hash bearing FeS mottling rare | vertical burrows abundant t-out | moist & malleable | | | |
| 21 | II | 304 | 339 | 359 | 333 | 20 | KR21 13 | clay | light gray | shell hash bearing FeS mottling rare | vertical burrows abundant t-out | moist & malleable | | | |
| 21 | II | 304 | 304 | 329 | 299 | 25 | KR21 14 | clay | light gray | foram bearing; shell hash bearing FeS mottling rare | vertical burrows abundant t-out | moist & malleable | | | |
| 21 | II | 304 | 269 | 294 | 264 | 25 | KR21 15 | clay | light gray | foram bearing; shell hash bearing FeS mottling rare; light gray-white mottling | vertical burrows abundant t-out | moist & malleable | | abundant lenses, white in | |
| 21 | II | 304 | 234 | 259 | 229 | 25 | KR21 16 | clay | light gray | shell lens with bivalve fragments ~3cm wide FeS mottling rare | bioturbation common with foram bearing interiors | moist & malleable | | | |
| 21 | II | 304 | 199 | 224 | 194 | 25 | KR21 17 | clay | 50% gray - 50% light gray/white mottled together | | | | | | |
| 21 | II | 304 | 164 | 189 | 154 | 25 | KR21 18 | clay | 50% gray - 50% light gray/white mottled together | | | | | | |
| 21 | II | 304 | 115 | 149 | 261 | 34 | KR21 19 | clay | 50% gray - 50% light gray/white mottled together | 30cm of bivalve rich clay; 30 cm bed with clam fragments and whole shells FeS mottling rare | bioturbation abundant t-out | very moist & malleable | X | X | |
| 21 | III | 115 | 75 | 95 | 69 | 20 | KR21 20 | clay | 50% gray - 50% light gray/white mottled together | 3cm layer of bivalve abundant clay FeS mottles faint/rare t-out | bioturbation abundant t-out | very moist & malleable | | | |
| 21 | III | 115 | 40 | 65 | 33 | 25 | KR21 21 | clay | 50% gray - 50% light gray/white mottled together | 10cm layer of bivalve abundant clay FeS mottles faint/rare t-out | bioturbation abundant t-out | very moist & malleable | | | |
| 21 | III | 115 | 0 | 25 | 49 | 25 | KR21 22 | clay | light gray | foram rich FeS mottles rare; pyrite grains <1mm | bioturbation abundant t-out | extremely moist & malleable | | disturbed sample due to | |

| | | | | | | | | | | | | | |
|----|----|-----|-----|-----|---------------|----|---------|---|-------------|---------------|---|---|---|
| 22 | I | 242 | 450 | 510 | 520 | 20 | KR22 01 | clay | light brown | foram bearing | FeS mottling common; Flesh colored mottling rare common; Flesh and teal colored mottling rare common; | moist but firm | *Section III was not sampled but was measured at 193cm total length |
| 22 | I | 242 | 420 | 540 | 550 | 20 | KR22 02 | clay | light brown | foram bearing | Flesh and teal colored mottling rare common; Flesh and teal colored mottling rare common; | moist but firm | |
| 22 | I | 242 | 390 | 570 | 580 | 20 | KR22 03 | clay | light brown | foram bearing | Flesh and teal colored mottling rare common; Flesh and teal colored mottling rare common; | moist & malleable | |
| 22 | I | 242 | 355 | 600 | 613 | 25 | KR22 04 | thick, FeS stained, well sorted, medium | light brown | foram bearing | Flesh and teal colored mottling rare common; Flesh and teal colored mottling rare common; | moist & malleable | |
| 22 | I | 242 | 320 | 635 | 648 | 25 | KR22 05 | clay | light brown | foram rich | Flesh and teal colored mottling rare FeS mottles common | moist & malleable very moist & malleable | |
| 22 | I | 242 | 280 | 670 | 685 | 30 | KR22 06 | clay | light gray | foram rich | FeS mottling rare | very moist & malleable | |
| 22 | I | 242 | 248 | 710 | 721 | 22 | KR22 07 | clay | light gray | foram rich | FeS mottling rare | very moist & malleable | |
| 22 | II | 55 | 213 | 258 | 271 | 25 | KR22 08 | clay | light gray | foram rich | FeS mottling rare | very moist & malleable | |
| | | | | | 7620 Total | | | | | | | | |